

Examining The Predictability of Genetic Background Effects in The
Drosophila Wing

Caitlyn Daley

A thesis

Submitted to the School of Graduate Studies in Partial Fulfillment of the
Requirements for the Degree Master of Science

McMaster University © Caitlyn Daley, December 2019

McMaster University, Master of Science (2019), Hamilton, Ontario
(Biology)

Title: Examining The Predictability of Genetic Background Effects
in The *Drosophila* Wing

Author: Caitlyn Daley, BSc Honours Biology, Nipissing University

Supervisor: Dr. Ian Dworkin

Number of pages: 1-162

Abstract

Background dependence is a ubiquitous attribute of eukaryotic gene systems that modulates the phenotypic effects of a mutant allele due to segregating genetic variation among different wildtype strains. Despite the wealth of literature demonstrating the presence of genetic background effects, very little is known about how they functionally or mechanistically contribute to the relationship between genetic variation and phenotypic expression. It has been postulated that background dependent effects may be highly specific to the activity of individual alleles or genes. A recent examination of mutant alleles in two interacting genes in the *Drosophila* wing network demonstrated the magnitude of phenotypic effect of a mutant allele may predict its sensitivity to the genetic background. To further understand this, I examined the background dependence of many alleles for genes across the regulatory network of *Drosophila* wing development in many inbred strains. Our goal was to understand whether effects of the genetic background are an attribute of individual alleles, alleles of the same gene, or genes with similar phenotypes or developmental roles. Our analysis suggests that background dependence is highly positively correlated among alleles of the same gene, especially between alleles with similar magnitudes of phenotypic effect. Similarly, the background dependence of genes within the same regulatory network were also positively correlated. Alleles from different genes, but of the same magnitude of phenotypic effect, generally demonstrated the highest degree of intergenic correlation. However, the background dependence of mutant alleles were generally not

well correlated with the wildtype allele. Interestingly, we also found no recovery of any lethal alleles, despite thousands of individuals screened and evident suppression of mutant effects in some strains. We also analyzed the magnitude of intra-line variance in among a subset of our genes. This demonstrated a strong positive relationship between the magnitude of intra-line variation and the severity of phenotypic effects, regardless of the identity of the mutant allele. However, we show no correlation between intra-line variability in the wildtype and the magnitude of perturbation for a given mutant allele. To confirm the quantitative estimates of mean wing size accurately reflected subtle perturbations to wing tissue, we conducted a semi-quantitative analysis and compared it to our quantitative estimates. We demonstrate a high degree of correlation between the quantitative and semi-quantitative approaches, indicating semi-quantitative analysis is a useful way to capture subtle phenotypic effects. In addition, we repeated the quantitative analysis with a subset of the genes and inbred strains from the original data. Importantly, results of the repeated study largely recapitulate our original results.

Acknowledgments

I would like to begin by thanking my supervisor and mentor, Dr. Ian Dworkin, for his unwavering encouragement and support over the course of this project. Your patience and willingness to listen anytime I was stumped, had a new idea, or just needed to talk things out, challenged me to develop my ability to think more critically and independently. I would also like to thank my committee member Dr. Roger Jacobs for always welcoming me into your lab, and being open to chat about anything without notice. I also extend my gratitude to Dr. Lesley Macneil for serving on my committee and often suggesting insightful scientific perspectives related to my research that I had not ever considered. Thank you to my fellow Dworkin lab members Sarah, Maria, Katie, Darcy and Audrey, for being awesome friends, listening ears, and making our lab a great place to study. I would also like to thank Ana Vera-Cruz and Abood Abubakr for their contributions during their fourth year thesis projects, which were critical components of our study. I will also take this opportunity to acknowledge the contributions of the undergraduate volunteers that helped dissect the thousands of wings that went into this project, and I especially thank Genevieve Dietrich for all the hours she spent dissecting in the summer of 2018. Lastly, but not the least, I would like to thank my family and friends for their continued support over the course of my program. I can't name all of you, but I could not have completed this project without your support.

Table of Contents

Title page.....	i
Descriptive note.....	ii
Abstract.....	iii
Acknowledgements.....	v
Table of Contents.....	vi
List of figures.....	viii
List of tables.....	xi

1. Introduction

1.1 What are genetic background effects?.....	1
1.2 Limitations of genetic analysis in genetically invariant laboratory strains.....	3
1.3 Making sense of background dependence for mutations implicated in human disease.....	5
1.4 Biological robustness, canalization and phenotypic variance.....	8
1.5 Outstanding research questions.....	13
1.6 Project overview: Examining two models of background dependence.....	15
1.7 Drosophila wing morphology: A model system to study genetic background effects.....	16
1.8 An overview of key genes in Drosophila wing development.....	18
1.9 Predicting background dependent phenotypic expressivity of mutant alleles: Chandler et al. (2017).....	21
2.0 The Drosophila Genetic Reference Panel (DGRP Lines).....	23
2.1 Project Overview.....	25
2.2 Objectives.....	26
2.3 Hypothesis.....	27

2. Methods

2.1 Experimental Methods.....	29
2.1.1 Backcrossing of mutant alleles that have P-element mini-white insertions.....	32
2.1.2 Backcrossing of mutant alleles without P-element mini-white insertions.....	33

2.1.2 Crossing scheme for F1 Oregon-R/DGRP mutants.....	35
2.1.3 Methods to titrate gene expression in <i>Drosophila</i>	36
2.1.4 Crossing scheme for <i>sd</i> and <i>vg</i> knockdowns.....	37
2.2.5 Rearing environment of <i>sd</i> and <i>vg</i> knockdowns.....	37
2.2 General Methods.....	38
2.2.1 Fly rearing and collections	38
2.2.4 Wing dissection and imaging.....	39
2.2.3 Semi-quantitative scale.....	39
2.3 Experimental Design and Statistical Methods.....	40
2.3.1 Randomized blocking design for DGRP crosses.....	40
2.3.2 Quantitative analysis of <i>sd</i> , <i>ct</i> , <i>bx</i> and <i>bi (omb)</i>	41
2.3.3 Linear mixed models.....	42
2.3.4 Estimating broad sense heritability.....	43
2.3.5 Levene’s statistic as a measure of within genotype variability.....	44
2.3.6 Choosing lines for further analysis.....	45
3. Results	
3.1 Quantitative estimate of wing size, variance and H^2 for <i>sd</i> , <i>ct</i> , <i>bx</i> and <i>bi (omb)</i>	48
3.2 Correlation among quantitative estimates for <i>sd</i> , <i>ct</i> and <i>bx</i>	58
3.3 Semi-quantitative analysis of <i>sd</i> and <i>bi (omb)</i>	65
3.4 The relationship between intra-line variability and mutant effects in <i>sd</i>	75
3.5 The relationship between variability of wildtype size and deviations in <i>sd</i>	81
3.6 The relationship between intra-line variance of wildtype size and deviations in <i>sd</i>	84
3.7 Further analysis of <i>sd</i> and <i>bx</i> in a subset of 20 DGRP strains.....	86
3.2 Titrated knockdown of <i>sd</i> and <i>vg</i> expression.....	100
4. Discussion	107
5. References	127
6. Supplemental figures	142

List of Figures

- 1.1 The *Drosophila* wing regulatory network
- 1.2 Wildtype strains differ with respect to mutational robustness and wild type gene activity
- 2.1 Backcrossing of mutant alleles with P-element mini-white insertions
- 2.2 Backcrossing of mutant alleles without P-element mini-white insertions
- 2.3 Crossing scheme for F1 Oregon-R: DGRP mutants
- 2.4 Crossing scheme for *scalloped* and *vestigial* knockdowns
- 2.5 The randomized block design for the *scalloped*: DGRP crosses
- 2.6 Choosing select DGRP lines by quantitative estimates of wing size
- 3.1 Average wing size of *scalloped* mutants alleles
- 3.2 Average wing size of *cut* and *beadex* mutants alleles
- 3.3 Variation in *scalloped* wing size line means among DGRP strains
- 3.4 Variation in *beadex* wing size line means among DGRP strains
- 3.5 Variation in *cut* wing size line means among DGRP strains
- 3.6 Variation in *bifid* wing size line means among DGRP strains
- 3.9 Correlation of mutant effects in *scalloped* wing size among DGRP strains
- 3.10 Correlation of mutant effects in *beadex* wing size among DGRP strains
- 3.11 Correlation of mutant effects in *cut* wing size among DGRP strains
- 3.12 Correlation of mutant effects in *scalloped* and *cut* wing size among DGRP strains

- 3.13 Correlation of mutant effects in *scalloped* and *beadex* wing size among DGRP strains
- 3.14 Correlation of *scalloped* alleles wing size and wing score estimates
- 3.15 Average effect of *scalloped* mutant wing scores among DGRP strains
- 3.16 Average effect of *bifid* mutant wing scores among DGRP strains
- 3.17 Variation in *scalloped* wing score line means among DGRP strains
- 3.18 Variation in *bifid (omb)* wing score line means among DGRP strains
- 3.19 Correlation of mutant effects in *scalloped* wing scores among DGRP strains
- 3.20 Correlation of mutant effects in *bifid (omb)* wing scores among DGRP strains.
- 3.21 Correlation of mutant effects in *scalloped* and *bifid* wing scores among DGRP strains
- 3.22 Average estimate of *scalloped* mutant interline variability among DGRP strains
- 3.23 Intra-line variability in wing size among *scalloped* alleles across 73 DGRP strains
- 3.24 Correlation of intra-line variability and wing size among *scalloped* mutant alleles
- 3.25 Correlations of intra-line variation and wing score among *scalloped* mutant alleles
- 3.27 The relationship between wildtype deviation and magnitude of intra-line variability
- 3.28 The relationship between intra-line variance in wing size among in the wildtype and deviations from wild type wing size
- 3.29 Average size effect of *scalloped* mutants wing size among (subset) DGRP strains

- 3.30 Average size effect of *beadex* mutants wing size among (subset) DGRP strains
- 3.31 Variation in *scalloped* wing size line means among (subset) DGRP strains
- 3.32 Variation in *beadex* wing size line means among (subset) DGRP strains
- 3.33 *scalloped* and *beadex* line means correlations mutant effect among DGRP
- 3.34 Average estimate of *scalloped* mutant interline variability among DGRP strains
- 3.35 Average estimate of *beadex* mutant interline variability among DGRP strains
- 3.36 Among line variability in environmental sensitivity (variation within lines) across *scalloped* mutant alleles
- 3.37 Intra-line variability in wing size among *beadex* mutant alleles
- 3.38 Correlation of intra-line variability and wing size among *scalloped* mutant alleles
- 3.39 Correlation of intra-line variability and wing size among *beadex* mutant alleles
- 3.40 Mean wing size in Oregon and Samarkand by *nubbin-GAL4 / UAS-vg.RNAi*
- 3.41 Mean wing size in Oregon and Samarkand by *nubbin-GAL4 / UAS-sd.RNAi*
- 3.42 Temperature modulation of *scalloped* expression by *nubbin GAL4/ UAS-sd.RNAi*

List of Tables

- 2.1 Summary of *beadex* and *cut* mutant alleles. All alleles on the X-chromosome
- 2.2 Summary of *scalloped* mutant alleles. All alleles on the X-chromosome
- 2.3 Summary of *Beadex* and *cut* mutant alleles. All alleles on the X-chromosome
- 2.4 DGRP lines that were chosen for further analysis
- 2.5 Experimental Crosses of *scalloped* and *vestigial* knockdowns
- 3.1 The statistical model estimates of the *scalloped* alleles
- 3.2 The statistical model estimates of the *beadex and cut* alleles
- 3.4 The statistical model estimates of the *bifid* alleles
- 3.6 The statistical estimates for interline variance and correlations among *scalloped* alleles
- 3.7 The statistical estimates of the relationship between the deviation from wildtype wing size and intra-line wing size variation
- 3.8 The statistical estimates of the relationship between the intra-line variance in the wildtype strain and the deviation (severity) of *scalloped* alleles.
- 3.9 The statistical estimates of the *scalloped* and *beadex* alleles from the subset experiment

1.0 Introduction

What are genetic background effects?

It might be expected that a given mutation will generally have consistent phenotypic effects among strains. Yet evidence indicates that the interaction of mutant alleles with naturally occurring genetic variants across the genome, or genetic background, generates considerable variation in phenotypic expression (in terms of both penetrance and expressivity). Genetic background effects, can be defined as “alleles at other genes throughout the genome that interact with the focal gene/allele of interest” (Yoshiki & Moriwaki, 2006), are a pervasive feature of eukaryotic systems across taxa, affecting bacteria, yeast, nematodes, flies, mice and some plant systems (Burnett et al., 2011; Kebaara, Nazarenu, Taylor, & Atkin, 2003; Korona, 1996; Lessel, Parkes, Dickinson, & Merritt, 2017; Ungerer, Linder, & Rieseberg, 1996.). Although the mechanisms for mediating background dependence of mutational effects are still largely unclear, accumulating evidence suggests that the effects of the genetic background may be a common phenomenon to genetic perturbation, as background dependence occurs across the spectrum of mutant classes. This includes hypomorphs (Johnson, Zheng, & Noben-Trauth, 2006), hypermorphs (Tissenbaum & Guarente, 2001), neomorphs (Fowler & Freeling, 1996) and null mutations (Bonyadi et al., 1997). Background dependence has also been observed for mutations with varying degrees of severity, including lethal mutations, and genes critical for viability (Dowell et al., 2010). In the yeast *Saccharomyces cerevisiae*, systematic deletion of 5100 genes in two different wildtype

laboratory strains identified several candidate genes that are conditionally essential for viability (Dowell et al., 2010). The functional discrepancy of these “essential genes” is thought to arise through complex interactions of essential genes with genetic modifiers that are likely strain specific (Dowell et al., 2010). Strikingly, the two yeast strains *S1278b* and *S288c* that display such disparate phenotypic effects are genetically similar; genetic differences observed between the two strains were mostly due to small insertions, small deletions, and single nucleotide polymorphisms (Dowell et al., 2010). Similarly, Threadgill et al. (1995) show the phenotypic manifestation of an amorphic allele for epidermal growth factor receptor (EGFR) in mice is strain-specific, causing lethality at different developmental stages. In the CF-1 background, EGFR deficiency was lethal during implantation of the embryo, causing degradation of the embryo’s inner cell mass. However, lethality of the same mutant allele in the 129/Sv strain is delayed until placental formation. Strikingly, the CD-1 strain proceeds through embryonic development with the EGRF deficiency, with lethal organ abnormalities delayed until three weeks postnatal (Threadgill et al., 1995). This study also illustrates the background dependent response to perturbation of highly pleiotropic genes can display novel phenotypes that appear to be strain specific. In other words, pleiotropic genes that influence the expression of several other traits may interact with genetic modifiers unique to specific genetic backgrounds, resulting in phenotypes that either cannot be reproduced in other strains, or are not yet characterized (Nadeau, 2001). For example, two modifier variants unique to two separate mice strains have both been implicated in

novel expression of neural tube defects (Estibeiro, Brook, & Copp, 1993; Helwig et al., 1995).

Limitations of genetic analysis in genetically invariant laboratory strains

While it is now well understood that modulation of mutant phenotypes by segregating allelic variation among wild type genetic backgrounds is more likely a rule than an exception, the role of such allelic variation has historically been treated as nuisance variation, and thus remains poorly understood. The classic approach to mutational analysis has been to design forward genetic screens that are both repeatable and reduce sources of variation, which is routinely achieved by conducting experiments in controlled environments, limiting genetic analysis to single genes, and using isogenic (or near isogenic) strains as the substrate for mutagenesis. This method minimizes any potential confounding effects from segregating genetic variation with that of the focal gene. However, an important caveat to this approach rests on the assumption that the results from one set of conditions will be generalizable, such that inferences derived from one genetic strain will be true of other strains, and perhaps even to orthologous genes in other species (Sittig et al., 2016). Yet in many circumstances, genetic inferences of mutant phenotypes become clouded or convoluted by segregating allelic variation among genetic backgrounds of different wildtype strains. For example, in *Drosophila melanogaster*, the *indy* gene was demonstrated to extend lifespan, with follow up experiments to understand a mechanistic explanations, including differential expression of genes in the oxidative phosphorylation pathway (Neretti et al., 2009) and the

interaction of calorie restriction and downregulated *indy* expression to promote longevity (Wang et al., 2009). However, Toivonen et al. (2007) later report that the increases in longevity by *indy* mutants was dependent on modifiers in the genetic background, as outcrossing these mutants to both laboratory strains and natural populations diminished these effects.

Nonetheless, minimizing the effect of segregating allelic variation by controlling for genetic background, in conjunction with classic genetic tools such as forward mutant screens, UAS-GAL4 systems, and RNA interference, has made remarkable progress in discerning genotype-phenotype relationships, particularly in fields that aim to study trait *expression* (in contrast to studies of trait *variation*). Phenotypic analysis of mutants generated in standard isogenic laboratory strains has uncovered tremendous insights into the link between genotype and phenotype by identification of countless causal genetic variants, spatial developmental domains of expression, as well as characterization of important gene-gene interactions by non-complementation that contribute to the expressivity of mutant alleles. Moreover, these findings have helped in the construct gene networks, bettered our understanding of gene function, gene interactions in signalling pathways, and revealed how developmental gene networks influence cellular and organ level processes. While the contribution of these experimental designs should not be negated, one limitation in this approach is the potential to uncover the expression of mutant phenotypes is largely limited to traits with large mutational target size, lower degrees of canalization, and expression that occurs

later in development (Houle, 1998). Consequently, there are likely multitudes of mutant phenotypes, epistatic interactions, and allelic variants implicated in quantitative trait variation that remain to be discovered. Additionally, analysis of inbred laboratory adapted strains may overestimate the effect of genetic variants to ecologically relevant trait variation in natural populations. For example, Hoekstra (2006) highlight an extensive number of genes that affect vertebrate pigmentation patterns, most of which were identified through mutagenesis screens in laboratory mouse strains. However, only a select few of these genes have been implicated in variation of vertebrate pigmentation patterns in natural populations to date (Hubbard, Uy, Hauber, Hoekstra, & Safran, 2010). The exposure of such genetic variants in laboratory mice may be because conditions of the laboratory environment are more favourable than in nature (Hoffmann, Hallas, Sinclair, & Partridge, 2001). Controlling the effects of allelic variation and microenvironment may thus limit the gene by environment interactions that contribute to diminished phenotypic expressivity of these genetic variants in natural populations.

Making sense of background dependence for mutations implicated in human disease

With growing evidence for the ubiquity of genetic background effects in model organisms, clinicians have begun to research how these effects modulate human traits, especially those associated with disease. Cystic fibrosis, an autosomal recessive disorder, has become one of the most well studied human diseases with regard to genetic background, as most patients are homozygous for the same perturbation, yet there is substantial variation in how the disease manifests (Castellani et al., 2008). Although

screening for the protective variants that modulate the disease using genome wide association studies has been thought to hold the key to understanding why such heterogeneity exists, this approach often lacks power to identify modifier genes in circumstances where the genetic risk of disease is highly polygenic, and/or arise from the contribution of many genes with smaller and more subtle effects (Tam et al., 2019). Indeed, even the genetic variants identified through genome wide association that demonstrate modest modulating effects, often only account for a small fraction of heritability and disease risk, and are rarely causal variants that explain the mechanisms of the disease (Tam et al., 2019). Consequently, the clinical application of such loci as potential therapeutic targets or disease biomarkers is often limited (Tam et al., 2019).

The central goal of genome wide association studies is to understand the genetic underpinnings associated with disease risk, and ultimately develop treatment strategies personalized to your unique genetic background (Bush & Moore, 2012). However, given that most human genetic diseases are highly polygenic, and an astonishing number of allelic variants are often implicated (McCarroll & Hyman, 2013), carrying out personalized regimens in practice remains a formidable task. So in spite of the fact genome wide association studies have been very successful in locating thousands of loci associated with disease risk, and have identified potentially many new pathways implicated in disease development, current approaches fail to capture the full breadth of the genetic variants, particularly allelic variants with relatively small modifier effects. This also includes any non-additive epistasis, which has been thought to explain missing

heritability of disease risk (Green et al., 2017). Consequently, the ability to integrate any understanding we have of the genetic basis of human diseases into clinical practice is limited. Moreover, our understanding of the underlying genetic architecture of diseases like cystic fibrosis is likely confounded by the substantial amount of small effect allelic variants residing in the genetic background, despite some alleles of large effect. Albeit detecting more subtle gene-gene interactions may be alleviated through larger sample sizes (Tam et al., 2019), the current method of detecting modifier genes to better understand the genetic interactions that contribute to increased disease risk is ultimately impeded by the lack of framework that defines when and why background dependence occurs. For example, is increased disease risk an attribute of the causal allele(s), or is disease risk determined by an increased sensitivity of particular gene network(s) associated with the disease? In the former case, any identified modifier variants of cystic fibrosis patients that carry the most common perturbation may tell you nothing about other patients that carry alleles with one of the many other perturbations that cause the disease; in the latter case, the nature of the perturbation may not matter. Thus, a predictive framework of background dependence, as well as a comprehensive understanding of the scope of genetic variation that segregates in human populations, and the development of an approach that captures the effects of both small and large effect allelic variants in modulating disease risk, is critical to thoroughly characterizing both causal genes/alleles and any allelic modifier variants that contribute to the background dependence evidenced in the prognosis of many identified genetic diseases.

Biological robustness, canalization and phenotypic variance

An integral component of the functional relationship between genotype and phenotype is external sources of variation, whereby contributions of genetic variants are modulated by environmental, genetic and stochastic effects that contribute to phenotypic expressivity. Although these sources of variation are integral to the capacity of a system to evolve (as phenotypic variability is the substrate on which natural selection acts), new mutations are often detrimental to an organism (Bataillon, 2003). Biological robustness, or genetic canalization, is a ubiquitous feature of gene regulatory networks that evolves to cope with aberrant genetic variation, including the effects of deleterious mutations (Félix & Barkoulas, 2015). Robustness in gene networks is characterized by quantitative non-linear relationships between genes and gene products, which permit compensatory actions in the genetic background in response to perturbation (Félix & Barkoulas, 2015). Consequently, gene networks evolve thresholds for gene activity that minimizes phenotypic variance to an optimal (or “wildtype”) range. Gene activity that falls outside this range demonstrates an increased sensitivity to the perturbation, as indicated by increased phenotypic variability. (Félix & Barkoulas, 2015). This control of gene activity during development is especially evident in the extent of trait variation within a population, as generally speaking, the overwhelming majority of individuals will exhibit the so-called “wildtype” phenotype(s) that correspond to the optimal range (Félix & Barkoulas, 2015; Flatt, 2005). This phenomenon is called canalization (Waddington, 1959), which is a more specific term used to describe a trait

that is robust to sources of environmental perturbation (environmental canalization), such as temperature fluctuation or availability of nutrients, and sources of genetic perturbation (genetic canalization), such as the accumulation of new mutations (Flatt, 2005). It has been hypothesized that genetic canalization of wildtype phenotypes occurs through the evolution of non-linear epistatic responses in the genetic background (Green et al., 2017). Epistasis, or non-additive genetic interactions, describes the non-independence of a mutational effect by the interaction of alleles at different loci (Barkoulas, van Zon, Milloz, van Oudenaarden, & Félix, 2013; Poelwijk, Krishna, & Ranganathan, 2016). This is in contrast to dominance effects, or the interaction of alleles at the same loci (Kacser & Burns, 1981). Epistatic interactions in classic model organisms, including plants, flies, worms, and mice, reveals epistatic interactions are very common among genes that function in the same regulatory network. For example, in the *C. elegans* vulval network, perturbation to *epidermal growth factor* (EGF) signalling prompts a function shift in genes in the *Notch* pathway from cell inhibition to cell induction, ensuring the correct vulval cell fate (Barkoulas et al., 2013). Similarly in *Arabidopsis*, the *clavata* and *wuschel* genes conditionally regulate the function of themselves and each other in a negative feedback loop, ensuring correct meristem development (Muller, 2006). Epistatic interactions have been observed to be context dependent (Domingo, Baeza-Centurion, & Lehner, 2019). In *Drosophila*, the majority of epistatic modifiers that influence the severity of perturbations to the wing appear to be background dependent (Chari & Dworkin, 2013). Similarly, in *Saccharomyces cerevisiae*,

epistatic interaction in the metabolic network depends on the conditions of the local environment (Harrison, Papp, Pál, Oliver, & Delneri, 2007).

Understanding the mechanisms that promote robustness during development and trait canalization have important implications in understanding the function of background dependence, as background dependent phenotypic variance may simply reflect differences in the genetic capacities of a different strains to minimize the magnitude of phenotypic deviation from the wildtype. In other words, the magnitude of severity of a mutant allele may be explained by how much the mutant allele perturbs the regulatory network, and how well that strain is canalized to the genetic perturbation. Under this pretense, phenotypic variance among strains may be minimal for alleles with weak effects, as they only marginally perturb the function of the regulatory network. Similarly, phenotypic variability may be minimal for alleles with severe effects, as evolving canalization mechanisms to overcome drastic reductions in gene function may be rare. In contrast, alleles with moderate effects may demonstrate the most phenotypic variability (background dependence), and best reflect differences in canalization of gene networks among strains (Félix & Barkoulas, 2015; Hallgrímsson et al., 2019).

Mechanisms of robustness and genetic compensation

It is evident that epistasis often plays a role in mitigating the phenotypic effects of mutant alleles, and there are many known mechanisms that underlie these compensatory genetic effects. Consideration of known mechanisms that induce genetic

compensation are important to understanding background dependence, because any mechanisms of suppression utilized by different strains to suppress the phenotypic effects of deleterious alleles may depend on the nature of the mutant allele itself. Excluding any compensation mechanisms by altering the expression of other genes, genetic compensation mechanisms may be broken down into two distinct classes; compensation that occurs either upstream of protein function (also called transcriptional adaptation), or downstream of protein formation (post-translational modification) (El-Brolosy & Stainier, 2017). Transcriptional adaptation has been observed in most standard model organisms, including bacteria (Taneja, Dhingra, Mittal, Naresh, & Tyagi, 2010), yeast (Strassburg, Walther, Takahashi, Kanaya, & Kopka, 2010), flies (Hojland, Jensen, & Kristensen, 2014), worms (Boer, Roelofs, Vooijs, Holmstrup, & Amorim, 2018) and mice (Wright et al., 2008). Similarly, post-translational modification is well documented (Pejaver et al., 2014). Despite the abundance of literature demonstrating transcriptional adaptation, it is unclear if transcriptional adaptation becomes active by the DNA lesion itself, or in response to fragmented mRNA. The compensation response to lesions in the DNA have been shown to occur through chromatin remodeling (Wright et al., 2008) and the recruitment of small non-coding RNA's (d'Adda di Fagagna, 2014; Rossi et al., 2015). Changes in interchromosomal interactions and the activity of micro-RNA's are also postulated to be involved (Li et al., 2015; Rossi et al., 2015). In contrast, mutations that produce fragmented mRNA have mostly been demonstrated to induce the nonsense-mediated decay pathway

(Schuermann, Helker, & Herzog, 2015) and the activity of RNA binding proteins (Keene, 2007; Rossi et al., 2015). Mutant mRNA decay has recently been shown to be necessary to trigger transcriptional adaptation, or upregulation of genes that can assume the developmental function of the gene producing mutant mRNA (El-Brolosy et al., 2018). However, transcriptional adaptation is not observed for most mutations that fail to trigger this response, despite decreased transcription of the mutant gene (El-Brolosy et al., 2018). This discordance demonstrates an importance to consider the transcriptional effect of a deleterious allele, as the molecular mechanisms of genetic compensation are evidently sometimes different. As such, the background dependence of alleles with differing transcriptional effects may vary in their ability to be suppressed. Additionally, molecular mechanisms that induce the activity of heat shock proteins and microRNA's have also been thought to buffer the phenotypic expression of genetic perturbation (Green et al., 2017). For example, in *C. elegans*, the loss of microRNA's are known to influence the mutant phenotypes in strains sensitized to the effects of the mutation (Brenner et al. 2010). However, the behaviour of microRNA's themselves have been shown to be background dependent (Kiessling et al. 2017).

Outstanding research questions

Understanding the scope of segregating allelic variation among strains or populations, and how it contributes to the background dependence of large effect alleles, is critical to deepening our understanding of phenotypic expression. A comprehensive understanding of segregating allelic variation, particularly small effect allelic variation, therefore requires deliberate integration of genetic variation into time-tested methods of genetic analysis. However, before we can begin to employ these genetic effects as a largely untapped resource, there are several outstanding questions to be addressed. First and foremost among these is the degree of predictability of which mutations will vary due to interactions with genetic backgrounds. Previous work (Chandler et al. 2017), demonstrated a relationship between magnitude of mutational effects and background dependence for *scalloped* and *vestigial*, two *Drosophila* wing genes that encode transcription factors that together form a heterodimer central to wing development. Yet the degree to which there may be similar predictable effects of background dependence in mutations of other genes involved with these developmental processes is largely unknown. It is also unclear whether any generalized patterns underlying background dependence exist. For example, can we identify any common tendencies towards background effects among genes or alleles that function in the same pathway, or among genes or alleles with either similar phenotypes or developmental roles? That is, do alleles with similar phenotypic effects respond to different wild type backgrounds in the same way? Similarly, is there a relationship between the magnitude

of individual mutations, and the potential for background dependence? Finally, can discordant background dependent phenotypes simply be explained by differences in robustness or intrinsic sensitivity in the regulatory network to sources of external variation? Addressing these types of questions will aid in determining whether background dependence has any predictive potential to explain the incongruence of mutant phenotypes among strains, as well as building our understanding of the genetic architecture implicated in both phenotypic expression and phenotypic variation of small effect genetic variants hidden in the genetic background.

Project overview: Examining two models of background dependence

There are at least two distinct views with respect to the causes of genetic background effects. On the one hand, It has been thought that the effects of the genetic background may be highly specific to every allele or gene, regardless of intragenic or intergenic relation. This notion implies that background effects are due to either the nature of the perturbation of the mutant allele itself (i.e. the DNA lesion), the distinguishing function that is served by the alleles of that gene, or extends more generally to the alleles/genes that execute specific developmental roles. In contrast, background dependence may be explained by an intrinsic sensitivity in the genetic network, or even the trait in question. In this circumstance, background dependent phenotypic variance may reflect differences in the robustness of connections within a gene network. Given that developmental genes often exhibit functional threshold boundaries, regulatory networks are consequently characterized by ubiquitous, nonlinear quantitative relationships between genes and gene products (Félix & Barkoulas, 2015). As such, the apparent strain specific sensitivity to mutation, or genetic background effects, may be due to intrinsic differences in the ability to buffer sources of variation, which may mechanistically be explained by differences in the threshold ranges of genes in each genotype's regulatory network. It is important to note that these explanations need not be mutually exclusive. Here, I will examine both ideas. First I will address whether patterns of background dependence are predictable by the identity of an allele or gene, using a comprehensive allelic series across several genes in the

Drosophila wing network. To do this, I will utilize an allelic series in four genes, *scalloped*, *cut*, *bifid* and *beadex*. Notably, all four of these genes are transcription factors and on the X-chromosome. Secondly, I examine the more mechanistic explanation of background dependence to determine whether background effects occur due to naturally occurring variation in transcript expression among strains.

***Drosophila* wing morphology: A model system to study genetic background effects**

The *Drosophila* wing presents an ideal model to study how the genetic background modulates phenotypic variance because its relatively simple adult structure allows the wings to be easily phenotyped for small or subtle changes in wing size and wing shape. In addition, every cell in the adult wing structure has its own trichome bristle, providing a means to quantify cell density. As illustrated in Figure 1.1, the genetic interactions and the mechanisms underlying development in the wing regulatory network are well characterized, which makes the *Drosophila* wing very conducive to studying epistasis and other types of genetic interactions. In the larvae, wing imaginal discs are easily isolated from other developmental tissues, making them excellent models for developmental and cellular research.

The *Drosophila* wing regulatory network

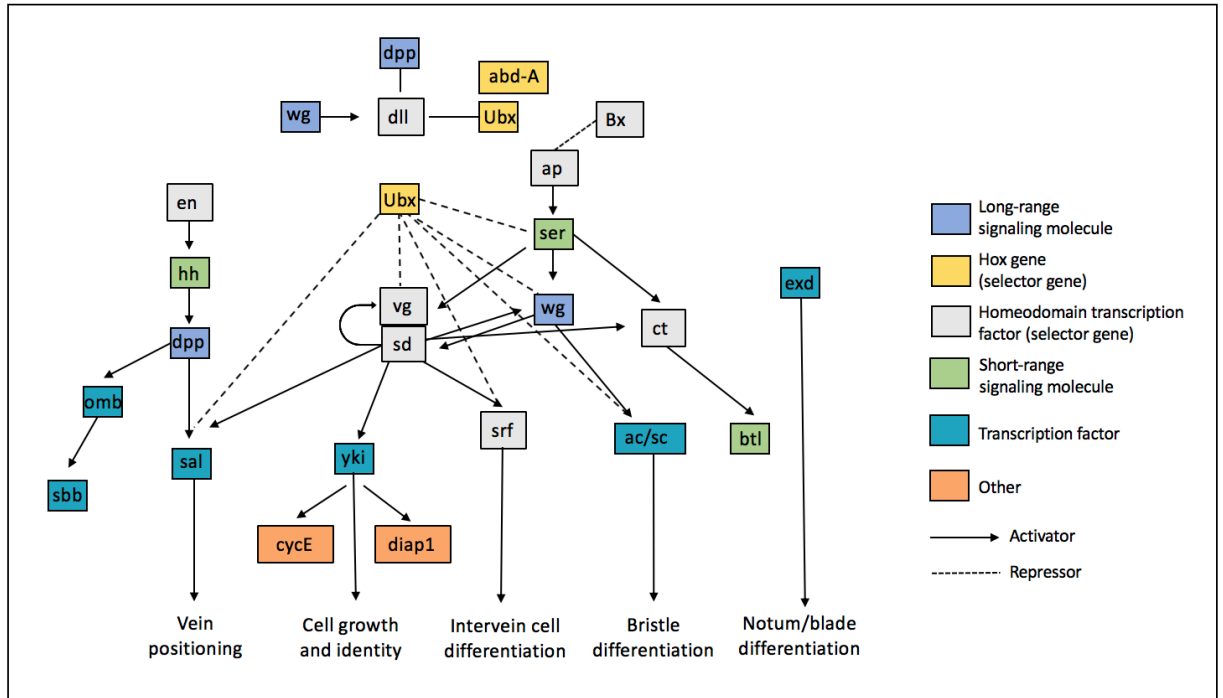


Figure 1.1: A simplified overview of the *Drosophila* wing regulatory network. This figure represents some of the key genes involved with wing determination and cell differentiation during wing development, but is not meant to be comprehensive. Figure adapted from (Connahs, Rhen, & Simmons, 2016).

An overview of key genes in *Drosophila* wing development

While a large scale review of wing development is beyond the scope of this thesis, there are a few key developmental events, and genes that govern such events, that are relevant to the current work. *scalloped* (*sd*) encodes a transcription factor that encodes a TEA protein with a DNA binding domain, and is critical for proper wing development (Srivastava, 2004). Its activity regulates the *cis*-regulatory elements of genes that promote wing morphogenesis (Kirsten A. Guss et al., 2013). In wing tissues, the Scalloped (SD) promotes both wing tissue differentiation (as a part of a heterodimeric transcription factor) with the Vestigial protein, and regulates cell growth and proliferation of the wing with Yorkie (also as a heterodimeric transcription factor). *vestigial* (*vg*) expression is initially limited early on to the dorsal/ventral boundary by Wingless (Simmonds et al., 1998). *vg* then becomes expressed in the wing primordia in response to Decapentaplegic (Dpp) (Simmonds et al., 1998). During early second instar, *sd* and *vg* are expressed ubiquitously at low levels in the wing imaginal disc (Paumard-Rigal, Zider, Vaudin, & Silber, 1998). As development proceeds into the third larval instar, both *sd* and *vg* expression become well defined in progenitor cells of the future wing margins via induction by WG (Simmonds et al., 1998). In late third instar, *scalloped* and *vestigial* expression spreads throughout the wing imaginal disc to become ubiquitously expressed in both the wing pouch and hinge regions (Paumard-Rigal et al., 1998).

In addition to its role for directing wing development via regulation of downstream genes with Vg, SD also regulates cell growth and proliferation of the developing wing tissue through its interaction with Yki in the hippo signalling pathway. In the absence of Hippo signaling, Yki is shuttled into the nucleus where it binds with SD to promote cell proliferation and inhibit apoptosis (Guo et al., 2013). This is achieved with Yki-SD regulating the activity of genes downstream of the *hippo* pathway, including *diap1*, cell cycle regulator *cyclin-E* and the *bantam* micro-RNA (Guo et al., 2013). In the presence of *hippo* signalling, Yki is shuttled into the cytoplasm, inactivating it (Guo et al., 2013).

Although expressed later in development than either *wingless* or *dpp*, *scalloped* and *vestigial* are described as the earliest genes to promote wing differentiation, as their expression is independent of both *wingless* and *dpp* in the wing (Williams, Paddock, & Carroll, 1993). Together, SD and Vg physically interact to form a heterodimer that acts as a “master switch”, regulating the transcription of each other and additional wing specific genes (Guss et al., 2013) including *spalt* (Guss et al, 2001), *blistered* (Montagne et al., 1996) and *cut (ct)* (Liu, Grammont, & Irvine, 2000). *cut* encodes a long range homeodomain transcription factor, and it’s expression is critical for the formation of the dorsal/ventral (DV) boundary in the wing imaginal disc, and consequently the formation of the margin of the wing blade (Micchelli, Rulifson, & Blair, 1997). The DV boundary is first formed during mid-second instar in part by *apterous (ap)* expressing cells in the dorsal region. *cut* expression then becomes well defined in mid-late third instar via the

Ap dorsal boundary in a narrow row of “edge” cells along the wing margin. Ct protein in edge cells serves to distinguish bristle precursors on the dorsal and ventral regions, which go on to express *ct* during early pupal development (Blochlinger, Jan, & Jan, 1993.; Micchelli, Rulifson, & Blair, 1997). However, when *ct* is perturbed, *ct* expression becomes diminished in edge cells, bristle precursor cells, and adjacent epithelial cells, eventually leading to cell death during pupal development. It is thought that this is the mechanism by which *ct* mutants develop notched wings (Micchelli, Rulifson, & Blair, 1997).

The formation of the DV boundary by Ap LIM-homeodomain protein is modulated by another protein, dLMO, encoded by the *Beadex (Bx)* gene. Bx and Ap function in an antagonistic feedback loop to regulate *ap* expression, via competitive binding of Bx to Chip (Milan, Diaz-Benjumea, & Cohen, 1998). However, it is important to note that while Bx competes with Ap for Chip binding, the reciprocal is not true. This discrepancy may be explained by a higher affinity of Bx LIM binding domains to Chip than in those in Ap (Weihe, Milán, & Cohen, 2001). Nonetheless, the binding of cofactor Chip to Ap is critical for Ap activity (and consequently the formation of the DV boundary), as together they form a functional complex (Weihe, Milán, & Cohen, 2001). Ap activity is thereby modulated by the relative amount of Chip bound to Bx. *Beadex* gain of function alleles that result in overexpression of the dLMO protein drastically reducing Ap activity by disrupting the relative amount of Chip available to bind with Ap (Milan *et al.*, 1998). The mutant phenotype of *Beadex* overexpression mutant alleles are

thus effectively due to *apterous* loss of function (Bejarano et al., 2008). Loss of function in *apterous* via *Beadex* perturbation is consequential, as binding of Chip to Ap is crucial for Ap stability. The stability of Ap expression is reduced when unbound to DNA with Chip in the functional complex (Weihe et al., 2001). Disruption of *apterous* activity in the DV boundary by *Beadex* may be the mechanism by which *Beadex* mutants have phenotypically excised wings (Bejarano et al., 2008).

Predicting background dependent phenotypic expressivity of mutant alleles:

Chandler et al. (2017)

Recent work by Chandler et al. (2017) in *Drosophila* examined how the genetic background affects patterns of phenotypic expressivity, complementation among alleles, and the rank ordering of an allelic series of the two functionally related *Drosophila* genes, *sd* and *vg*, in two distinct isogenic wildtype laboratory strains. Although they did not observe reordering of their allelic series for either *sd* or *vg* between strains, they did observe a notable relationship between the sensitivity to background dependence (among strain variability) and the magnitude of phenotypic effects. Background dependence was most pronounced for mutant alleles with, on average, intermediate phenotypic effects. In contrast, alleles with relatively weak or severe phenotypic effects demonstrated less background dependence among strains. This pattern, observed for both homozygous females and hemizygous males, suggests that the sensitivity to genetic background effects may be predictable at the allelic level. Further analysis of hemizygous, homozygous, and trans-heterozygotes determined this relationship relates

to the magnitude of genotypic effects overall, rather than properties of specific alleles themselves. The allelic effects of trans-heterozygotes, which in combination sometimes exhibited increased background dependence, were not always background dependent in isolation

Chandler et al. (2017) also demonstrate between genotype variability was not indicative of within genotype variability. While variability *between* genotypes (i.e. background dependence) was highest for alleles and genotypes with intermediate effects, variability within a *single* genotype (i.e. stochastic differences between otherwise identical individuals) was most pronounced for alleles with severe phenotypic effects. This suggests an independence of the sensitivity to genetic background and sensitivity to the micro-environment or intrinsic stochastic variation.

To confirm the generalizability of their results, Chandler et al. (2017) tested their model with additional inbred strains. In follow up experiments, they crossed a few *sd* alleles with weak, moderate and severe phenotypic effects (*sd*¹, *sd*^{e3} and *sd*^{58d} respectively) introduced into the *Samarkand* laboratory strain and then crosses to 16 randomized strains from the *Drosophila* Genetic Reference Panel (DGRP). The DGRP are a panel of wild type strains generated from a collection from a farmers market in North Carolina, that were inbred and sequenced. The DGRP thus provide an important resource for the study of segregating genetic variation in natural populations. In Chandler et al, the crosses between the mutant alleles and the 16 DGRP lines produced F1 hemizygous male progeny that were heterozygous on the autosomes for the

Samarkand and unique *DGRP* genome. These results recapitulated the general phenomenological model outlined by their original data, reiterating their prior findings. However, of note, the phenotypic range of effects across backgrounds was substantially less for the alleles crossed to the 16 DGRP as compared to the two lab strains. Two potential explanations were provided for this result. On one hand, the 16 randomly chosen DGRP were not collectively segregating for the modifier alleles that act as strong enhancers of the *sd* phenotypes. On the other hand, the allele(s) contributing to the strong enhancement of the *sd* alleles were recessive (and in the Oregon-R background). In this circumstance, starting with the mutant alleles in the *Samarkand* background meant that the modifier alleles were always present in the F1 males as heterozygotes on the autosomes, resulting in a relatively “suppressed” distribution of phenotypes.

The *Drosophila* Genetic Reference Panel (DGRP Lines)

As briefly mentioned above, the *Drosophila* Genetic Reference Panel is a collection of isogenic, inbred lines derived from 192 isofemale lineages of a natural outbred population of *Drosophila melanogaster* collected in Raleigh, North Carolina (Mackay et al., 2012). In aggregate, the DGRP lines are representative of naturally segregating genetic variation typical of a natural population, making them a powerful tool to study the scope of phenotypes in quantitative traits. Many of the DGRP lines also harbour allelic variants present at low frequencies in the natural population. This is a valuable attribute because rare variants in novel genes may have a large effect on

phenotypic variance (Mackay et al., 2012). In addition, the DGRP strains are all fully sequenced, making them conducive to genomic analysis.

Project Overview:

Examining two predictive models of background dependence

In my first chapter, I sought to confirm the utility of phenomenological model outlined by Chandler et al. (2017) with a more comprehensive allelic series with a complete range of phenotypic effects in a different laboratory strain, Oregon-R. I also expanded on Chandler et al. (2017) results to test their model among 73 unique *DGRP* strains. Their work included an allelic series of the *scalloped* gene: *sd*¹, *sd*^{etx4}, *sd*^{e3}, *sd*^{58d} and *sd*^{G0309}. In addition to these, I added alleles to expand the range of phenotypic expressivity of the *scalloped* gene; this included alleles *sd*^{29.1}, *sd*^{G0239} and *sd*^{G0483} (Table 2.2). Importantly, some of these alleles are partially lethal, which provided an additional phenotype to assess the magnitude of background dependence. In particular analysis of these severe alleles is useful to determine if DGRP strains that strongly suppress *sd* mutant wing phenotypes for viable alleles also reduce lethality, as that may provide insight about whether genetic background effects are due to an intrinsic sensitivity of the background per se. To address whether the patterns of background dependence extend throughout the gene regulatory network influencing wing development, I also included multiple alleles from *cut*, *beadex* and *bifid (omb)*. Analysis of alleles in these genes in conjunction with the *scalloped* alleles aids in determining whether background dependence is correlated among alleles within genes, among genes influencing a single developmental process, or specific to particular phenotypes or developmental roles.

Objectives

Quantitative Analysis of *scalloped*, *cut*, *beadex* and *bifid*

1. Confirm the utility of the Chandler et al. (2017) phenomenological model and discern whether background dependence is predictable at the allelic level
2. Determine whether the pattern of background dependence is specific to individual alleles, or is correlated in alleles of the same gene, or genes with common phenotypic effects.
3. Assess the relationship between background dependence among strains, and intraline variance, in effect to understand the contribution of genetic and environmental effects.

Knockdown of *scalloped* and *vestigial* with nubbin-Gal4 driver

1. Determine the relationship between reduction in gene expression and phenotype *within* each genetic background, and whether this relationship is the same for both *scalloped* and *vestigial*.
2. Determine the relationship between gene expression and phenotype *between* genetic backgrounds, and whether this relationship is consistent for *scalloped* and *vestigial* across both backgrounds.

Hypothesis

Quantitative Analysis of *scalloped*, *cut*, *beadex* and *bifid*

Consistent with the model proposed by Chandler et al. (2017), the magnitude of background dependence will be predictable given the average magnitude of phenotypic effect of a given mutant allele. Alleles with either weak or severe magnitudes of phenotypic effects will demonstrate limited background dependence, indicated by the reduced phenotypic variance in wing size among DGRP strains. Alleles with relatively moderate phenotypic effects will be most sensitive to the effects of the genetic background.

Phenotypic Analysis of *scalloped* and *vestigial* knockdown with Nubbin-Gal4 driver

Wildtype strains differ with respect to mutational robustness and wild type gene activity

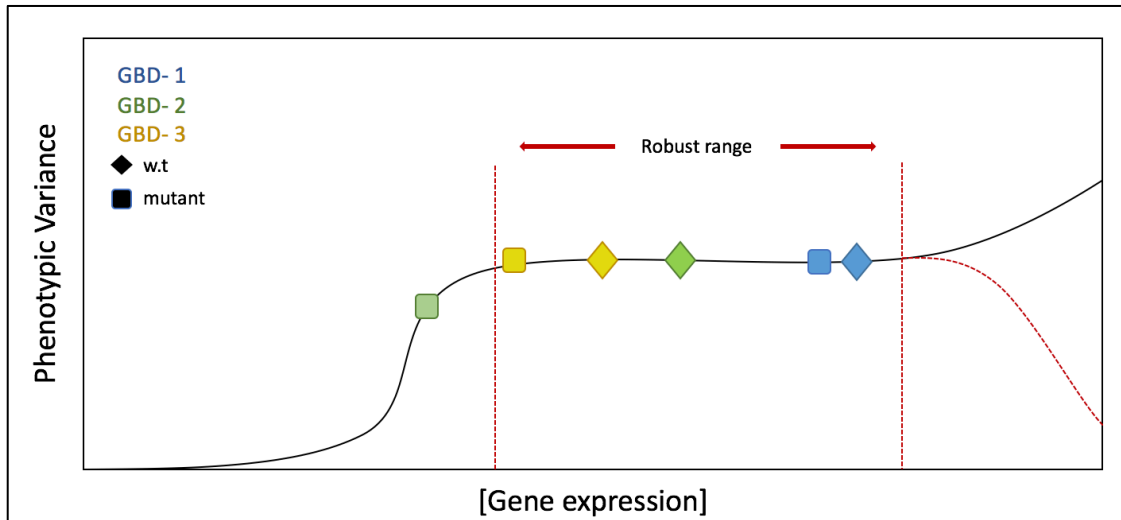


Figure 1.2: Each wild-type strain starts with a different amount of gene activity that is sufficient to produce the wild type phenotype (the robust range). A hypomorphic mutant allele behaves differently in each genetic background (GBD) reducing gene activity unequally between strains. See supplemental figures for other potential models (Supplemental Figures 3-5).

2.0 Methods

Experimental Methods

Table 2.1: Summary of *beadex* and *cut* mutant alleles. All alleles on the X-chromosome.

Allele	Allele Class	Mutagen	DNA Lesion	Description of Allele	Reference
<i>bx[1]</i>	Weak, dominant	Spontaneous	Ro- element is inserted into the 3' region of the UTR.	Hypermorph. Hemizygotes show loss of the posterior wing margin.	(Bejarano, Smibert, & Lai, 2010)
<i>bx[2]</i>	Weak-moderate, dominant	Spontaneous	Gypsy- element is inserted into the 3' region of the UTR.	Hypermorph. Hemizygous males wings are excised along both margins. Heterozygous females display weaker phenotype, overlaps with wildtype. Some venation defects.	Shoresh et al., 1998 & Rabinow et al., 1993
<i>bx[3]</i>	Moderate, dominant	Spontaneous	Ro- element is inserted into the 3' region of the UTR.	Hypermorph. Hemizygous males wings are long, narrow and excised along both margins. Heterozygous females display weaker phenotype, overlaps with wildtype. Some venation defects.	Shoresh et al., 1998 & Rabinow et al., 1993
<i>ct[6]</i>	Moderate, recessive	Spontaneous	Insertion of a gypsy element between the <i>ct</i> promoter and a distal wing-margin enhancer. Polytene chromosomes normal.	Hypomorph. Hemizygous males show reduction in margin tissue in distal and posterior regions of the wing.	Cai and Levine, 1997) & Johnson and Judd, 1979)
<i>ct[k]</i>	Severe, recessive	Spontaneous	Insertion of gypsy element 6kb upstream of the 5'-most identified exon, in orientation opposite to that of <i>cut</i>	Hypomorph. Partially lethal, reduced viability. Viable hemizygous males show weak reduction in wing tissue at posterior region of the wing.	Hoover et al., 1992) & Johnson and Judd, 1979)

Table 2.2: Summary of *scalloped* mutant alleles. All alleles on the X-chromosome.

Allele	Allele Class	Mutagen	DNA Lesion	Description of Allele	Reference
<i>sd[29.1]</i>	Weak, recessive	Transposable element insertion	insertion in the first large intron after the translational start site, close to the 5' splice site.	Hypomorph. Hemizygous males show minor loss of the posterior wing margin. Incompletely penetrant.	Shyamala and Chopra, 1999.
<i>sd[1]</i>	Weak, recessive	X-Ray	Cytogenetically normal (no rearrangements in the <i>scalloped</i> region detected).	Hypomorph. Hemizygous males have scalloped wing margins thickened wing veins, as well as ectopic bristles on the wing blade. Does not overlap wild-type.	Campbell et al., 1991 & Chandler et al. 2017.
<i>sd[ETX4]</i>	Moderate, recessive	Transposable element insertion	P-element insertion in the first intron, approximately 400bp upstream of the translation site.	Hypomorph. Hemizygous males show nicking of the anterior and lateral margins of the wing blade.	Campbell et al. 1992 & Chandler et al. 2017
<i>sd[E3]</i>	Moderate, recessive	Transposable element insertion	P-element insertion in an intron, approximately 5kb downstream of the transcription start site.	Hypomorph. Hemizygous males have heavily scalloped wings.	Campbell et al., 1991, Inamdar et al. 1993 & Chandler et al. 2017
<i>sd[58d]</i>	Severe (viable), recessive	Gamma Ray	Gamma ray induced.	Hypomorph. Hemizygous males have strong reduction in wing tissue.	Campbell et al., 1991, Chandler et al. 2017
<i>sd[G0309]</i>	Severe (mostly lethal), recessive	Transposable element insertion	P-element in intron 7 of sd-RA transcript.	Hypomorph. Hemizygous lethal (except in rare circumstance). Heterozygotes appear wildtype.	Inamdar et al. 1993 & Chandler et. al 2017
<i>sd[G0239]</i>	Severe (mostly lethal, recessive)	Transposable element insertion	P-element insertion not mapped.	Hypomorph. Hemizygous lethal (except in rare circumstance). Heterozygotes appear wildtype.	Inamdar et al. 1993 & Chandler et. al 2017
<i>sd[G0483]</i>	Severe (mostly lethal, recessive)	Transposable element insertion	P-element insertion predicted to be inserted in the 3' UTR.	Hypomorph. Hemizygous lethal (except in rare circumstance). Heterozygotes appear wildtype.	Inamdar et al. 1993 & Chandler et. al 2017

Table 2.3: Summary of *Beadex* and *cut* mutant alleles. All alleles on the X-chromosome.

Allele	Allele Class	Mutagen	DNA Lesion	Description of Allele	Reference
<i>bi[1]</i>	Weak, Recessive	Spontaneous	Insertion into the first intro of the <i>bifid</i> gene.	Hypomorph. Hemizygous males have. The proximal longitudinal veins in the hinge region are fused. Phenotype is temperature sensitive. Wing size is slightly reduced.	(Shen, Dorner, Bahlo, & Pflugfelder, 2008)
<i>bi[QD]</i>	Weak, dominant	X ray	Unknown	Hypermorph. Hemizygous males exhibit wing venation defects.	(Kopp & Duncan, 1997)
<i>bi[GAL4]</i>	Weak, Recessive	P-element insertion	Enhancer trap	Hypomorph. Hemizygous males have weak delta-like venation defects	(Dworkin & Gibson, 2006)
<i>bi[md653]</i>	Weak, Recessive	P-element insertion	Enhancer trap	Hypomorph. Hemizygous males have weak venation defects	(Apidianakis, Nagel, Chalkiadaki, Preiss, & Delidakis, 1999)

Backcrossing of mutant alleles with P-element mini-white insertions

Virgin females heterozygous for the transgene insertion were repeatedly backcrossed to males of the Oregon-R strain for at least 10 generations, to allow for recombination on the autosomes, and introgression of the insertion into the Oregon-R background. Oregon-R is a standard laboratory strain marked with a *white* (w^-) eye marker. As such, backcrossing virgin females heterozygous for the mutation/transgene into Oregon-R were easily traced by their P-element mini-*white* insertion, which partially rescues eye color. Females with *white* eyes were discarded.

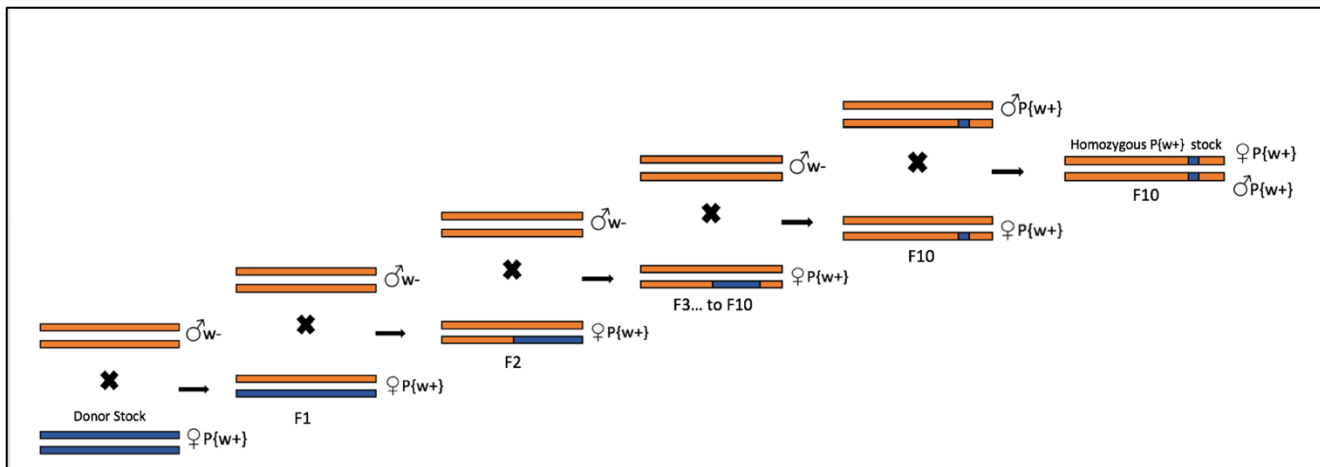


Figure 2.1: The crossing scheme for transgenic stocks carrying a P-element insertion.

Donor stocks with the target mutation or transgene are backcrossed to the desired strain for 10 generations, replacing most of the genome via recombination in female progeny. The target mutation/transgene was retained and traced by the mini-*white* p-element insertion during backcrossing into the Oregon-R (with w^-) strain.

Backcrossing of mutant alleles without P-element mini-white insertions

The remaining mutant alleles without a visible P-element mini-*white* eye marker associated with the mutant allele were all X-chromosome mutants. The mutant allele was retained instead during backcrossing by the mutant wing phenotype. Since the wing phenotypes of these alleles is only apparent in hemizygous males and homozygous females, backcrossing of these alleles into the Oregon-R background required altering the selection of either males with the mutant X-chromosome and heterozygous females every other generation. Since recombination only occurs in females, recombination events only occurred every other generation. To account for this limitation, balancer mediated replacement of the second and third chromosome was performed (Figure 2.2).

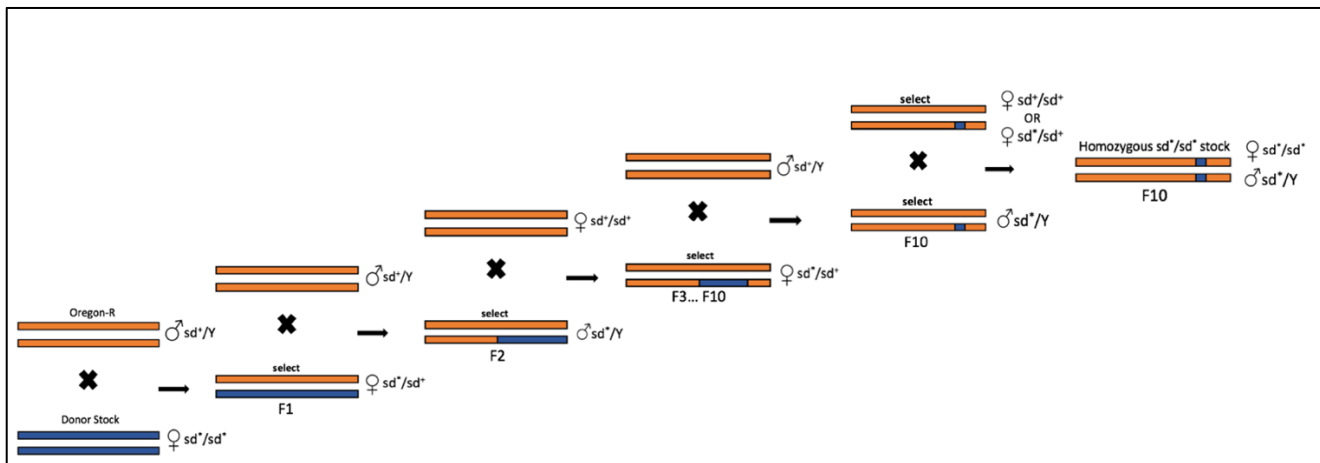


Figure 2.2: The crossing scheme for X-chromosome mutant stocks without a P-element mini-*white* insertion. Donor stocks with the target mutation were backcrossed to the Oregon-R strain for 10 generations, alternating selection of the mutant allele in either heterozygous females or hemizygous males. Introgression occurs only in heterozygous females.

Balancer mediated chromosome replacement of X-chromosomes and autosomes

The X-chromosome mutant stock without a P-element mini-white insertion (donor stock) was backcrossed to the Oregon-R strain for 10 generations, alternating selection of the mutant allele in either heterozygous females or hemizygous males, while simultaneously replacing the donor autosomes with Oregon-R autosomes using balancer mediated chromosome replacement. A similar or simpler design can be used to do balancer mediated chromosome replacement for mutant alleles or transgenes on the autosome, or in stocks with mini-*white* insertions.

Crossing scheme for F1 Oregon-R: DGRP mutants

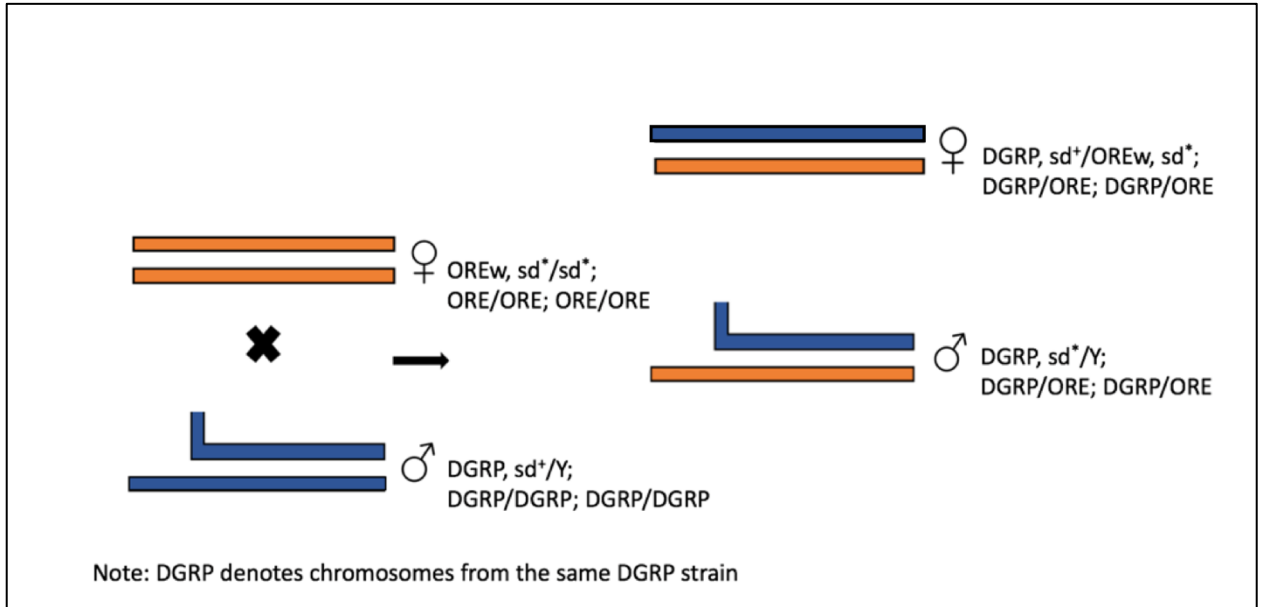


Figure 2.3: The crossing scheme to generate F1 male progeny hemizygous for the mutant Oregon-R X-chromosome. Females from the inbred homozygous Oregon-R stock for the mutant X-chromosome were crossed to males of the inbred homozygous DGRP strain. F1 progeny were either hemizygous for the mutant X-chromosome or heterozygous for the Oregon-R mutant X-chromosome and the DGRP wildtype X-chromosome. All F1 (from a given cross) were otherwise genetically identical and heterozygous on the autosomes for Oregon-R and unique DGRP strain.

Methods to titrate gene expression in *Drosophila*

There are a very proficient tools available in *Drosophila* to manipulate and study the dynamics of gene expression. Perhaps the most valuable is the bipartite UAS/GAL4 system, which can be used to drive tissue specific, temporal manipulation of a gene of interest, including expression knock down with *RNA interference (RNAi)* (Duffy, 2002). This UAS/GAL4 system is temperature sensitive; rearing developing flies at higher temperatures enhances the activity of *RNAi* by the UAS/GAL4 (Fortier & Belote, 2000). As such, it is also a useful tool to titrate the gene expression. Shifting developing embryos, larvae or pupae to alternate temperatures also provides an opportunity to exploit the temperature sensitivity of the UAS/GAL4 system to restrict or enhance the effects of the *RNAi* to desired critical periods of development (Fortier & Belote, 2000). An alternative means of titrating gene expression in *Drosophila* is through the use of loss or gain of function mutant alleles that cause perturbation to gene activity with varying degrees of severity. Selective crossing to combine mutant or wildtype alleles in allelic series can be used to create heterozygotes or trans-heterozygotes that differ along a spectrum with respect to gene activity (Green et al., 2017). Choosing one of these approaches to titrating *Drosophila* gene expression requires thoughtful consideration, as these methods may have different phenotypic consequences. There is evidence in many eukaryotic systems the compensation mechanisms to genetic perturbation through mutation and *RNAi* are different (Rossi et al., 2015). While effects of mutation have been

shown to trigger dosage compensation responses upstream of protein function, observation of these effects are limited in knockdown approaches (Rossi et al., 2015).

Crossing scheme for *scalloped* and *vestigial* knockdowns

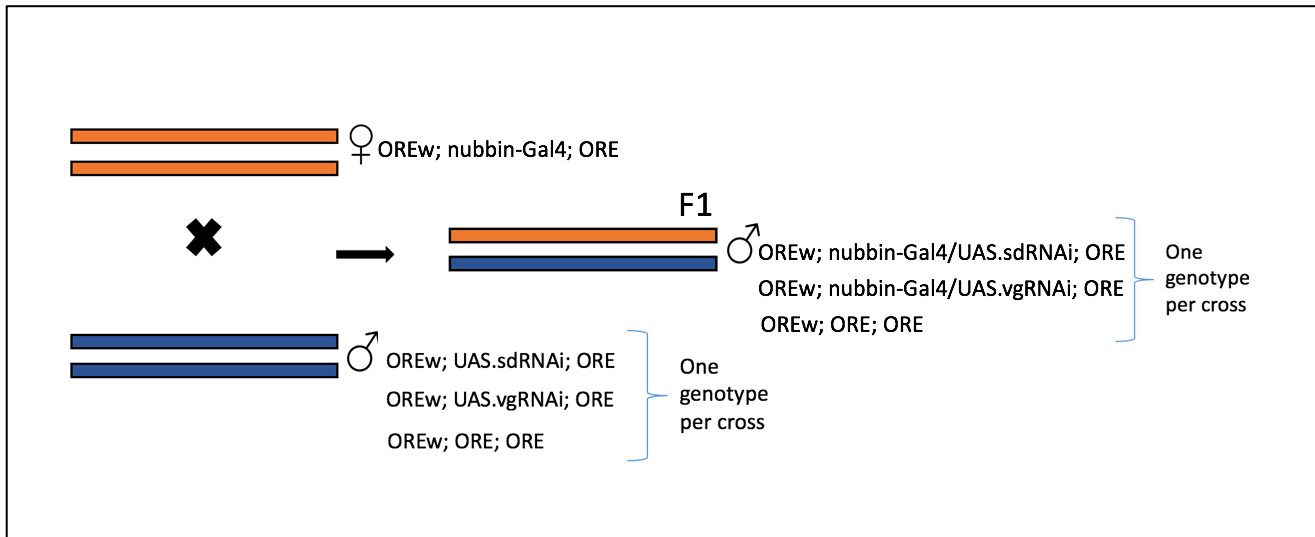


Figure 1: Crossing scheme to generate F1 knockdowns of *scalloped*, *vestigial* and the genetic control. Virgin females homozygous for the GAL4 transgene of either the Oregon-R or Samarkand strain were crossed to males homozygous for the *scalloped* RNAi construct, *vestigial* RNAi construct or wildtype.

Rearing Environment of *scalloped* and *vestigial* knockdowns

All experimental crosses were set with virgin females and males of the same age (<7 days). Parental flies were introduced at 24 degrees for 1 day before they were transferred on experimental vials. For experimental vials, parental flies were left to lay eggs in 12 hour intervals (replicate one). This was in effort to coarsely control for larval

density and age. After 12 hours, water and paper towel was added to the vials to control for moisture and provide a substrate for pupation. At the same time, eggs were distributed to their indicated temperature and parental were transferred to a new vial (replicate two). Flies remained at their indicated temperature regime until post-eclosion.

Table 2.5: Experimental Crosses of *scalloped* and *vestigial* knockdowns.

Female Parent	Male Parent	Rearing Temperatures	Replicate vials
ORE; nubbin-GAL4; ORE	OREw; UAS-sd.RNAi; ORE	16, 18, 22, 24, 29	2
ORE; nubbin-GAL4; ORE	OREw; UAS-vg.RNAi; ORE	16, 18, 22, 24, 29	2
ORE; nubbin-GAL4; ORE	OREw; ORE; ORE	16, 18, 22, 24, 29	2
OREw; ORE; ORE	OREw; ORE; ORE	16, 18, 22, 24, 29	2
SAMw; nubbin-GAL4; SAM	SAMw; UAS-sd.RNAi; SAM	16, 18, 22, 24, 29	2
SAMw; nubbin-GAL4; SAM	SAMw; UAS-vg.RNAi; SAM	16, 18, 22, 24, 29	2
SAMw; nubbin-GAL4; SAM	SAMw; SAM; SAM	16, 18, 22, 24, 29	2
SAMw; SAM; SAM	SAMw; SAM; SAM	16, 18, 22, 24, 29	2

General Methods

Fly rearing and collections

Unless stated otherwise, all flies were reared at 24°C in a Percival incubator (RH ~ 60%) on a 12:12 hour day:night cycle. All flies were reared on Dworkin lab standard media recipe (cornmeal-molasses-yeast based, with Carageenan as a gelling agent) (Supplemental figure 6). Once flies from crosses emerged, progeny were collected post-eclosion and post-wing expansion (typically 12-24 hours after eclosion) with standard CO₂ procedures. Collections of F1 hemizygous males continued until the 20th day after

the cross was set, to prevent accidental collection of F2 progeny. Flies were stored by genotype in 70% ethanol until wing dissections were completed.

Wing Dissections & Imaging

Once flies were sorted by genotype and sex, the left wing of each fly was dissected and mounted onto a standard microscope slide in 70% glycerol and 30% PBS using standard dissection procedures. Once dissected, wings were imaged using an Olympus BX43 microscope with a 4X objective (total 40X magnification), and images were generated with an Olympus DP80 camera using cellSens Standard (V1.14) software. Image resolution was 4080 x 3072 pixels. Wing area was computed from images using a custom ImageJ (version 1.52a) macro.

Semi-quantitative scale

Two separate scoring systems were created to measure the degree of perturbation in the wing; one for *scalloped* and the other for *bifid (omb)* mutant alleles. Each scoring system was comprised of a series of images that capture the range of phenotypic variation among alleles of the same gene. Each image corresponds to a wing score. Scoring of all samples within one gene was done by the same experimenter, to prevent scoring bias. Higher scores indicate increasing severity of the perturbation, relative to a score of zero for a wildtype phenotype (Supplemental Figure 2).

Experimental Design and Statistical Methods

Randomized blocking design for the DGRP

A randomized blocking design was implemented for the experimental crosses of the *scalloped* alleles to the DGRP strains to account for any variability that could occur throughout the time it took to set up all 1022 crosses. Given that these mutant phenotypes are sensitive to sources of external variation (Chandler et al., 2017), strategically arranging the crossing scheme to include both consistency (among subgroups) and randomization (among blocks) provides an opportunity to observe and account for any external sources of variation that may influence phenotypic variation in wing size during analysis.

Each DGRP strain was randomly assigned to a subgroup with 10 other strains, indicated in coloured columns (Figure). Two subgroups (coloured blocks) were strategically put together over the course of all eight blocks, such that the 10 DGRP strains in each subgroup always stayed together, but were included with a different subgroup in different blocks. Each DGRP/mutant cross was represented in at least two independent biological replicates over the course of all blocks. However, in some circumstances, a cross that failed for one or more mutant/DGRP combinations in the prior block was included in the next. Consequently, some combinations of mutant allele/DGRP are represented in more than two blocks or more than two biological replicates.

The randomized block design for the *scalloped*: DGRP crosses

Block 1		Block 2		Block 3		Block 4	
21	45	129	195	319	391	502	843
26	48	158	208	348	392	508	894
28	57	177	217	354	395	517	897
31	69	195	228	367	399	596	900
32	73	208	229	371	427	703	907
35	75	217	235	373	437	757	908
38	83	228	239	375	439	765	911
40	85	129	301	379	443	774	913
41	88	158	307	385	491	799	
42	91	177	315	390	492	808	
Block 5		Block 6		Block 7		Block 8	
319	129	391	21	195	45	502	843
348	158	392	26	208	48	508	894
354	177	395	28	217	57	517	897
367	195	399	31	228	69	596	900
371	208	427	32	229	73	703	907
373	217	437	35	235	75	757	908
375	228	439	38	239	83	765	911
379	129	443	40	301	85	774	913
385	158	491	41	307	88	799	
390	177	492	42	315	91	808	

Figure 2.5: The experimental design with randomized blocks. Each number represents a unique DGRP strain (i.e. DGRP 021). Each colored column represents a subgroup. Over the course of eight blocks, each subgroup was represented twice and grouped with two distinct subgroups. Each *scalloped* mutant allele was crossed to every DGRP lines in at least two independent biological replicates.

Quantitative analysis of *scalloped*, *cut*, *beadex* and *bifid* wing size

One aim of this study was to confirm if the phenotypic severity a mutant allele predicts sensitivity to background dependence. To understand this, the phenotypes of many alleles in the *Drosophila* wing regulatory network, in the genes *scalloped*, *beadex*, *cut* and *bifid* (*omb*), were examined with crosses to DGRP strains. Alleles of the *scalloped* gene were crossed to 73 unique DGRP strains over the course of eight randomized blocks. Across all blocks, each mutant by DGRP combination is represented in at least

two biological replicates represented by 6-20 individual samples. In two separate experiments, undergraduate students (Ana Vera-Cruz and Abood Abubakr) examined the alleles of *cut*, *beadex* and *bifid (omb)*. These alleles were phenotyped in 20 DGRP strains (a subset of those included in the study with the *scalloped* alleles), in two biological replicates across two temporally separated blocks. Alleles of *cut*, *beadex*, and *bifid (omb)* are represented by five individuals for each cross.

Linear mixed models

In the DGRP experiments, the linear mixed models were fit with wing area or wing score were the response variable. For the predictors, mutant alleles were fit as a fixed effect, while effects for DGRP (allowing allele specific variation for each DGRP, i.e. a “random slopes” model) and block were included as random effects. Models were fit using the `lmer()` and `glmer()` functions from the `lme4` library (V1.1-21). For Levene’s statistics (see below) where values are small, and forced to be positive, a generalized linear mixed model with an inverse link function and with data assumed to following a Gamma distribution was used. However, given that a gamma distribution cannot handle 0s, a very small positive value (0.0001) was added to all values of Levene’s Statistic to enable proper fitting. For the RNAi data, background (strain), temperature and genotype were modeled as fixed effects with interaction terms, as interaction between these three predictor variables were of primary interests. The effect of replicate vial was modelled as a nested random effect with background, temperature and genotype, which

just distinguishes each replicate vial from each other, as each biological replicate was of a specific strain, temperature and genotype.

For our statistical model examining the relationship between deviation of a mutant from its wild type, model based deviations were treated as a continuous predictor, and mutant *sd* allele and their interactions were all modeled. A random effect for DGRP was included to account for non-independence of observations.

Confidence intervals for all effects across studies were generated using the lme4 and emmeans libraries (1.4.2) in R (3.6.1).

Calculating broad sense heritability (H^2)

Broad sense heritability is an estimate typically used in quantitative genetics to estimate the heritable components of phenotypic variation for a trait. This measure is classically used to separate out the contribution of both additive and non-additive genetic effects to phenotypic variance from any contributing effects of the environment (Gonçalves, Carrasquinho, St. Aubyn, & Martins, 2013). However, the nature of this estimate also makes it a useful measure to determine how much genetic and environmental effects contribute to quantitative trait variation, even under laboratory conditions. Estimating broad sense heritability is possible in this dataset because the randomized blocking design allowed separation of environmental and genetic effects. This value is calculated through the following equation:

$H^2 = \text{Total Genetic Variance } (V_G) / \text{Phenotypic Variance } (V_p)$, where:

$V_G = \text{Additive Variance } (V_a) + \text{Dominance Variance } (V_A) + \text{Epistatic Variance } (V_e)$

$V_P = V_G + \text{Environmental Variance } (V_E)$

H^2 is calculated using output estimates of the variance components from the mixed linear models (Tables 3.1-3.3). Although a useful measure to distinguish additive and non-additive genetic effects, the experimental design of this dataset cannot provide information about narrow sense heritability. This is because all progeny from the cross are genetically identical. As such, any differences in phenotype within a given genotype will solely be the result of environmental effects.

Levene's statistic as a measure of within genotype variability (environmental sensitivity)

The introduction of mutations with large effects often not only influences the mean of traits, but the amount of phenotypic variation observed among otherwise genetically identical individuals (environmental variance or sensitivity). However, because of the common scaling relationship between means and variances, standard estimators of dispersion such as variance and standard deviation may be problematic, and a measure of relative variation is preferred. The coefficient of variation is a common measuring of relative variability, however the nature of it being a ratio (standard deviation over the mean) makes it difficult to conduct statistical inferences

with (Schultz, 1985; Dworkin, 2005). Levene's statistic is a preferred statistic for inferential use to assess any among group differences in variation within groups (Schultz, 1985). In this study, the Levene's statistic was calculated by first log transforming the data to reduce scale effects (mean variance relationship). Next, the median value was taken for each genotypic group (i.e. every mutant/DGRP combination). The arithmetic mean is also sometimes used to calculate the Levene's statistic, but the median is a more robust measure of central tendency as it is less impacted by outliers (Schultz, 1985; Dworkin, 2005). Finally, a deviation value was assigned to each sample (individual), which was calculated using the absolute value of the difference of the log transformed value of wing area for each individual, from the median of its respective genotypic group. This provides individual level deviations from their given group. Levene's Statistic was analyzed in the context of a generalized linear mixed model with an inverse link function and assuming a Gamma distribution.

Choosing lines for further analysis

After completing the first experiment with the 73 DGRP lineages, I performed a follow up experiment to both confirm the initial results and examine effects across a wider range of *sd* and *Bx* alleles simultaneously. To choose a subset of the DGRP lines for further analysis, phenotypic estimates from the quantitative and semi-quantitative data were considered. The goal of choosing these lines was to choose a suite of DGRP strains that in aggregate represented the full spectrum of phenotypic effects for all the

scalloped mutant alleles in the original dataset. This suite of DGRP strains was then used in a follow up experiment with more *scalloped* mutant alleles, including alleles *sd[29.1]* (very weak) and *sd[58d]* (very severe). Additionally, the phenotypes of *beadex* alleles *bx[1]*, *bx[2]* and *bx[3]* in this suite of DGRP strains were also analyzed.

Choosing select DGRP lines by quantitative estimates of wing size

Quantitative Scale	
very-small	<10%
small	10-25%
small-mid	25-46%
mid	46-54%
mid-large	55-75%
large	75-90%
very large	90-100%

Figure 2.6: The quantitative data was used to rank the mean wing area of each DGRP genotype relative to the other genotypes in the dataset by percentiles. These means were compared to the means of the semi-quantitative scores. Lines were selected based on similarity in both estimates, as well as the degree of phenotypic severity for each mutant allele.

Table: 2.4: DGRP lines that were chosen for further analysis. (see Figures 2.5, 2.6).

	DGRP Line		DGRP Line
1	28	11	319
2	38	12	371
3	48	13	385
4	75	14	391
5	83	15	392
6	88	16	443
7	229	17	491
8	239	18	492
9	301	19	517
10	315	20	757

3.0. Results

Quantitative estimates of wing size, variance and H^2 for *scalloped*, *cut* and *beadex*.

One aim of this study was to examine whether the magnitude of background dependence was highest for alleles with, on average, moderate phenotypic effects. Here we have examined many alleles in the *Drosophila* wing regulatory network, including *scalloped*, *beadex*, *cut* and *bifid (omb)*, across three separate studies. Mean wing size for each allele among all DGRP strains was estimated (Tables 3.1-3.3). For *scalloped*, the phenotypic range is confirmed in the mean estimates (Table 3.1). *sd[1]* has on average weaker effects than moderate phenotypic effects of *sd[e3]* and *sd[ETX4]* (Figure 3.1). Impressively, there was no recovery of any hemizygous males carrying any of the three lethal alleles, among any of the 8 blocks or 73 DGRP strains measured. Count data of the relative number of males with the wildtype X-chromosome and heterozygous females was collected for block three and four. Among both blocks, 6342 females and 3418 males were counted. Although count data was not collected in other blocks, this illustrates despite thousands of flies scored among all eight blocks, none of the genetic variation among the panel of DGRP was sufficient to overcome the lethal effects of these mutations.

For *beadex*, mean estimates illustrate the weak and moderate effects of *bx[1]* and *bx[3]*, and an intermediary effect of *bx[2]* (Figure 3.2). Mean estimates of the *cut* allele revealed both alleles have relatively weak phenotypic effects (Figure 3.2). In all cases, mutant effects significantly affected wing size estimates. However, estimates

for mean wing size among the *bifid (omb)* alleles were not statistically different from one another (Figure not shown). A notable trend among these estimates is *scalloped* alleles used in this study have a much bigger effect on wing size, relative to the other mutations.

The magnitude of phenotypic variance among DGRP strains for all alleles was measured by model adjusted estimates of variance (Tables 3.1-3.3). These estimates indicate the phenotypic variance among moderate *scalloped* alleles was dramatically increased, relative to *sd[1]* and the control (Figure 3.4). Yet among *beadex*, *cut* and *bifid (omb)* alleles, the magnitude of phenotypic variance was largely similar among alleles of the same gene (Figures 3.5-3.7). Crossing lines in Figures 3.4-3.7 indicate a reordering of alleles with respect to their phenotypic effect, illustrating the rank phenotypic effects of mutant alleles is not fixed.

After accounting for sources of environmental influence (i.e. block and residual variance), estimates of broad sense heritability (H^2) distinguished how much phenotypic variance for each allele can be attributed to allelic variation among DGRP strains (Tables 3.1-3.3). Strikingly, heritability estimates were very high among the moderate effect alleles, indicating allelic variation among DGRP strains explains more phenotypic variance than any environmental effects (Table 3.1). In contrast, heritability estimates among alleles of the other *beadex*, and *cut* were much more modest. This may reflect a reduced phenotypic range among alleles, relative to the allelic series of *scalloped*. This discrepancy may also be due to low sample sizes

among *beadex* and *cut* alleles (five individuals per cross), and a reduced number of DGRP strains analyzed. Consequently, the statistical power used to estimate these effects is reduced compared to *scalloped* alleles.

Table 3.1: The statistical model estimates of the *scalloped* alleles. N = 11164. ANOVA analysis: Mutant, P= 2.2^{-16}. In this table and below, the variance represents the among line (DGRP) variance for wing size (i.e. total genetic variance). The standard deviation is just the square root of this estimate.

Allele	Mean Estimate (mm ²)	Standard Error	Variance	Standard Deviation	H ²
wildtype	1.39	0.02	0.007	0.08	0.18
<i>sd</i> [1]	1.32	0.01	0.008	0.09	0.20
<i>sd</i> [E3]	0.76	0.03	0.045	0.21	0.94
<i>sd</i> [ETX4]	0.72	0.02	0.036	0.19	0.52
Block			0.003	0.06	
Residual			0.03	0.20	

Table 3.2: The statistical model estimates of the *bx* and *ct* alleles. *bx*, N=996, *ct*, N=225. ANOVA: Mutant, P= 2.2^{-16}.

Allele	Mean Estimate (mm ²)	Standard Error	Variance	Standard Deviation	H ²
wildtype	1.39	0.02	0.007	0.08	0.47
<i>Ct</i> [K]	1.37	0.02	0.006	0.08	0.43
<i>Ct</i> [6]	1.27	0.02	0.004	0.07	0.19
<i>Bx</i> [1]	1.5	0.02	0.006	0.07	0.43
<i>Bx</i> [2]	1.33	0.02	0.006	0.08	0.43
<i>Bx</i> [3]	1.16	0.02	0.006	0.08	0.43
Block			0.0001	0.01	
Residual			0.008	0.09	

Table 3.3: The statistical model estimates of *bifid* (*omb*) alleles. N=965. ANOVA: Mutant, P= 0.2033.

Allele	Mean Estimate (mm ²)	Standard Error	Variance	Standard Deviation	H ²
wildtype	1.39	0.02	0.007	0.08	0.28
<i>bi</i> [1]	1.53	0.04	0.006	0.08	0.25
<i>bi</i> [QD]	1.55	0.02	0.002	0.04	1
<i>bi</i> [GAL4]	1.54	0.02	0.002	0.04	1
<i>bi</i> [MD653]	1.58	0.02	0.003	0.05	0.14
Block			0.003	0.06	
Residual			0.015	0.12	

Average wing size of *scalloped* mutants

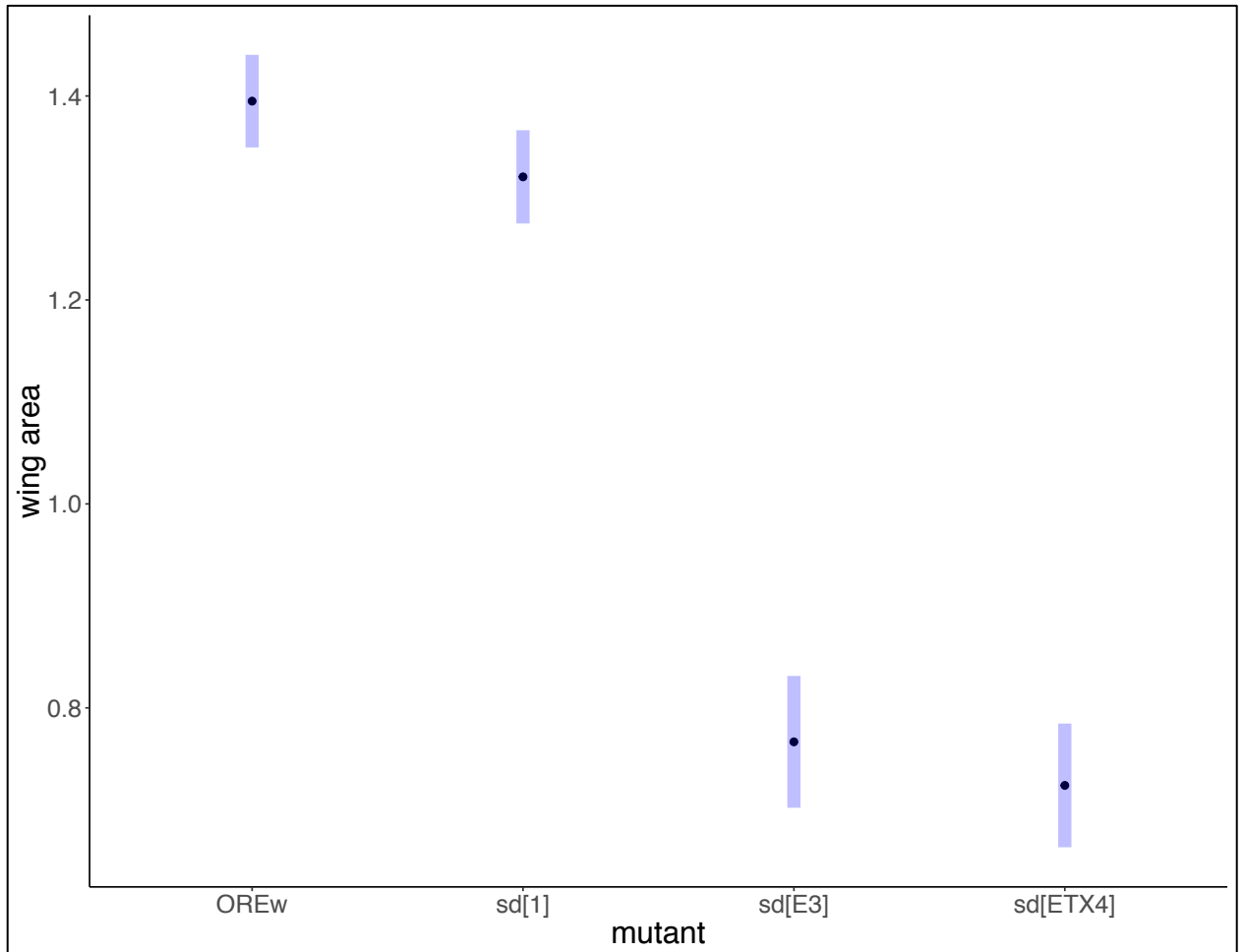


Figure 3.1: The mean phenotypic effect of each *scalloped* mutant allele averaged across 73 DGRP strains. Means reflect mixed model estimates (Table 3.1). Error bars are 95% confidence intervals (for all subsequent figures). N= 11164.

Average wing size of *cut* and *beadex* mutants alleles

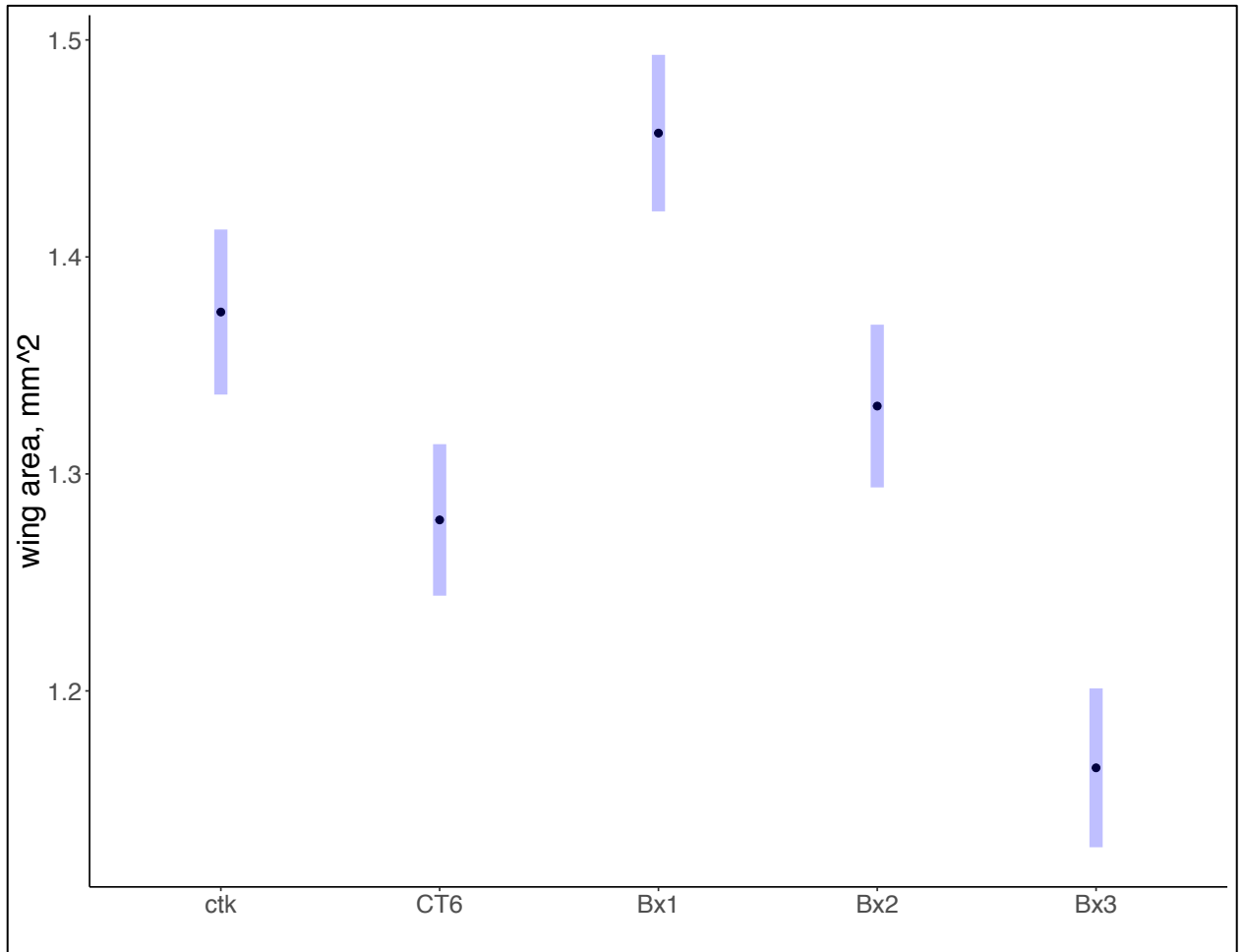


Figure 3.2: The mean phenotypic effect of each *cut* and *beadex* mutant allele in 25 DGRP strains Means reflect mixed model estimates (Table 3.2). *beadex*, N=996, *cut*, N=225.

Variation in *scalloped* wing size line means among DGRP strains

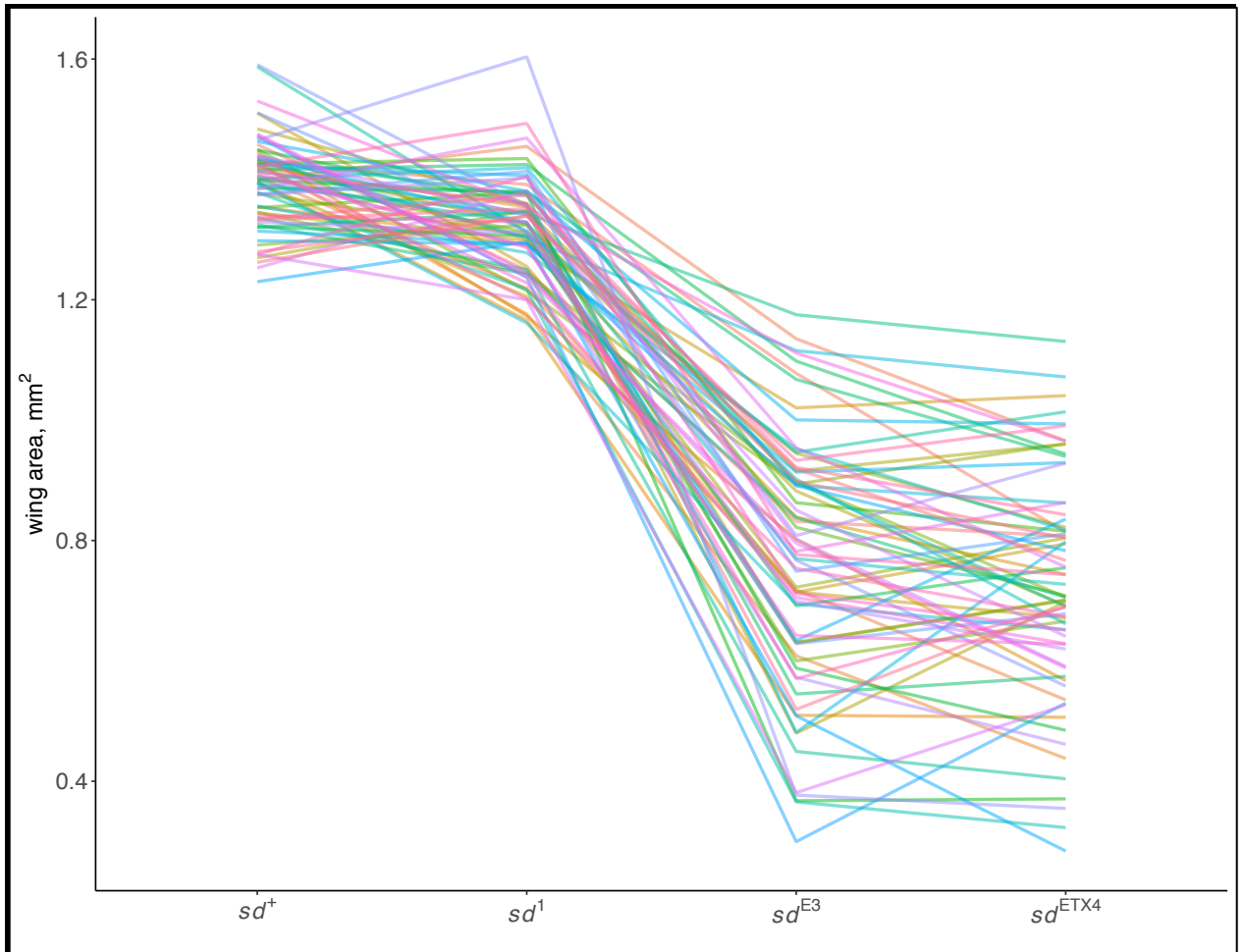


Figure 3.3: Reaction norms of *scalloped* mutant phenotypes among 73 DGRP strains.

Colours represent distinct DGRP lineages for a given *scalloped* allele. (Table 3.1). N= 11164.

Variation in *beadex* wing size line means among DGRP strains

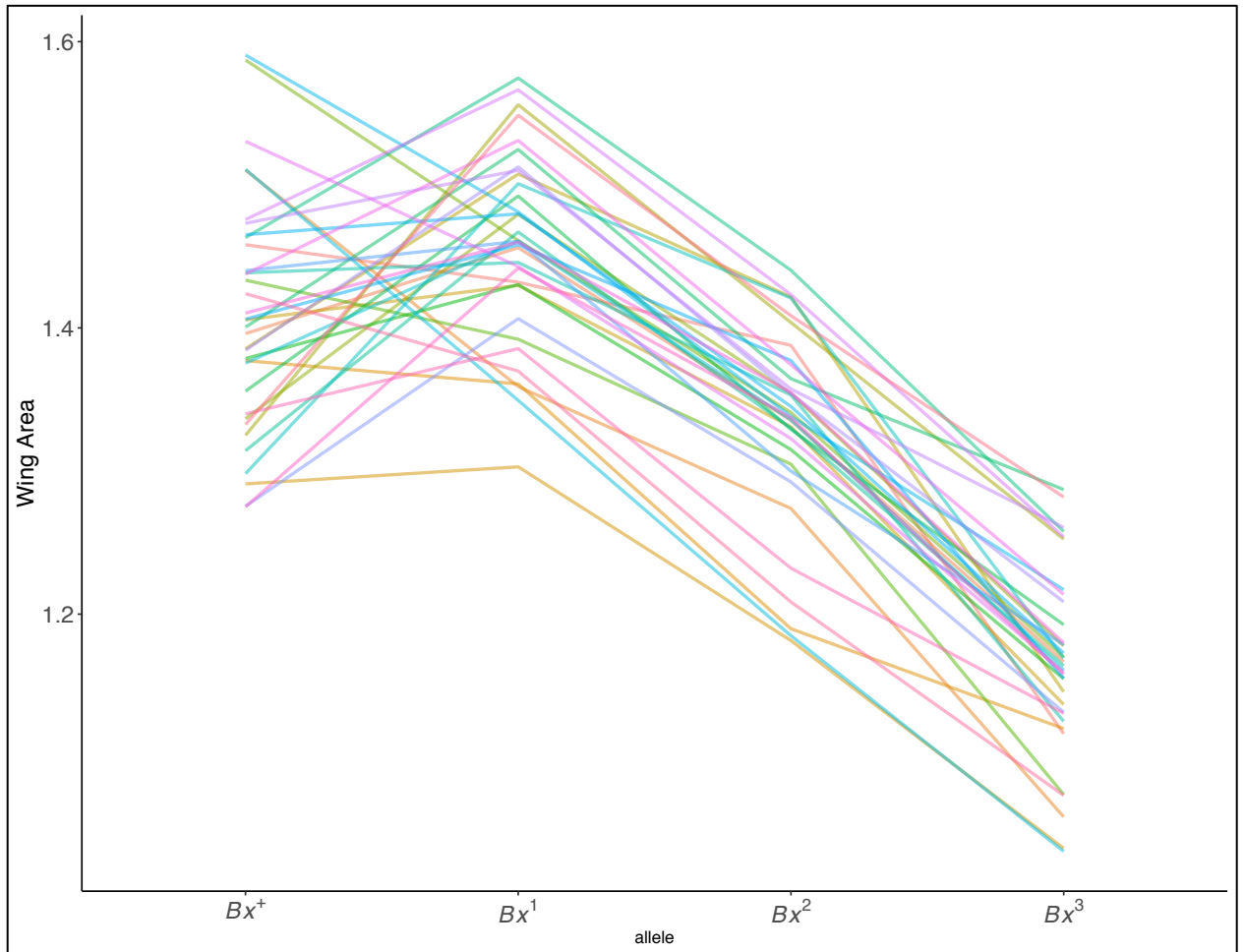


Figure 3.4: Reaction norms of *beadex* mutant phenotypes among 25 DGRP strains.

Colours represent distinct DGRP lineages for a given *Bx* allele. (Table 3.2). N=996.

Variation in *cut* wing size line means among DGRP strains

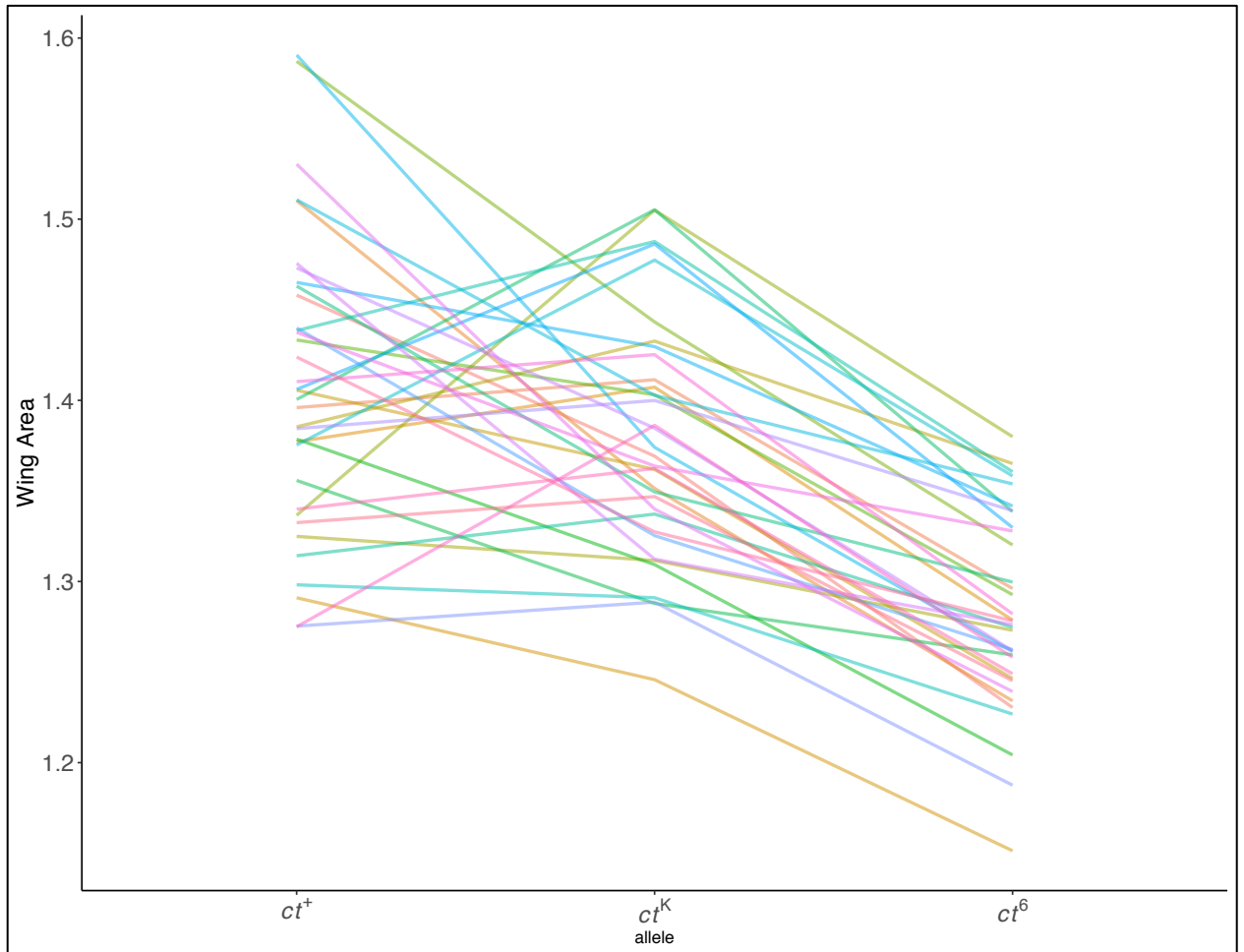


Figure 3.5: Reaction norms of *cut* mutant phenotypes among 25 DGRP strains. Colours represent distinct DGRP lineages for a given *ct* allele. (Table 3.2). N= 225.

Variation in wing size *bifid (omb)* line means among DGRP strains

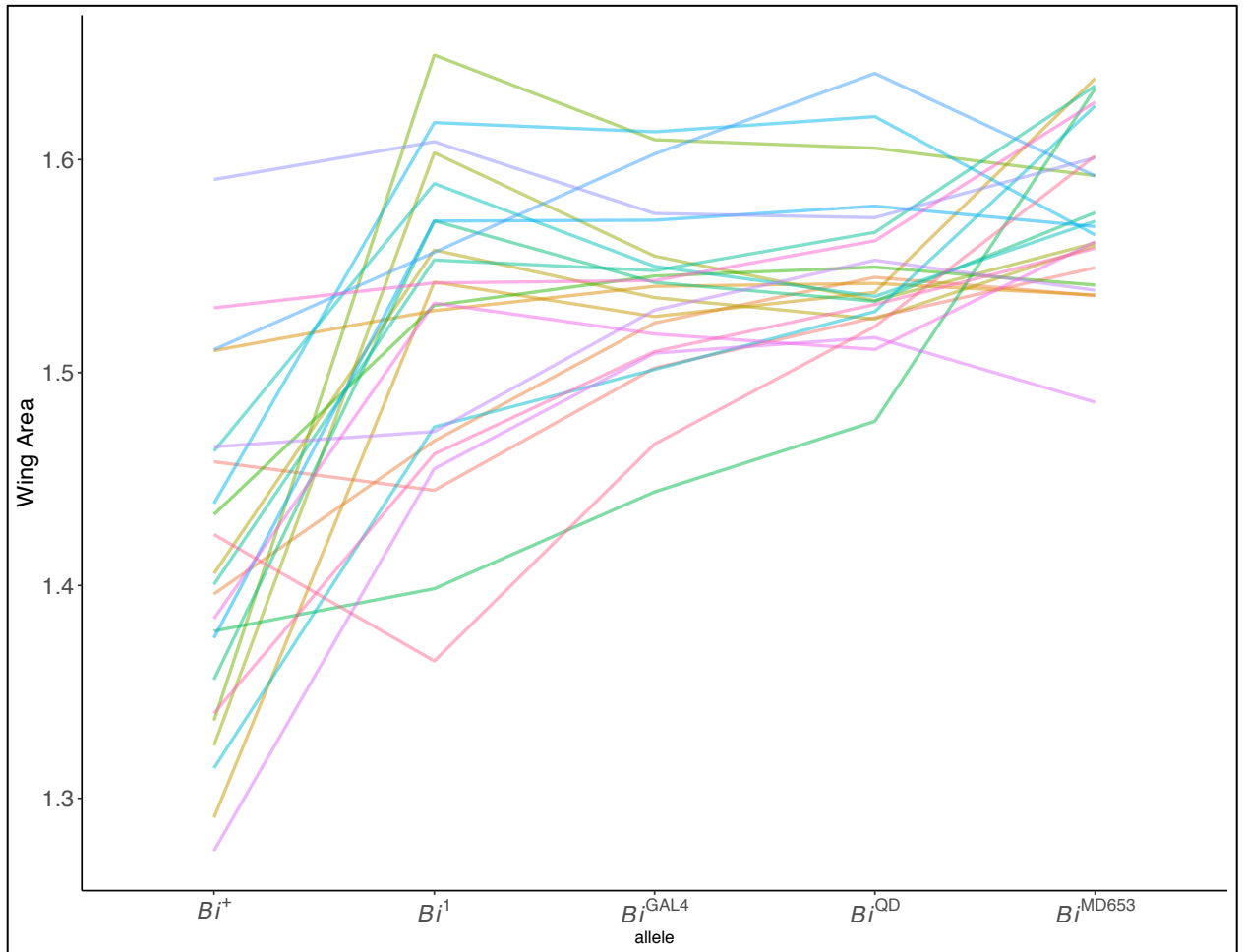


Figure 3.6: Reaction norms of *bifid (omb)* mutant phenotypes among 25 DGRP strains

Colours represent distinct DGRP lineages for a given *bifid/omb* allele. (Table 3.3). N=965.

Correlations among quantitative size estimates for *scalloped*, *cut* and *beadex*.

One central goal of this study was to examine whether the magnitude of background dependence is specific to individual alleles, similar for alleles of the same genes, or genes with similar mutant phenotypes or developmental roles. To assess this I estimated the Pearson correlation coefficient using model adjusted estimates (i.e. corrected for block effects) for background effects of alleles within and between *scalloped*, *beadex* and *cut*. Quantitative estimates for wing size in *bifid (omb)* were omitted, as there were no significant differences in wing size among the *bifid (omb)* alleles (data not shown). Among the other alleles, correlation estimates reflect model adjusted means for wing size in each DGRP line (blue dots). Correlations values between alleles indicate how similar the response to the effects of each DGRP strain are across different mutant alleles. For example, higher correlations indicate that if wings tended to be smaller for the first allele in a given DGRP strain, they tended to also be small for the contrasted allele in that same DGRP strain as well.

Significant correlations among mutant alleles of the same gene are common, and virtually all correlations are positive. For instance, in *scalloped*, size estimates in *sd[E3]* and *sd[ETX4]* are significantly correlated ($P= 0.02$) (Figure 3.9). In *beadex* (Figure 3.10), size estimates for every allele combination are significant; *bx[1]* and *bx[2]*, *bx[1]* and *bx[3]* and *bx[2]* and *bx[3]* are significantly correlated ($P= <0.001$). In *cut* (Figure 3.11), both mutant alleles (*ct[K]* and *ct[6]*), are significantly correlated ($P= <0.001$). However, alleles between distinct genes are generally less correlated (though generally positive).

Between *scalloped* and *cut*, *sd[1]* and *ct[6]* are significantly correlated ($P = <0.04$) (Figure 3.12). *sd[1]* and *ct[K]* are also significantly correlated ($P = <0.05$). Alleles of *scalloped* and *beadex* show no significant correlations with each other (Figure 3.12). Interestingly, for all genes, correlations between wild type alleles and the mutant alleles tends to be quite weak, although positive. One exception is the *ct* mutant alleles (Figure 3.11).

Correlation of mutant effects in *scalloped* wing size among DGRP strains

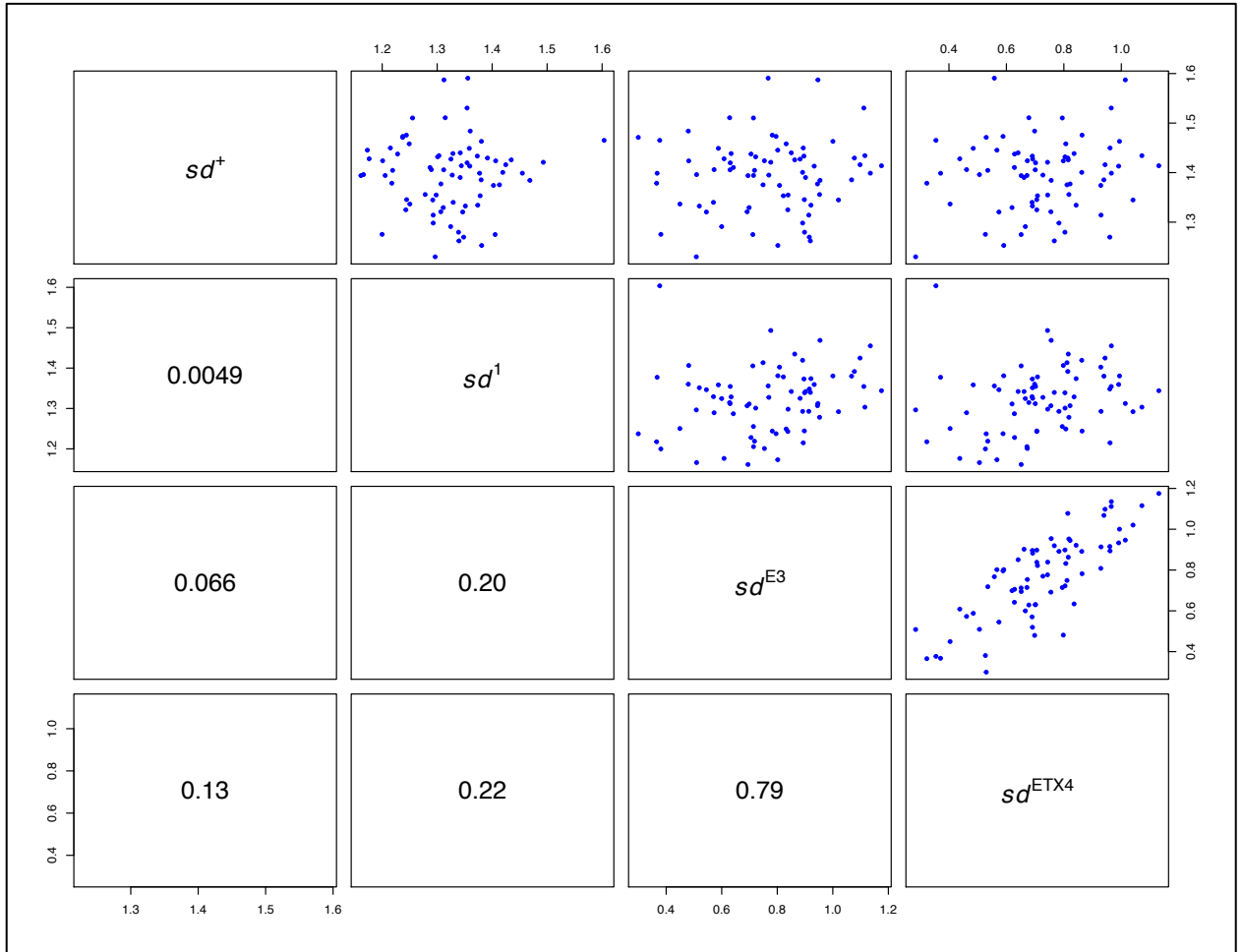


Figure 3.9: Pairwise correlations of *scalloped* mutant alleles for wing size in 73 DGRP

strains. Numerical boxes: The Pearson correlation coefficients between mutant alleles

adjacent to each numerical box. Scatter plots: Each blue dot represents the model

adjusted mean wing area for each of the 73 DGRP strains, where x and y of each plot are

the adjacent mutant alleles (Table 3.1). Correlation values reflect the R value of the

corresponding scatterplot. N= 11164. Pearson's correlation between: $sd[E3]:sd[ETX4]$, P=

0.02.

Correlation of mutant effects in *beadex* wing size among DGRP strains

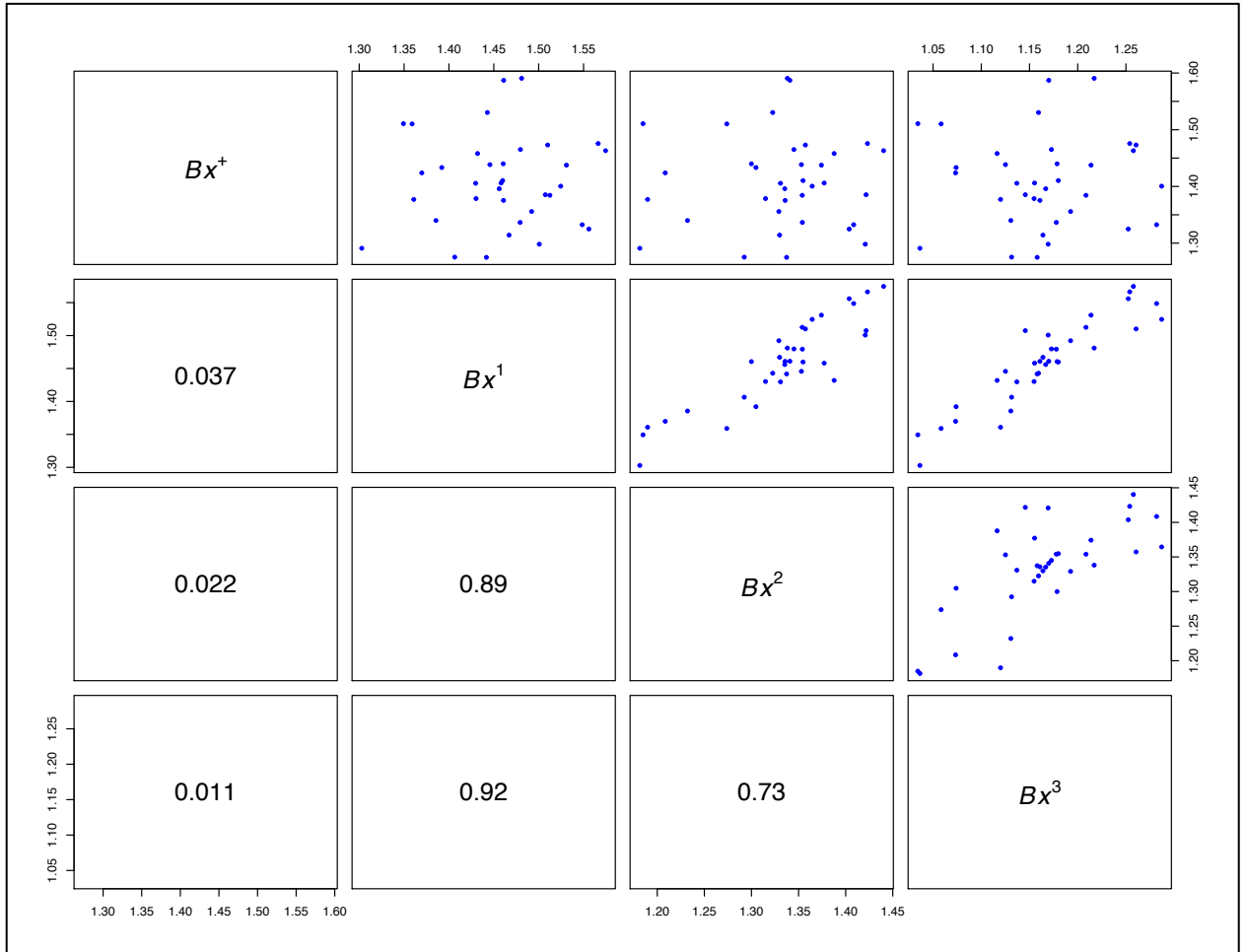


Figure 3.10: Pairwise correlation of *beadex* mutant alleles for wing size in 25 DGRP

strains. Each blue dot represents the model adjusted mean for a unique DGRP strain

(Table 3.2). N=996. Pearson's correlation between: $bx[1]:bx[2]$, $bx[1]:bx[3]$, $bx[2]:bx[3]$,

P= <0.001.

Correlation of mutant effects in *cut* wing size among DGRP strains

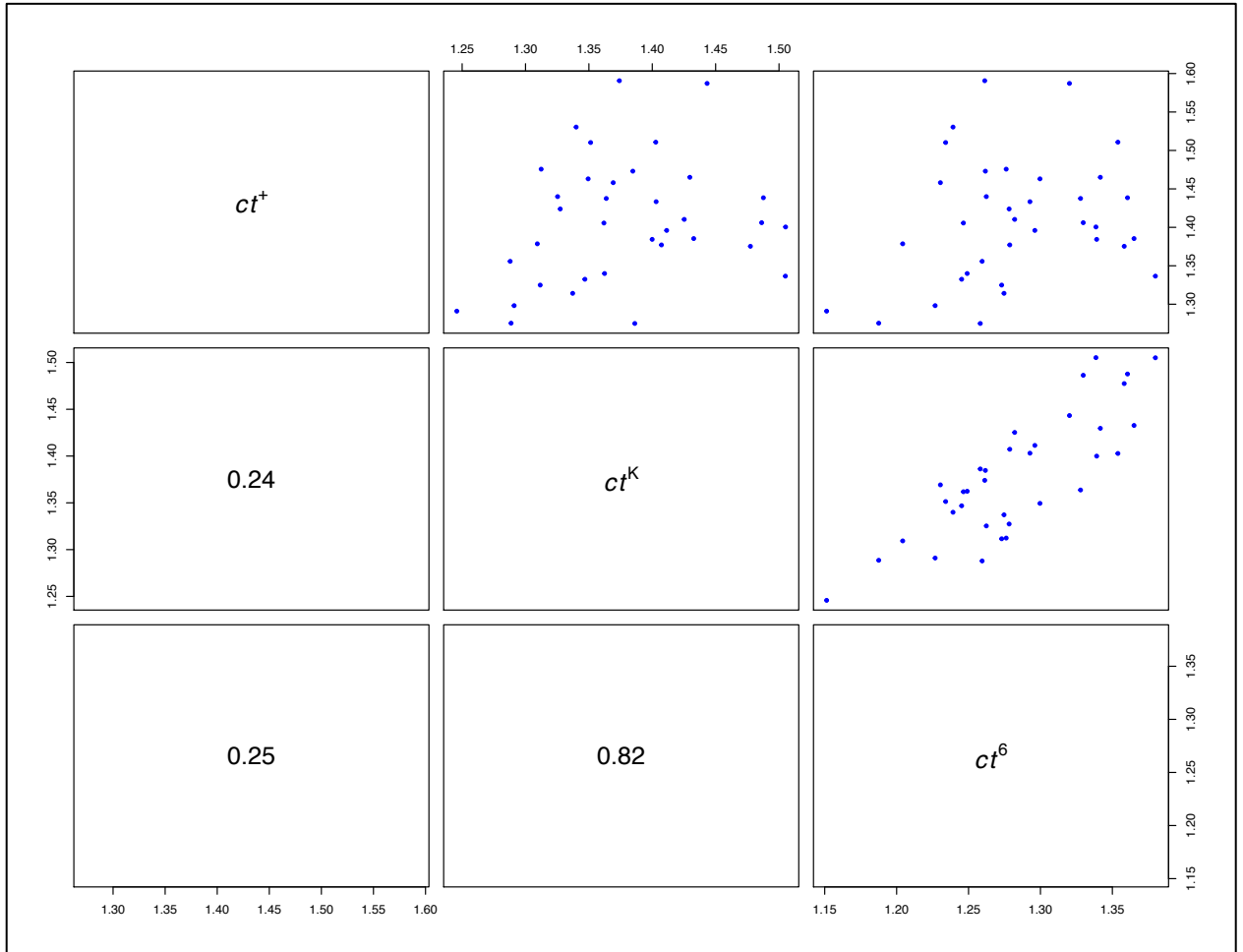


Figure 3.11: Correlation values among *cut* mutant alleles for wing size among 25 DGRP

strains. Each blue dot represents the model adjusted mean for a unique DGRP strain

(Table 3.2). N= 225. Pearson's correlation between: $ct[K]:ct[6]$, $P = <0.001$.

Correlation of mutant effects in *scalloped* and *cut* wing size among DGRP strains

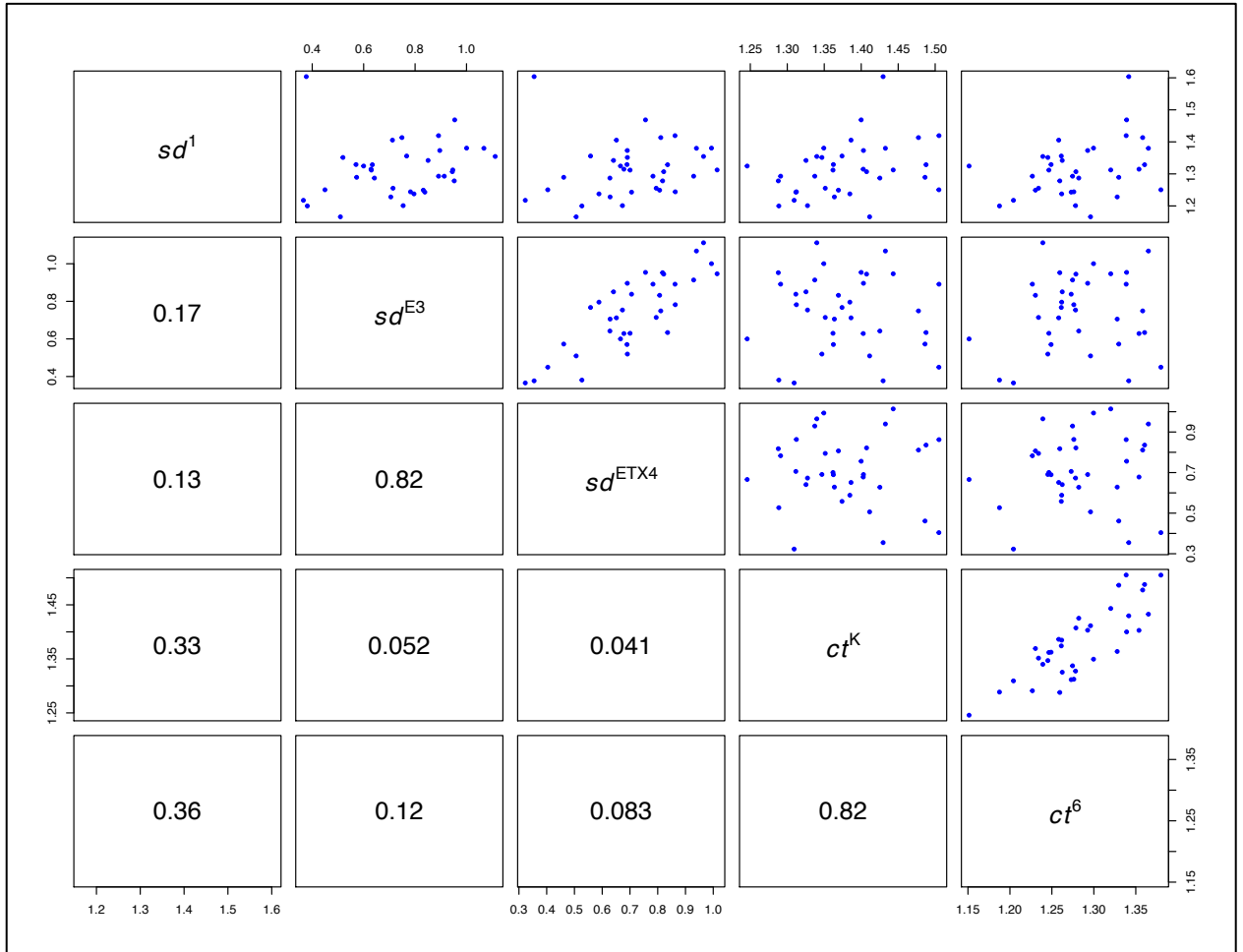


Figure 3.12: Correlation values among *cut* and *scalloped* mutant alleles for wing size

among 25 DGRP strains. Each blue dot represents the model adjusted mean for a unique

DGRP strain (Table 3.1, 3.2). Pearson's correlation between: *sd*[1]:*ct*[6], $P = < 0.04$,

sd[1]:*ct*[K], $P = < 0.05$.

Correlation of mutant effects in *scalloped* and *beadex* wing size among DGRP strains

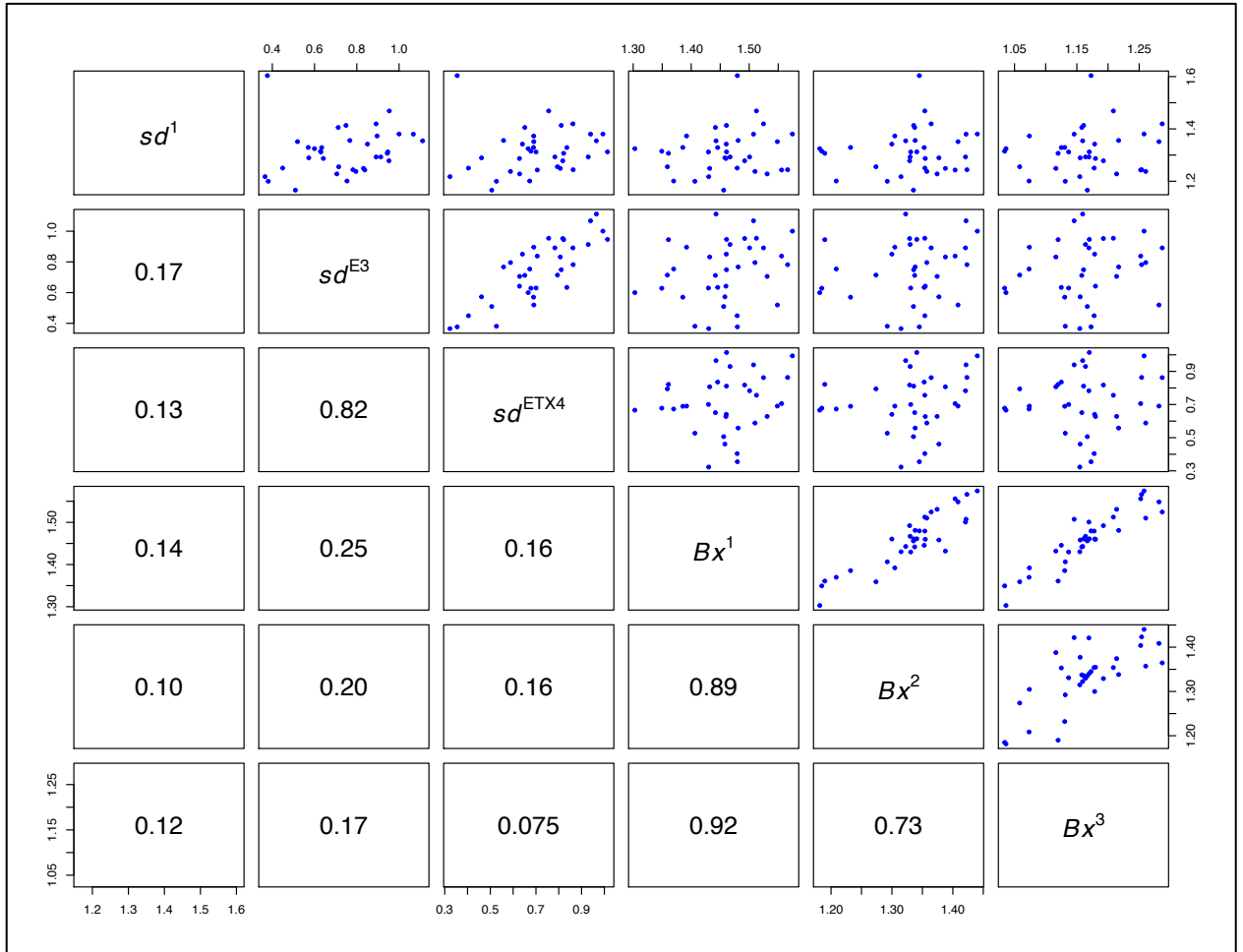


Figure 3.13: Correlation values among *beadex* and *scalloped* mutant alleles for wing size among 25 DGRP strains. Each blue dot represents the model adjusted mean for a unique DGRP strain (Table 3.1, 3.2).

Semi-quantitative analysis of *scalloped* and *bifid (omb)* alleles

One concern of our experimental design was whether wing area/wing size would be a good proxy to assess the degree of perturbation, particularly with respect to alleles with weak phenotypic effects. That is, the subtle defects (largely just removing bristles at the margin of the wing) for weak alleles may have little influence on overall wing area relative to natural variation among the DGRP for wing size. This is particularly acute for the *bifid (omb)* alleles, where there was little influence on wing size, despite the presence of wing venation defects. To address this concern, samples of the *scalloped* and *bifid (omb)* alleles were re-analyzed with two distinct semi-quantitative scales. “Score boards” that reflect the phenotype range of alleles in either gene were created to rank the degree of perturbation among mutant alleles (See supplemental). As is seen in Figure 3.14, the correlation between wing size and the semi-quantitative score is 0.95 for moderate effect alleles, and importantly this measure is able to capture subtle defects of wing morphology for the very weak *scalloped* alleles.

Similar to the statistical analysis of the quantitative measures (wing size), here we have estimated of mean wing score for each mutant/DGRP cross, and variance among all respective DGRP strains for *scalloped* and *bifid (omb)* in two separate mixed linear models (reflecting separation of experiments) (Table 3.4, 3.5). An interaction term between DGRP and Block was included in the *bifid (omb)* model terms, as there was a significant effect of the interaction and inclusion of the interaction term reflected a better model fit. Correlations of wing scores for alleles within and between *scalloped*

and *bifid (omb)* were also computed. Pearson's correlations tests were used to examine statistical significance and the strength of correlated response. In *scalloped*, the correlation between size estimates and wing scores was significantly correlated in alleles *sd[E3]* and *sd[ETX4]* ($P = <0.001$) (Figure 3.14). In *scalloped*, wing score estimates for every allele combination are all significantly different.

Notably, correlations among DGRP lines for the wing scores were generally as high or higher than for wing size. Indeed, the correlations between *sd[1]* and *sd[E3]*, *sd[E3]* and *sd[ETX4]*, and *sd[1]* and *sd[ETX4]* are significant ($P = <0.001$), and quite high (greater than 0.6, Figure 3.19). Among the *bifid (omb)* alleles, correlations vary between 0.36 and 0.94 (Figure 3.20). Correlation between *bi[1]* and *bi[QD]* is significant ($P = 0.02$). Correlation between *bi[GAL4]* and *bi[QD]* is significant ($P = 0.02$). Correlation between *bi[GAL4]* and *bi[MD653]* is also significant ($P = <0.001$). Despite the correlations between wing scores being quite high among mutant alleles within genes, and all of the correlations being positive, there was no significant correlations between the scalloped and bifid alleles. However, as statistical significance is very sample size dependent, this may reflect modest power, and these positive correlations may reflect some (albeit modest) shared response in background dependence.

Correlation of *scalloped* alleles wing size and wing score estimates

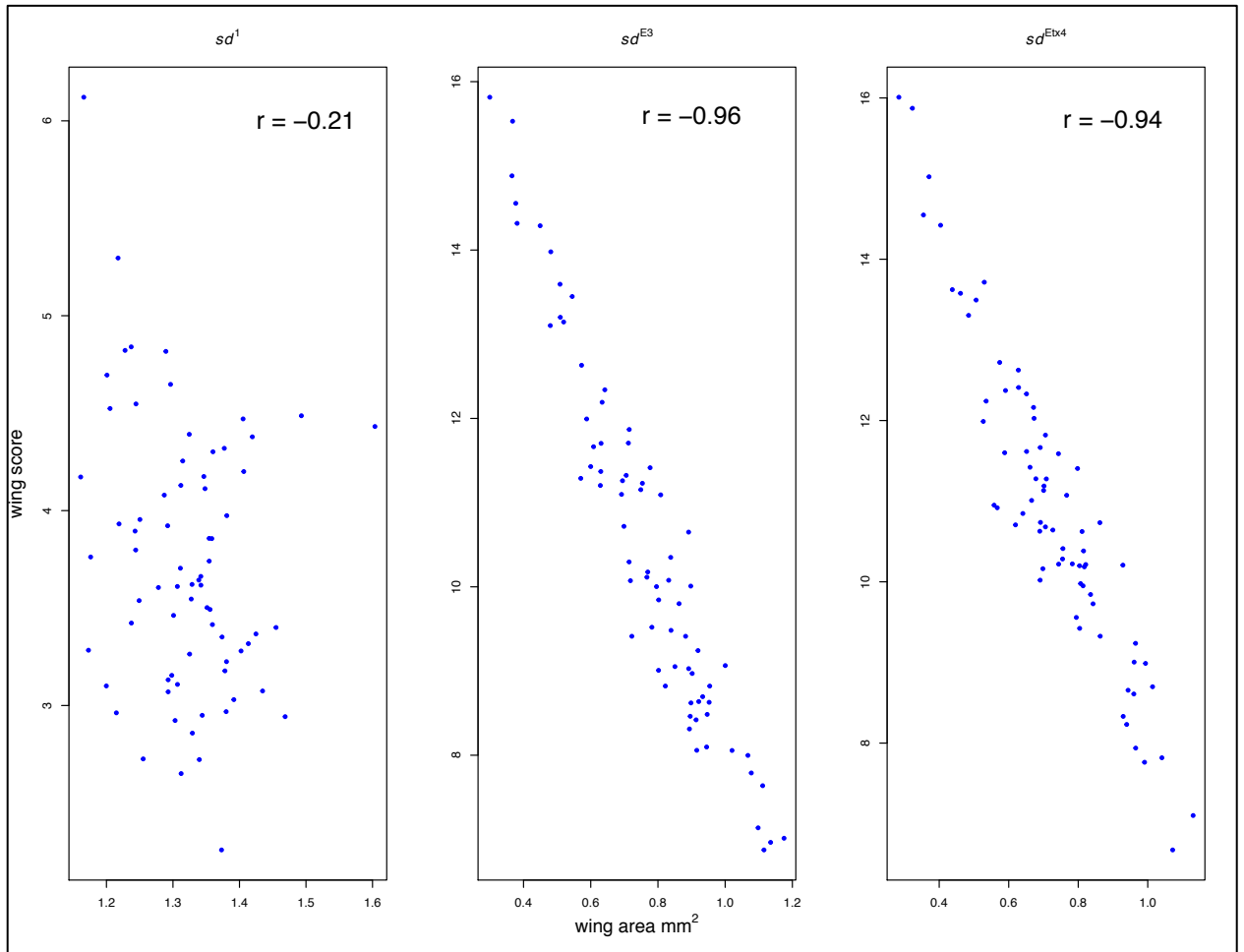


Figure 3.14: Pairwise correlations between the quantitative measure (wing area) and the semi-quantitative measure (wing score) among *scalloped* mutant alleles in 73 DGRP strains (Tables 1, 4). N=11164.

Average effect of *scalloped* mutant wing scores among DGRP strains

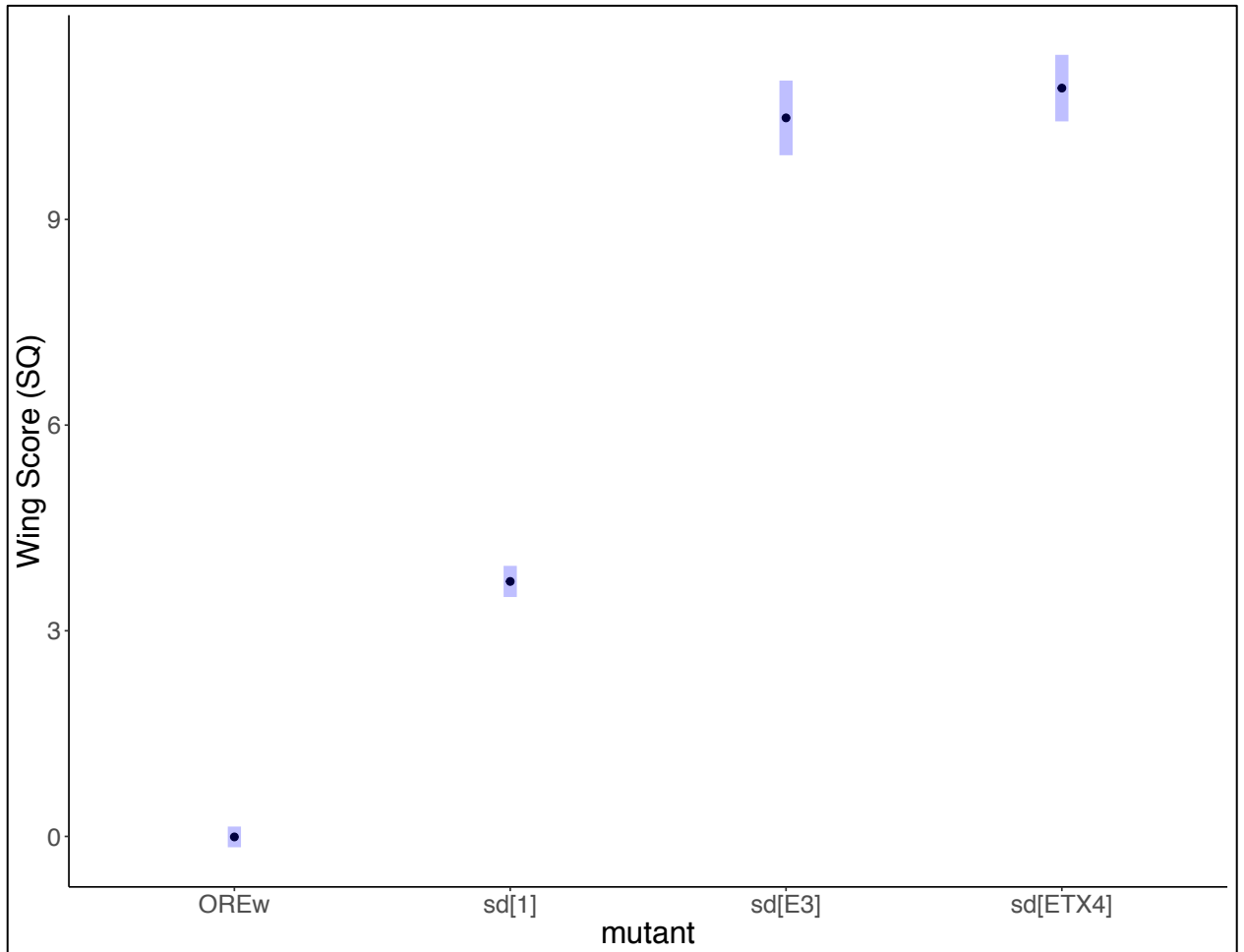


Figure 3.15: The mean phenotypic effect of each *scalloped* mutant allele in 73 DGRP strains. Means reflect fixed model estimates (Table 4). Note that the semi-quantitative wing score captures the subtle aspects on wing morphology. N=11164.

Average effect of *bifid (omb)* mutant wing scores among DGRP strains

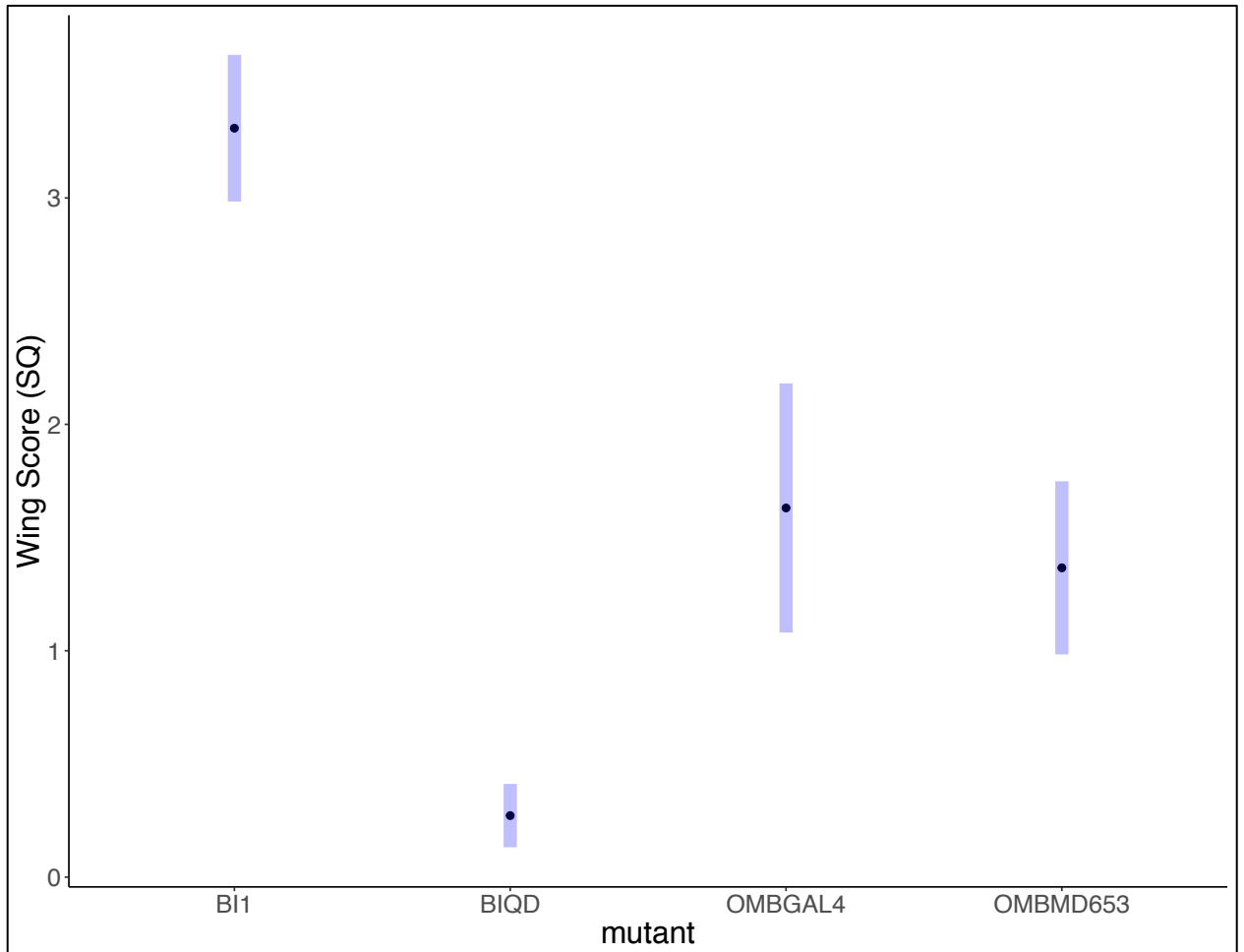


Figure 3.16: The mean phenotypic effect of each *bifid (omb)* mutant allele in 25 DGRP strains. Means reflect fixed model estimates (Table 5). Unlike wing area, the *omb* semi-quantitative wing score captures the overall effects on morphology. N=965.

Variation in *scalloped* wing score line means among DGRP strains

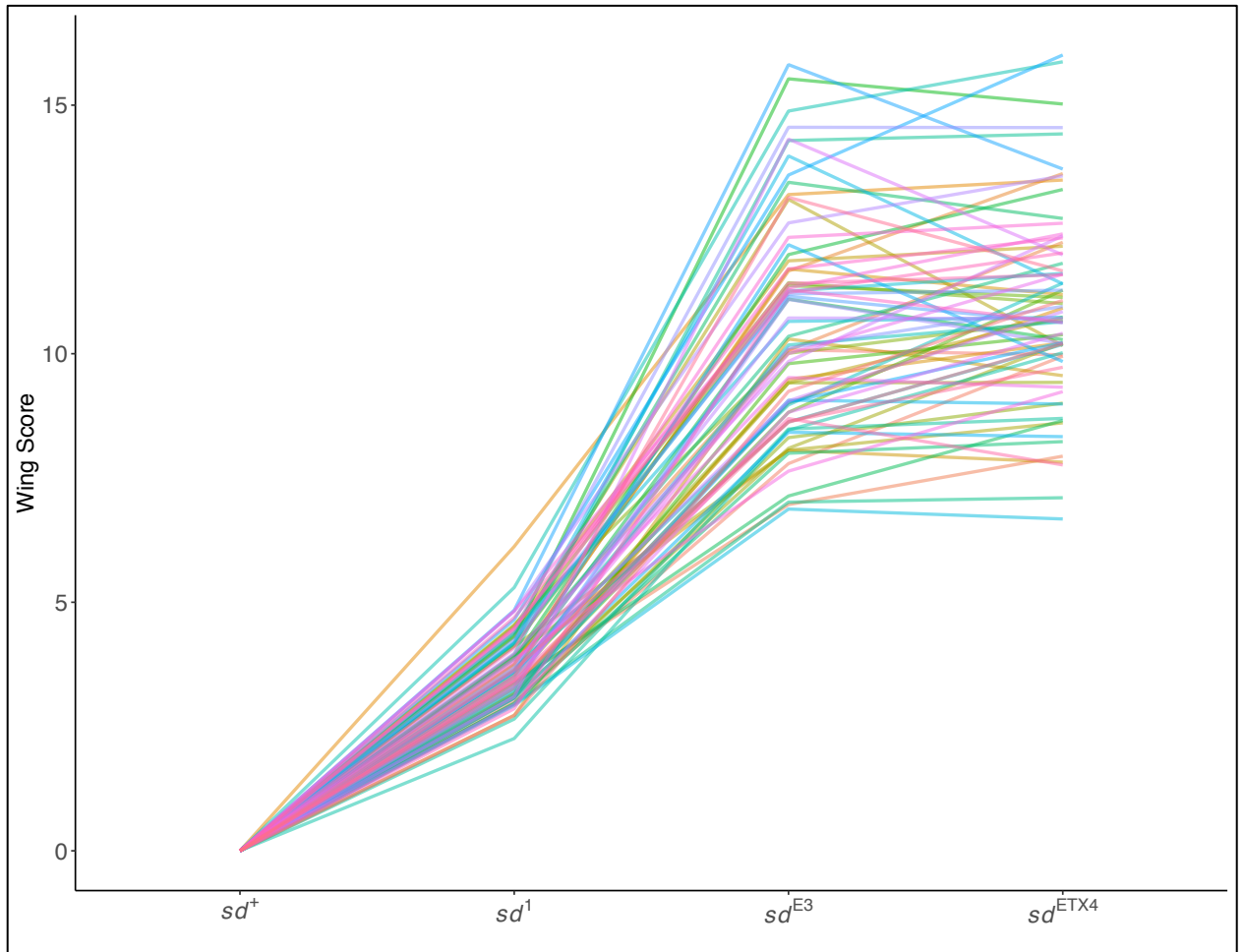


Figure 3.17: A reaction norms plot showing the variability of *scalloped* mutant wing scores among 73 DGRP strains. Colours represent distinct DGRP strains (Table 4). A score of 0 represents wild type wing phenotypes. N=11164.

Variation in *bifid (omb)* wing score line means among DGRP strains

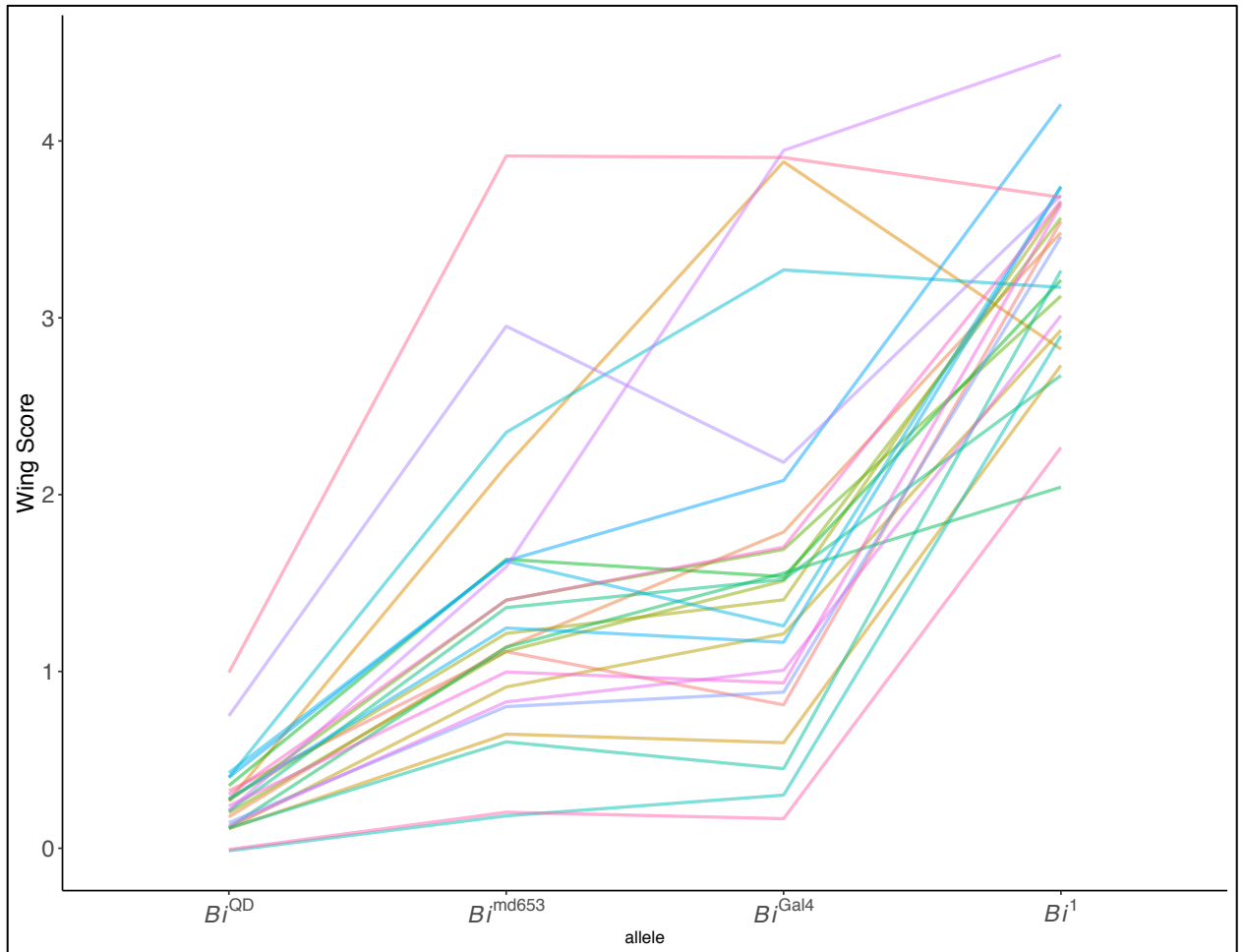


Figure 3.18: A reaction norms plot showing the variability of *bifid (omb)* mutant wing scores among 25 DGRP strains. Lines represent model adjusted means for each mutant allele (Table 5). N=965.

Correlation of mutant effects in *scalloped* wing scores among DGRP strains

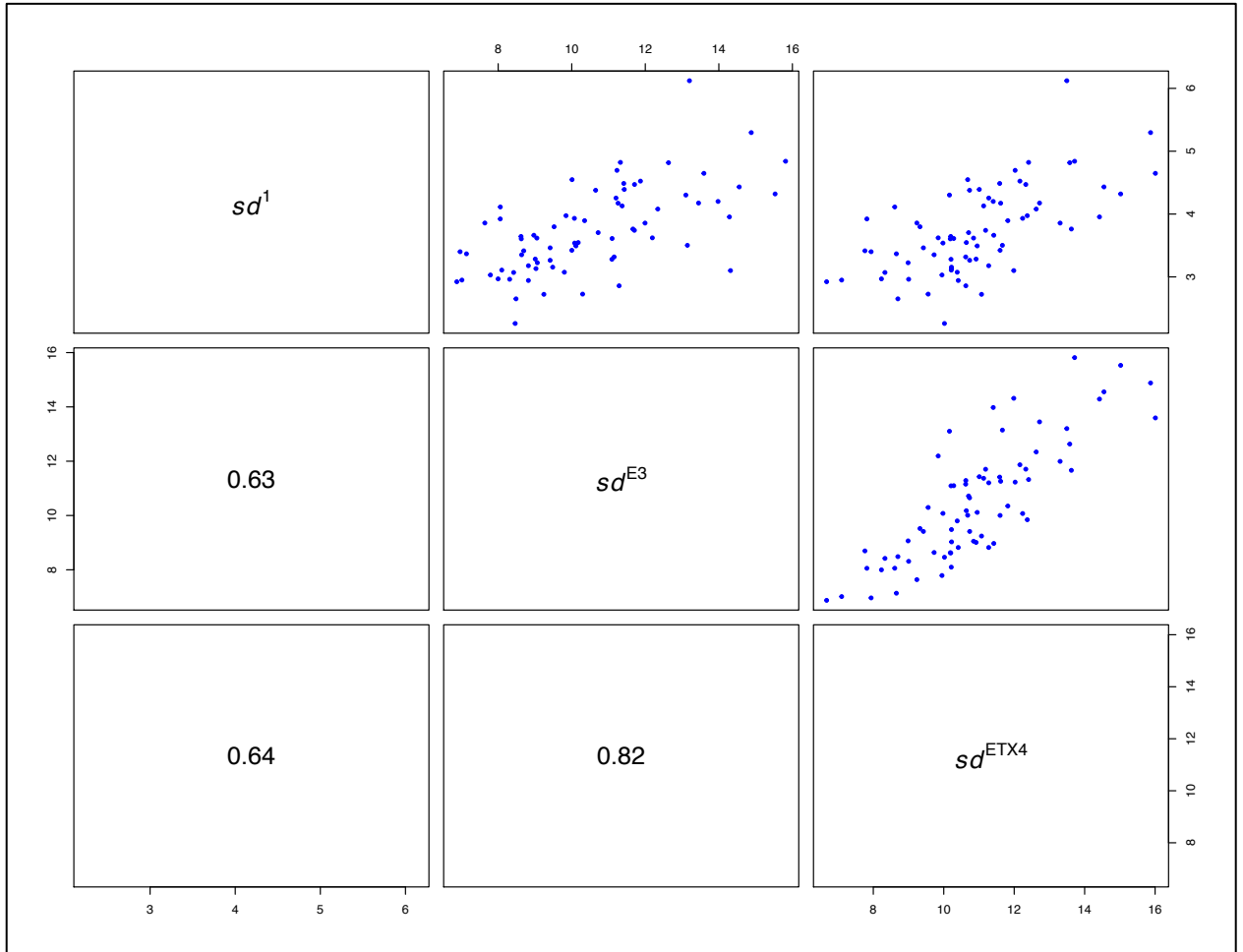


Figure 3.19: Pairwise correlations of *scalloped* mutant alleles for wing score in 73 DGRP strains. Each blue dot represents the model adjusted mean for a unique DGRP strain. N= 11164. Pearson's correlation: $sd[1]:sd[E3]$, $sd[E3]:sd[ETX4]$, $sd[1]:sd[ETX4]$, $P < 0.001$.

Correlation of mutant effects in *bifid (omb)* wing scores among DGRP strains

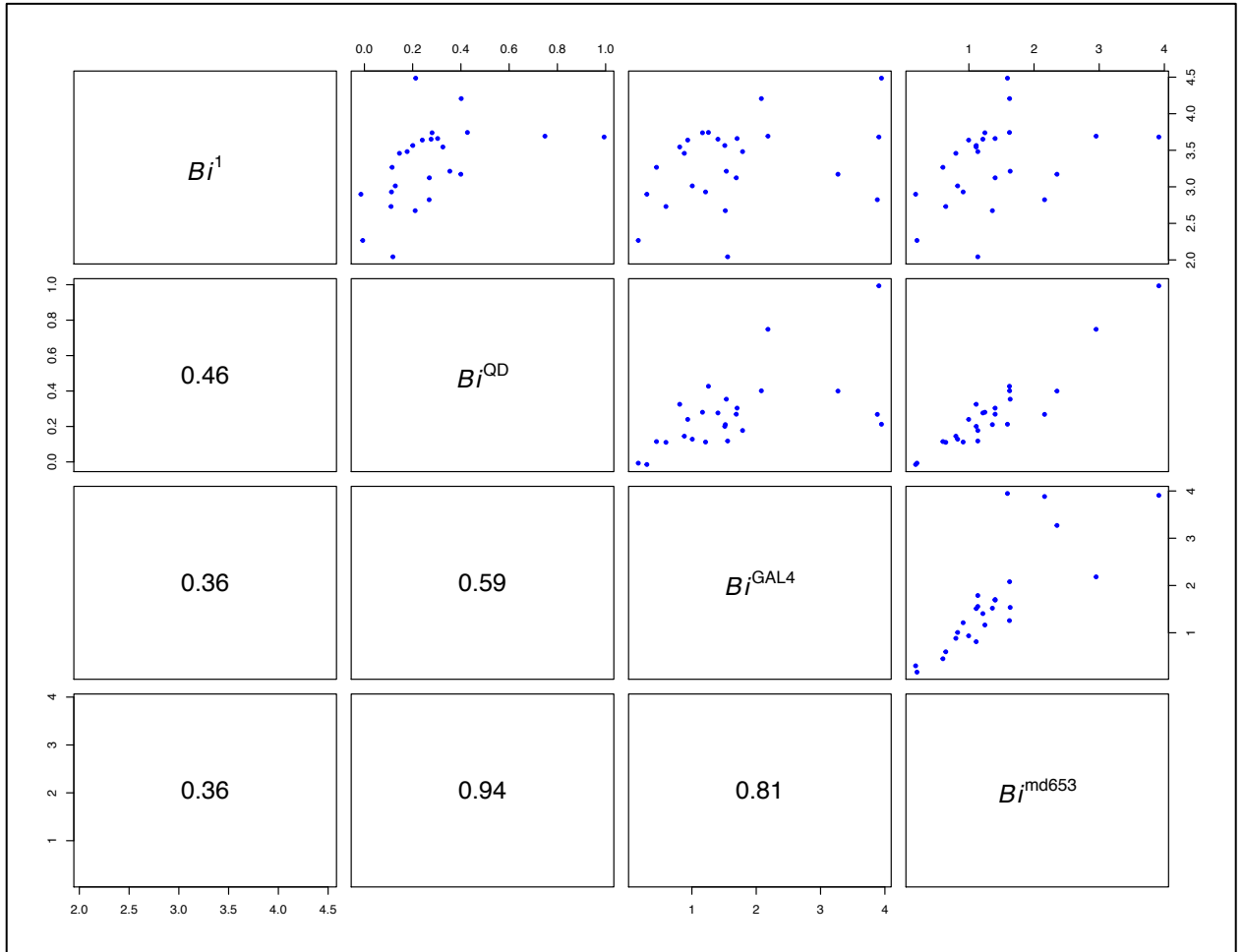


Figure 3.20: Correlation values among *bifid (omb)* mutant alleles for wing score among 25 DGRP strains. Each blue dot represents the model adjusted mean for a unique DGRP strain. N= 965. Pearson's correlation: $bi[1]:bi[QD]$, $P= 0.02$, $bi[GAL4]:bi[QD]$, $P= 0.02$, $bi[GAL4]:bi[MD653]$, $P= <0.001$.

Correlation of mutant effects in *scalloped* and *bifid* (*omb*) wing scores among DGRP

strains

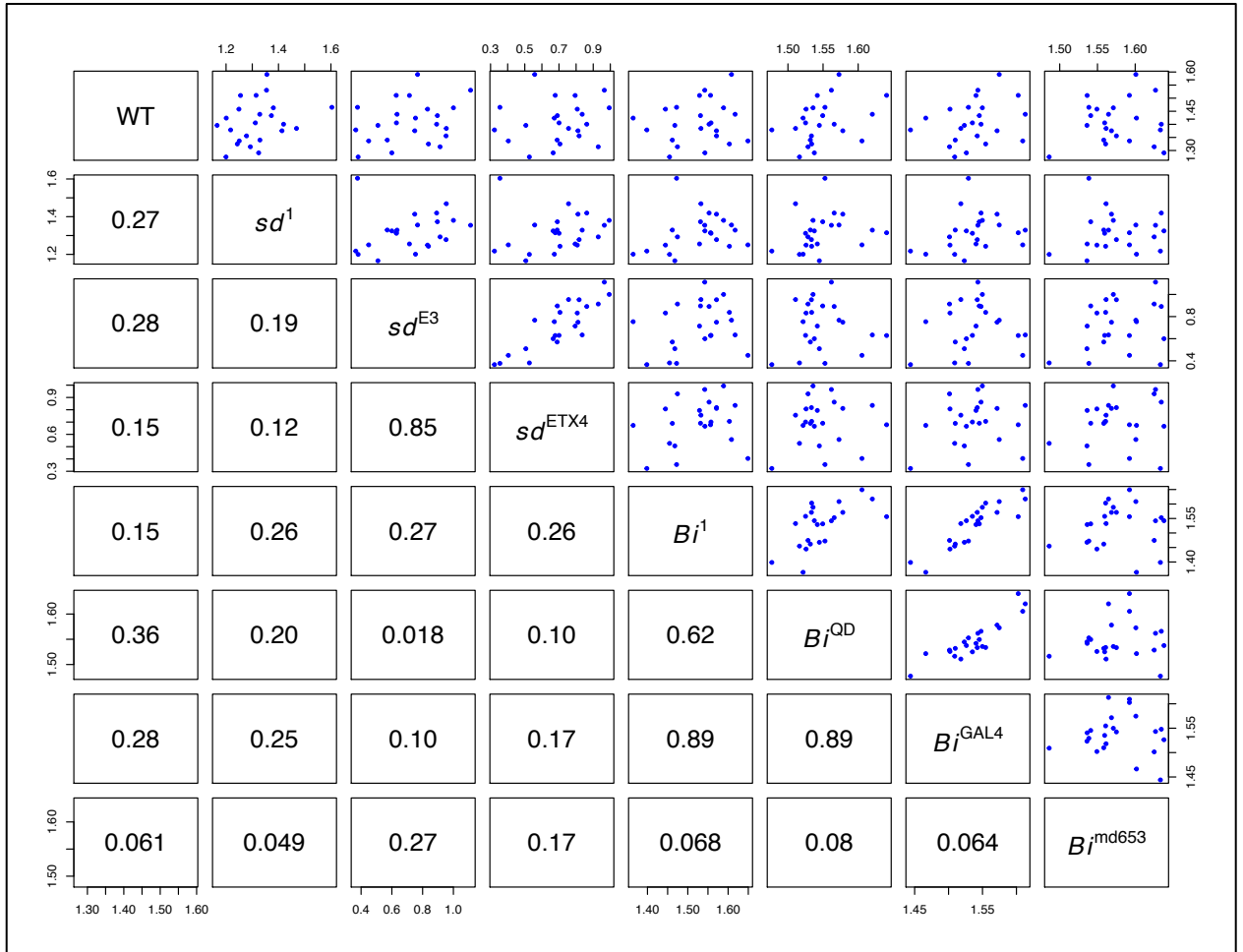


Figure 3.21: Correlation values among *scalloped* and *bifid* mutant alleles for wing score

in 25 DGRP strains. Each blue dot represents the model adjusted mean for a unique

DGRP strain.

The relationship between intra-line variability (environmental sensitivity) and mutant effects in *scalloped*

Despite mutant alleles influencing aspects of both the magnitude of background dependence, and environmental sensitivity (variation among genetically identical individuals), previous work has demonstrated a disconnect between the magnitude of background dependence among strains, and the magnitude of variability (environmental sensitivity) within strains (Debat, Debelle, & Dworkin, 2009). Other work focused largely on two standard wild type strains and comparing across many different mutant allelic combinations, with modest sample sizes within genotypes (Chandler et al. 2017). To understand the relationship between these effects more fully, we computed Levene's statistics of the crosses between the *scalloped* alleles and the 73 DGRP strains to measure of within-line (intra-line) variation as a proxy for environmental sensitivity. Importantly, not only were many more wild type strains tested in our study, but many individuals were sampled within each genotype to get much better estimates.

Average estimates of mean variability illustrate significant differences between the moderate alleles and *sd[1]* and the wildtype, where environmental sensitivity was highest for alleles with moderate effects (Table 3.6). In fact, variability among moderate alleles was at least twice the magnitude of the intra-line variance for *sd[1]* and wildtype among DGRP strains. This indicates a substantial increase in environmental sensitivity among moderate alleles. However, sensitivity to environmental effects does not appear to be a fixed attribute, as crossing of lines indicate reordering (Figure 3.23). Moreover,

intra-line variation is highly correlated among all alleles, especially between both moderate alleles (Figure 3.26). Similar correlations were demonstrated among wing scores (Figure 3.25). Collectively, these results largely echo results that demonstrate differences in magnitude of phenotypic variation among *scalloped* alleles (Table 3.1).

Table 3.6: The statistical estimates used to estimate interline variance and the correlations among *scalloped* alleles. Model estimates are converted from the logit link scale. N=11164. ANOVA: Mutant, P = <0.001

Allele	Mean Estimate (mm ²)	Standard Error	Variance	Standard Deviation
wildtype	0.078	0.16	0.091	0.302
<i>sd</i> [1]	0.084	1.35	0.075	0.274
<i>sd</i> [E3]	0.195	1.75	0.260	0.600
<i>sd</i> [ETX4]	0.238	1.82	0.652	0.808
Block			3.414	1.848
Residual			1.203	1.100

Average estimate of *scalloped* mutant interline variability among DGRP strains

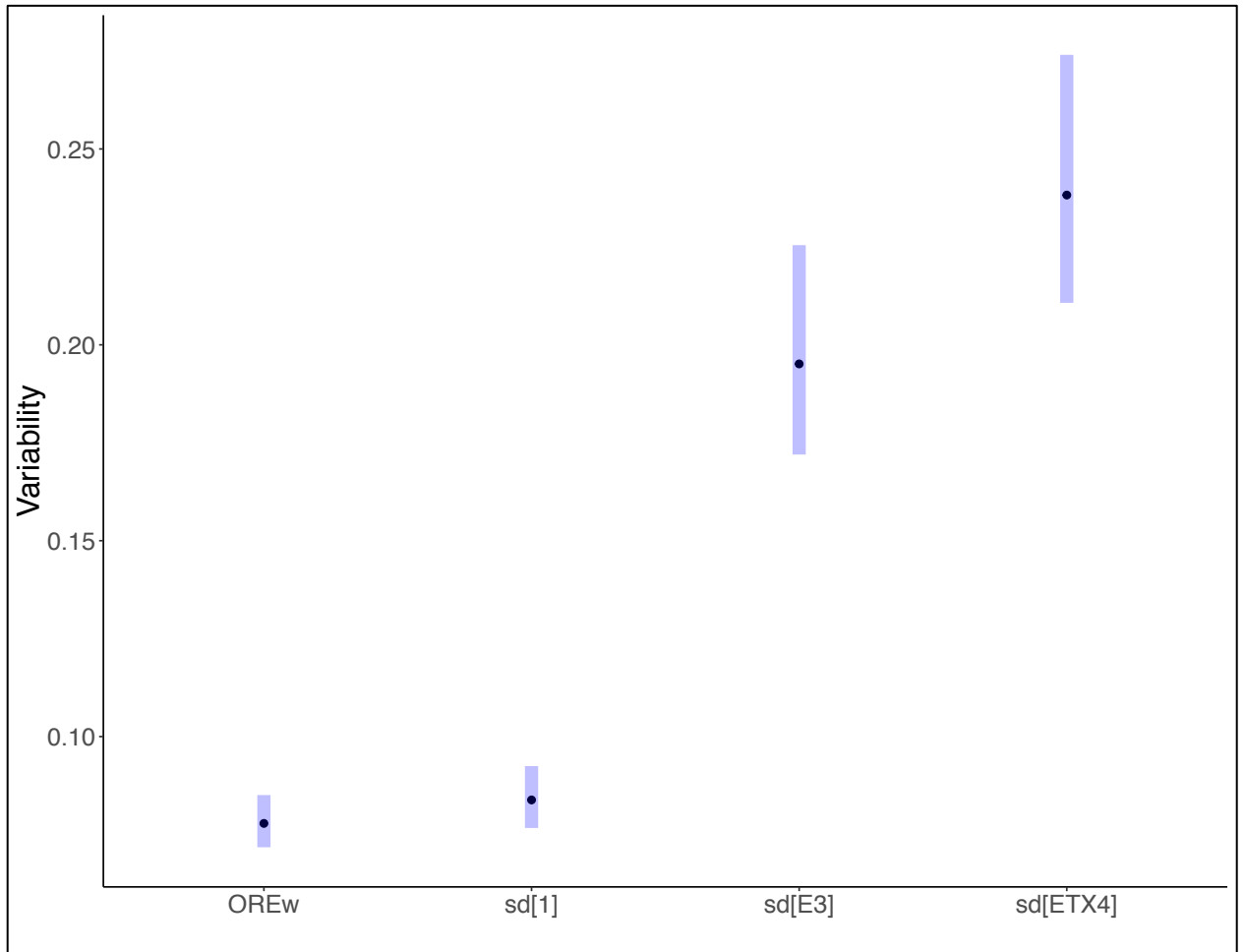


Figure 3.22: The mean variability effect of each *scalloped* mutant allele in 73 DGRP strains. Levene's means reflect mixed model estimates (Table 3.6). Error bars represent 95% CI. N=11164.

Intra-line variability in wing size among *scalloped* alleles across 73 DGRP strains

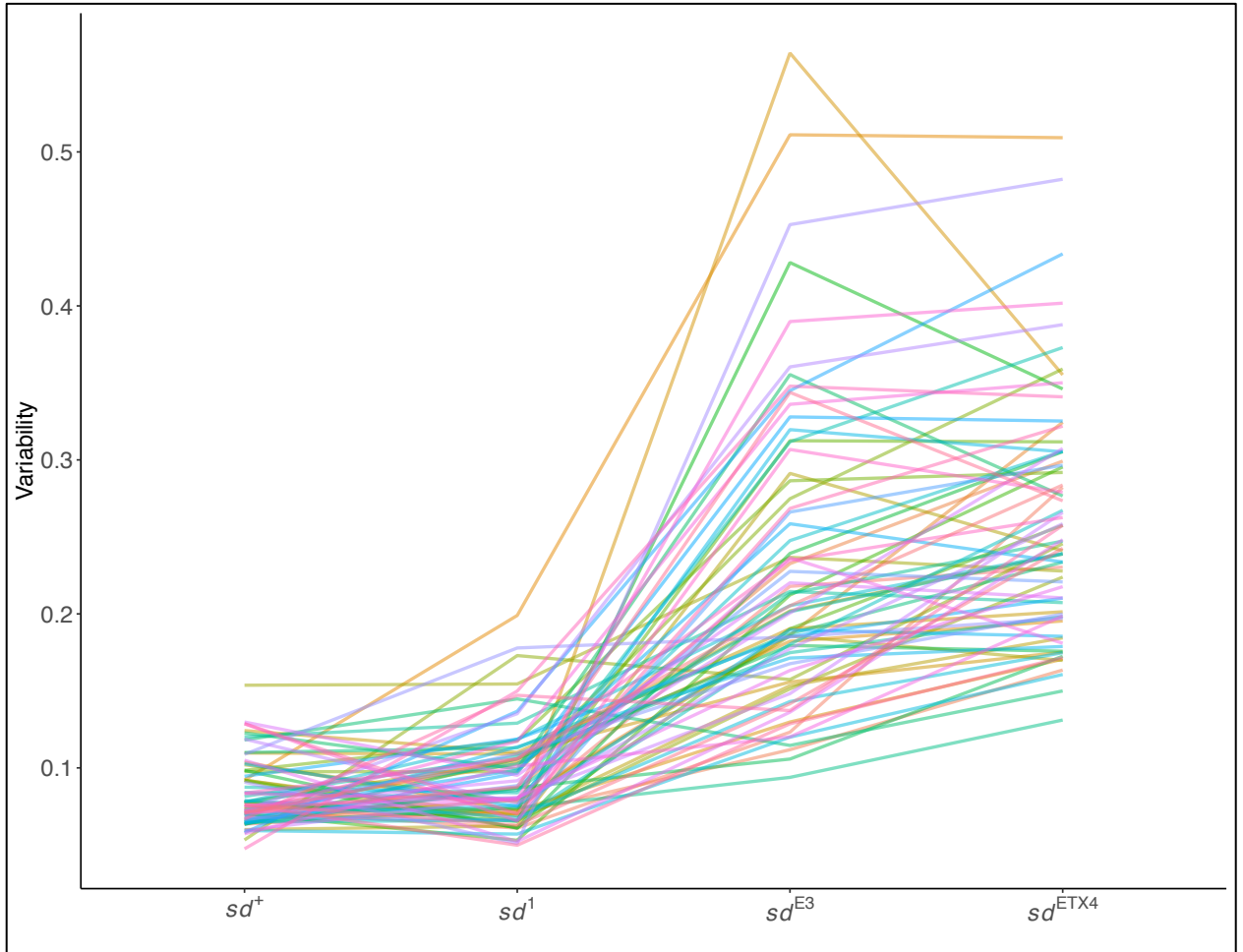


Figure 3.23: A reaction norms plot showing the interline variability in *scalloped* mutant wing size among 73 DGRP strains. Lines represent model adjusted Levene's estimates by DGRP (colour) for each mutant allele (Table 3.6). N=11164.

Correlation of intra-line variability and wing size among *scalloped* mutant alleles

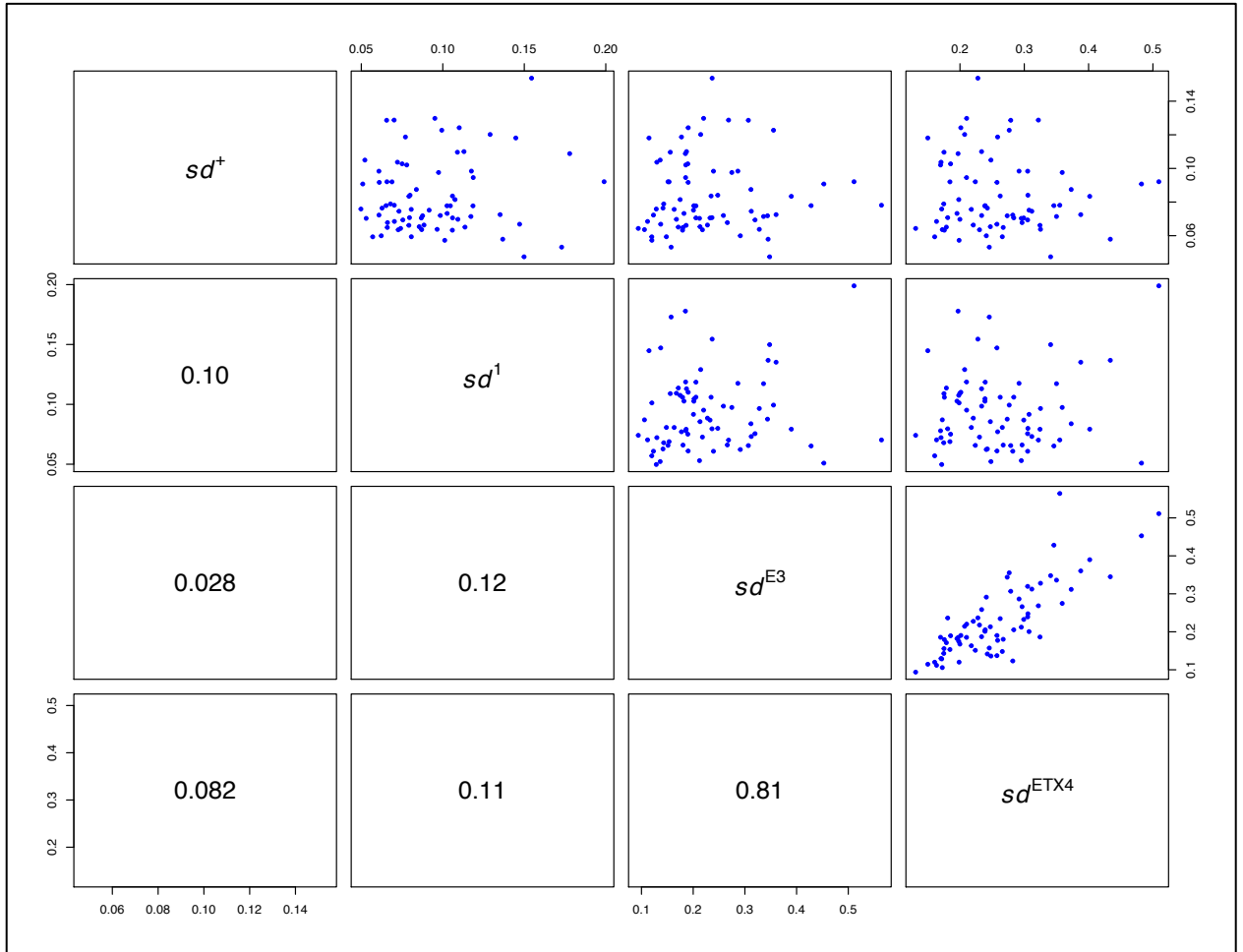


Figure 3.24: Correlation values among *scalloped* mutant alleles for Levene's statistic and in 73 DGRP strains. Each blue dot represents the model adjusted estimate for a unique DGRP strain. N= 11164. Pearson's correlation: $sd[E3]:sd[ETX4]$, $P= <0.001$.

Correlations of intra-line variation and wing score among *scalloped* mutant alleles

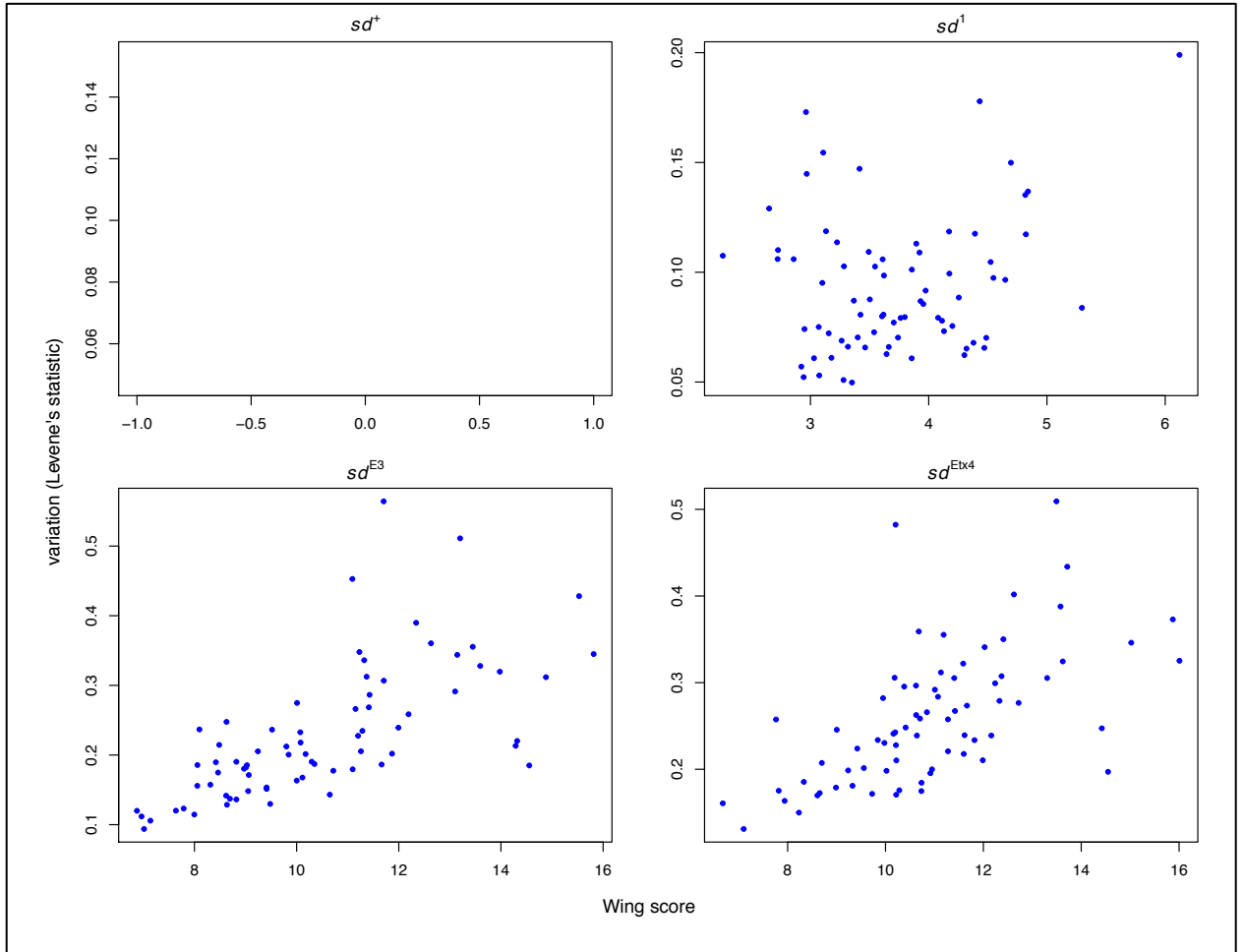


Figure 3.25: Correlation values among *scalloped* mutant alleles for Levene's statistic and wing score in 73 DGRP strains. Each blue dot represents the model adjusted estimates for a unique DGRP strain. N= 11164. Correlation values: $sd[1]$, Corr = 0.21, $sd[E3]$, Corr = 0.73, $sd[ETX4]$, Corr = 0.66.

The relationship between deviation from wildtype wing size and interline variability

Previous work has shown more severe mutants demonstrate more intra-line variability than alleles with weaker effects (Chandler et al., 2017). However, it is unclear whether there is a general relationship between magnitude of divergence from mean wildtype size and the magnitude of intra-line variation. In other words, how does the severity of perturbation predict how variable otherwise genetically identical individuals are? Answering this question will demonstrate if more severely perturbed individuals are also more sensitive to subtle environmental influences. To understand this, we examined the relationship between Levene's statistic, a measure of intra-line variability, and deviations of mutant alleles from their respective wildtype. Deviations were calculated by subtracting the raw value of wing size for each individual from the mean wildtype wing size of its respective mutant/DGRP strain. DGRP level estimates of Levene's statistic was modeled as a response with deviations values. Deviations were included as a continuous predictor along with the effects of each *scalloped* allele. DGRP was included as a random effect term to account for repeated measures within each DGRP line. Estimates of the wildtype allele are omitted, as deviation is zero.

Here we demonstrate a high correlation between the deviation from wildtype size, and the degree of intra-line variability. Regardless of the identity of the mutant allele, increasing deviation (i.e. mutant severity) is highly associated with intra-line variability ($R^2 = 0.78$, Figure 3.27). However, *scalloped* alleles varied in the degree to which they influenced intra-line variability within a DGRP line (Table 3.7). Notably,

estimates of intra-line variability is increased in both moderate alleles compared to *sd[1]*. In addition, variance of these alleles is also increased. Variance is interpreted as how much these alleles vary in intra-line variance among DGRP strains. In other words, moderate alleles exhibit greater differences in the degree of intra-line variation among DGRP strains.

Table 3.7: The statistical model used to estimate the relationship between the deviation from wildtype wing size (severity) and the degree of intra-line wing size variation in the wildtype strain. N=11164. ANOVA: Deviations, P= <0.001, Mutant, P=0.01.

Fixed effects	Estimate (mm ²)	Standard Error
<i>sd[1]</i> (intercept)	0.084	0.0086
<i>sd[E3]</i>	-0.014	0.022
<i>sd[ETX4]</i>	-0.048	0.025
Deviations (continuous)	-0.129	0.06

The relationship between wildtype deviation and magnitude of intra-line variability

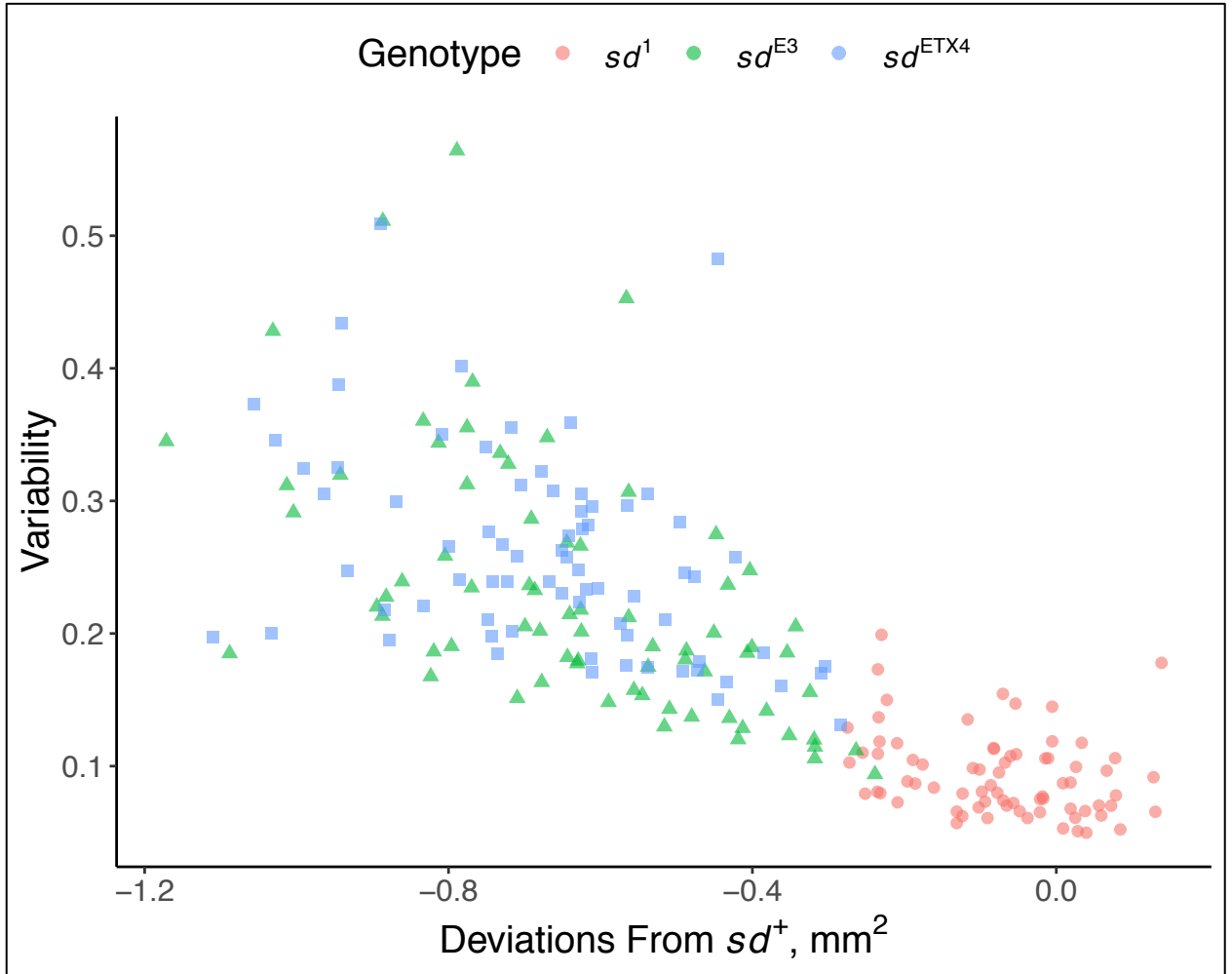


Figure 3.27: The mean Levene's estimate of each *scalloped* mutant allele in 73 DGRP strains associated with deviations of mutant alleles from their respective wildtype (i.e. comparisons within a DGRP). Levene's estimates reflect mixed model estimates (Table 3.7).

N= 11164. Pearson Correlation = 0.88 ($R^2 = 0.78$).

The relationship between variability of wild type size and deviations in *scalloped*

Given the relationship between deviation from wild type and environmental sensitivity, it was also considered whether the environmental sensitivity among wild type individuals (within a DGRP lineage) is predictive of the degree of background effects for a given mutation. The premise of this question relates to how the strength of environmental canalization in the wildtype predicts the severity of a mutant allele. Interestingly, we observe no relationship between the magnitude of intra-line variability in the wildtype and how severe mutant effects will be in that strain (Table 3.8).

Table 3.8: The statistical model used to estimate the relationship between the intra-line variance in the wildtype strain, and the deviation (severity) of *scalloped* alleles. N=11164. ANOVA: Mutant, P=0.01.

Fixed effects	Mean Estimate (mm ²)	Standard Error
<i>sd[1]</i> (intercept)	-0.14601	0.06760
<i>sd[E3]</i>	0.85907	0.77093
<i>sd[ETX4]</i>	-0.55401	0.02044
Deviations	-0.59673	0.02044

The relationship between intra-line variance in wing size among in the wildtype and deviations from wild type wing size

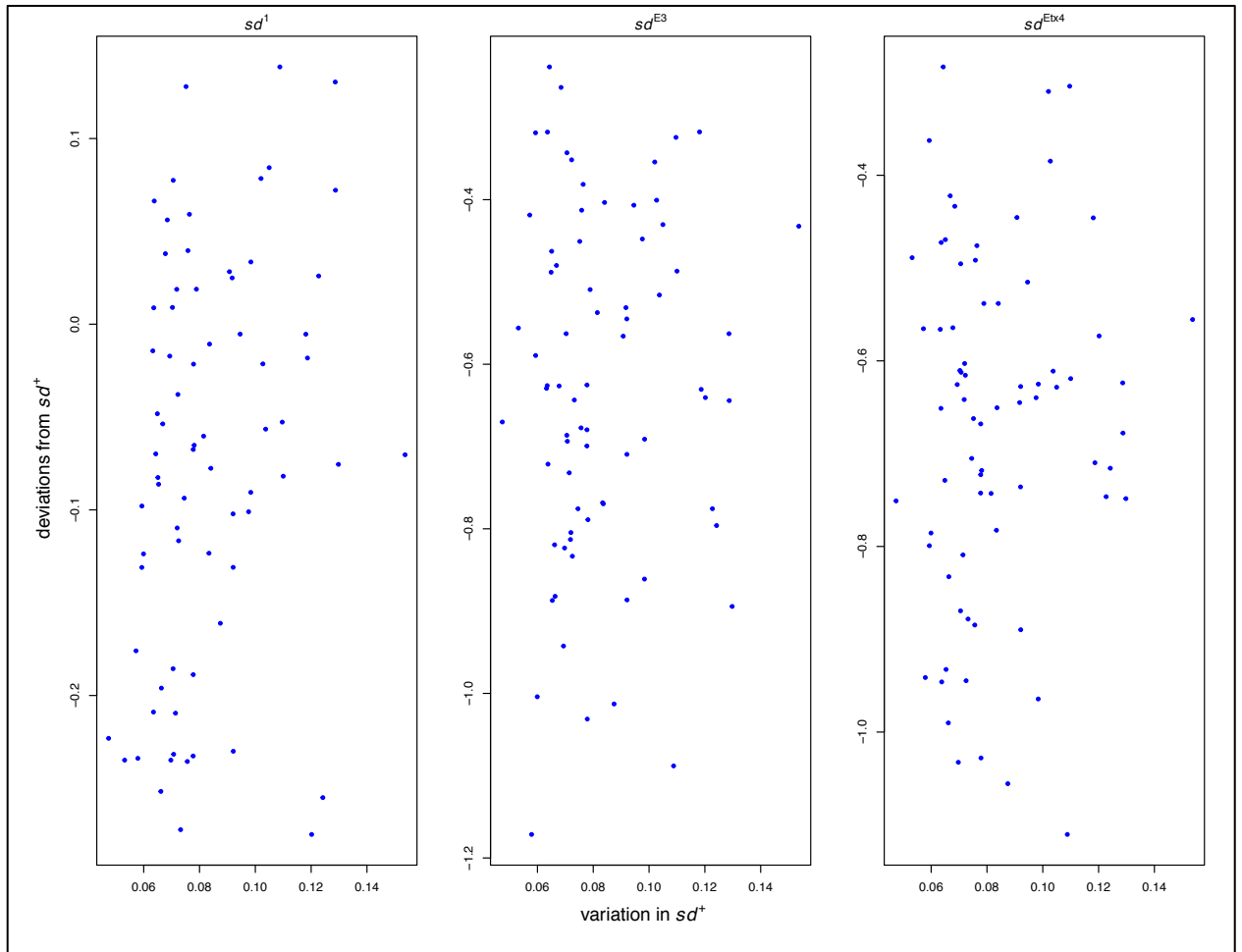


Figure 3.28: Interline variation in the wildtype (model adjusted Levene's statistics) and absolute deviation from the wildtype. Pearson Correlation coefficients, $sd[1]= 0.26$, $sd[E3] = 0.057$, $sd[ETX4] = 0.082$.

Further analysis of *scalloped* and *Beadex* in a subset of 20 DGRP strains

One limitation of the original study with the *scalloped* and *beadex* mutants was there was a limited distribution of *scalloped* phenotypic effects among the mutant alleles. Additionally, the *scalloped* and *beadex* alleles were also analyzed in different experiments at separate times (although there was overlap of *beadex* experiments with a few of the *scalloped* blocks). Given the evident contribution of environmental effects in modulating mutant phenotypes, correlations among genes may have been weaker due to these effects. As such, quantitative analysis of wing size was repeated for *scalloped* and *beadex* in a subset of 20 DGRP strains included in the original study. Additional *scalloped* alleles were also added to the allelic series complete the range of phenotypic effects (*sd[29.1]*, weak, and *sd[58d]*, severe).

The terms of the mixed linear models used to estimate mean mutant effects among DGRP strains, the magnitude of phenotypic variance for each mutant allele, and the degree of interline variation among mutant alleles was identical to the terms used in the original study. Mean estimates of mutant effect, variance and the Levene's statistics were thus computed the same way as the original data. However, due to computational convergence errors in modeling estimates of *beadex* mutant alleles, the Levene's statistics are represented by the raw Levene's statistics, not the model adjusted estimates (Figure 3.38). The estimates between the converged statistical model and the raw data are relatively similar (comparisons not shown).

The results of the second study with the subset of DGRP strains broadly recapitulates the results of the original data, although correlations between *scalloped* and *beadex* were notably higher (Figure 3.33). This may not be surprising, given that sensitivity of the mutant alleles to environmental effects and the temporal separation between analysis of these alleles in the original study. However, significant differences among correlations is less frequent, simply reflecting reduced statistical power due to a decreased number of DGRP strains analyzed with this subset. Nonetheless, the magnitude of correlations between alleles of the same gene are comparable (Figure 3.33). Estimates of mean wing size of the newly added *scalloped* alleles at opposite ends of the phenotypic spectrum (*sd[29.1]* and *sd[58d]*) demonstrate expected mean estimates of wing size (Table 3.9). In addition, variance estimates for these alleles were relatively modest compared to variance estimates of the moderate alleles, as anticipated with regard to results of the original study (Figure 3.31). Interestingly, the moderate *beadex* allele (*bx[3]*) demonstrated more phenotypic variance among DGRP strains in this study (Figure 3.32).

Table 3.9: The statistical model estimates of the *scalloped* and *beadex* alleles from the subset experiment. N= 5509. ANOVA analysis: Mutant, P= <0.001.

Allele	Mean Estimate (mm²)	Standard Error	Variance	Standard Deviation	H²
<i>wildtype</i>	1.45	0.08	0.012	0.11	0.27
<i>bx[1]</i>	1.37	0.04	0.016	0.12	0.33
<i>bx[2]</i>	1.40	0.03	0.008	0.09	0.20
<i>bx[3]</i>	1.10	0.04	0.010	0.10	0.23
<i>sd[29.1]</i>	1.45	0.03	0.006	0.08	0.15
<i>sd[1]</i>	1.38	0.03	0.016	0.13	0.33
<i>sd[E3]</i>	0.88	0.05	0.044	0.21	0.57
<i>sd[ETX4]</i>	0.79	0.05	0.035	0.20	0.51
<i>sd[58d]</i>	0.15	0.03	0.0002	0.01	0.03
Block			0.0163	0.13	
Residual			0.0167	0.13	

Average size effect of *scalloped* mutants wing size among (subset) DGRP strains

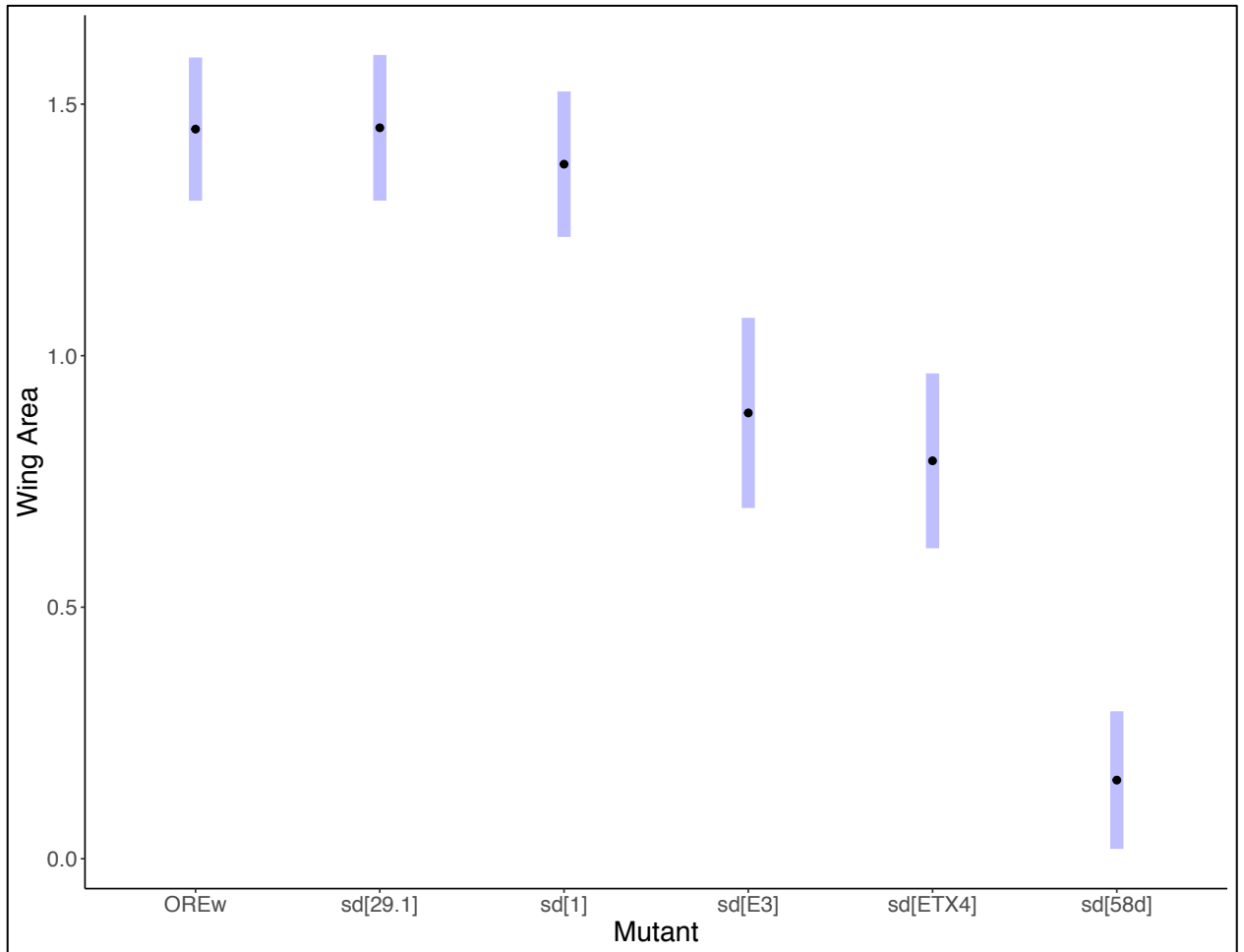


Figure 3.29: The mean phenotypic effect of each *scalloped* mutant allele across 20 DGRP strains. Means reflect mixed model estimates (Table 3.9). Error bars represent 95% CI. N=3632.

Average size effect of *beadex* mutants wing size among (subset) DGRP strains

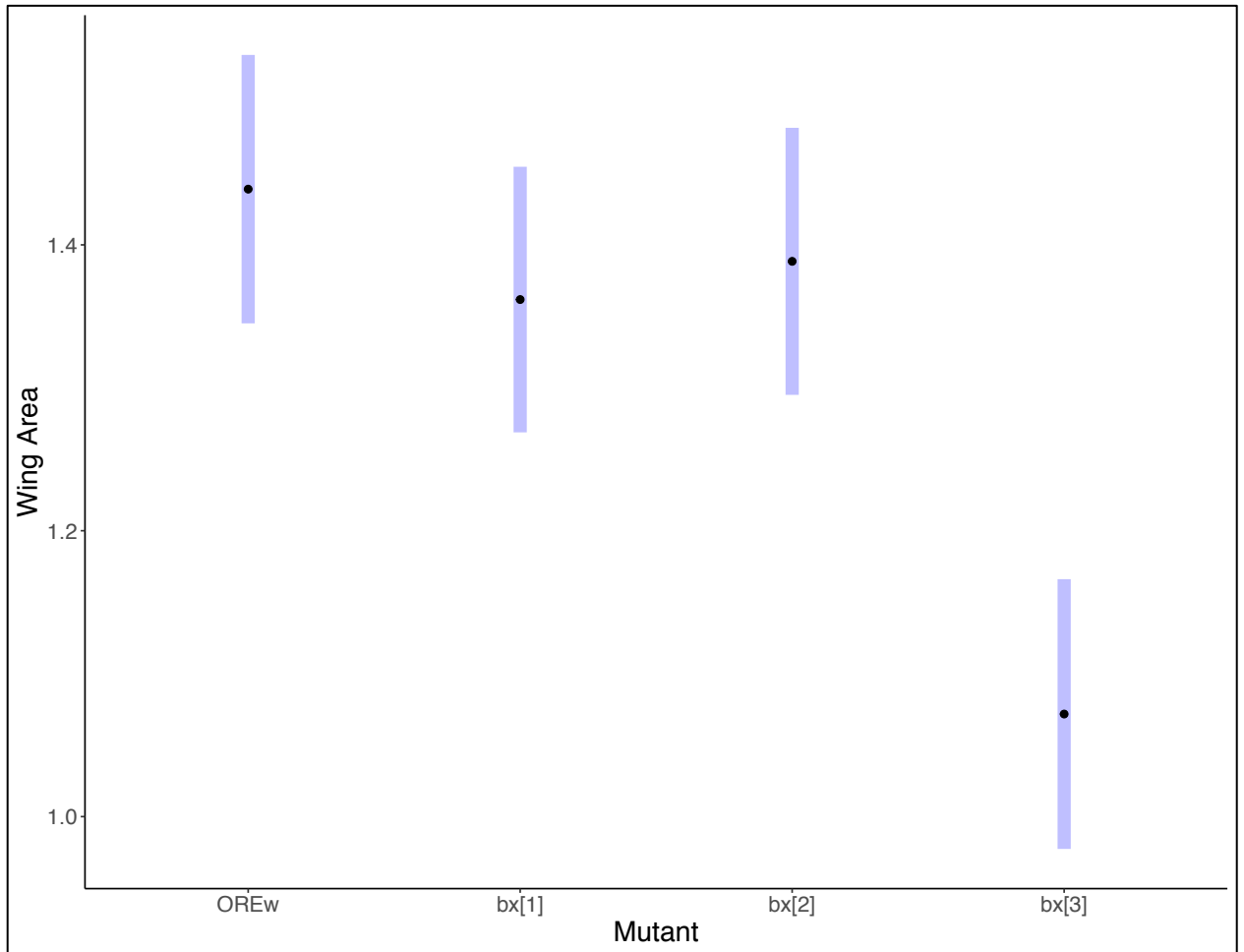


Figure 3.30: The mean phenotypic effect of each *Beadex* mutant allele in 20 DGRP strains. Means reflect fixed model estimates (Table 3.9). Error bars represent 95% CI. N =2494.

Variation in *scalloped* wing size line means among (subset) DGRP strains

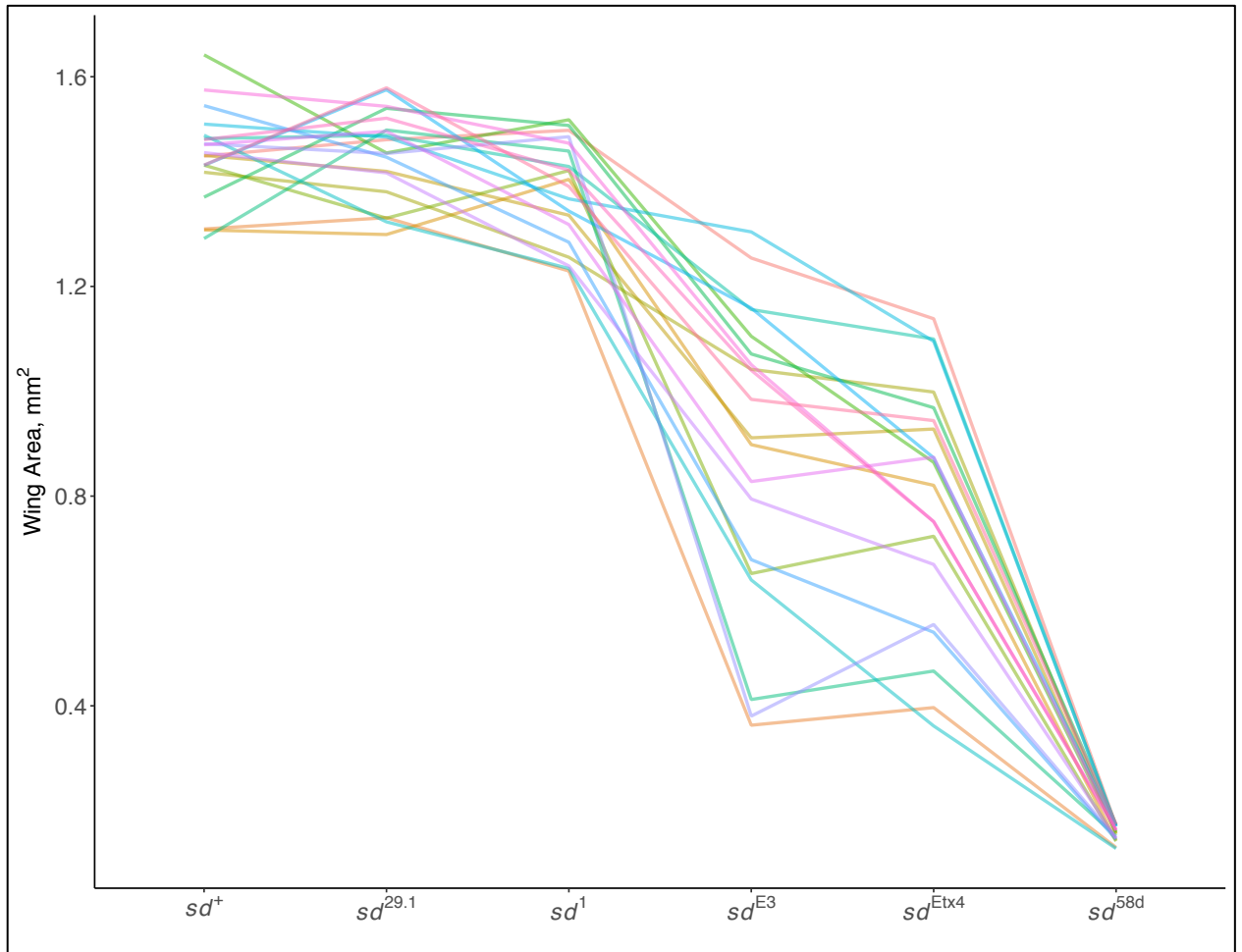


Figure 3.31: Reaction norms of *scalloped* mutant phenotypes among 20 DGRP strains.

Lines connect mixed model estimates (Table 3.9). N=3632.

Variation in *beadex* wing size line means among (subset) DGRP strains

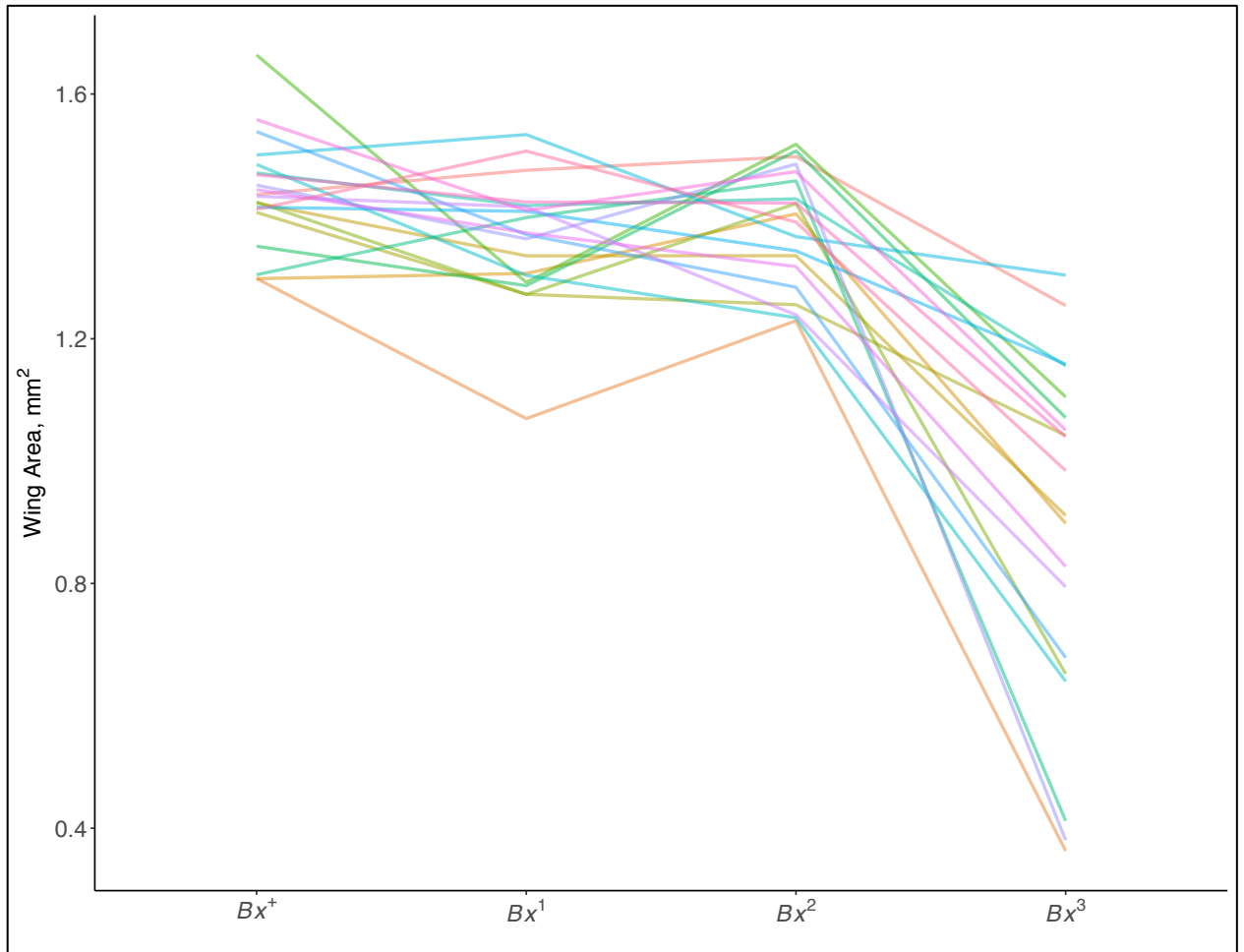


Figure 3.32: Reaction norms of *beadex* mutant phenotypes among 20 DGRP strains.

Lines connect mixed model estimates (Table 3.9). N =2494.

***scalloped* and *beadex* line means correlations mutant effect among DGRP**

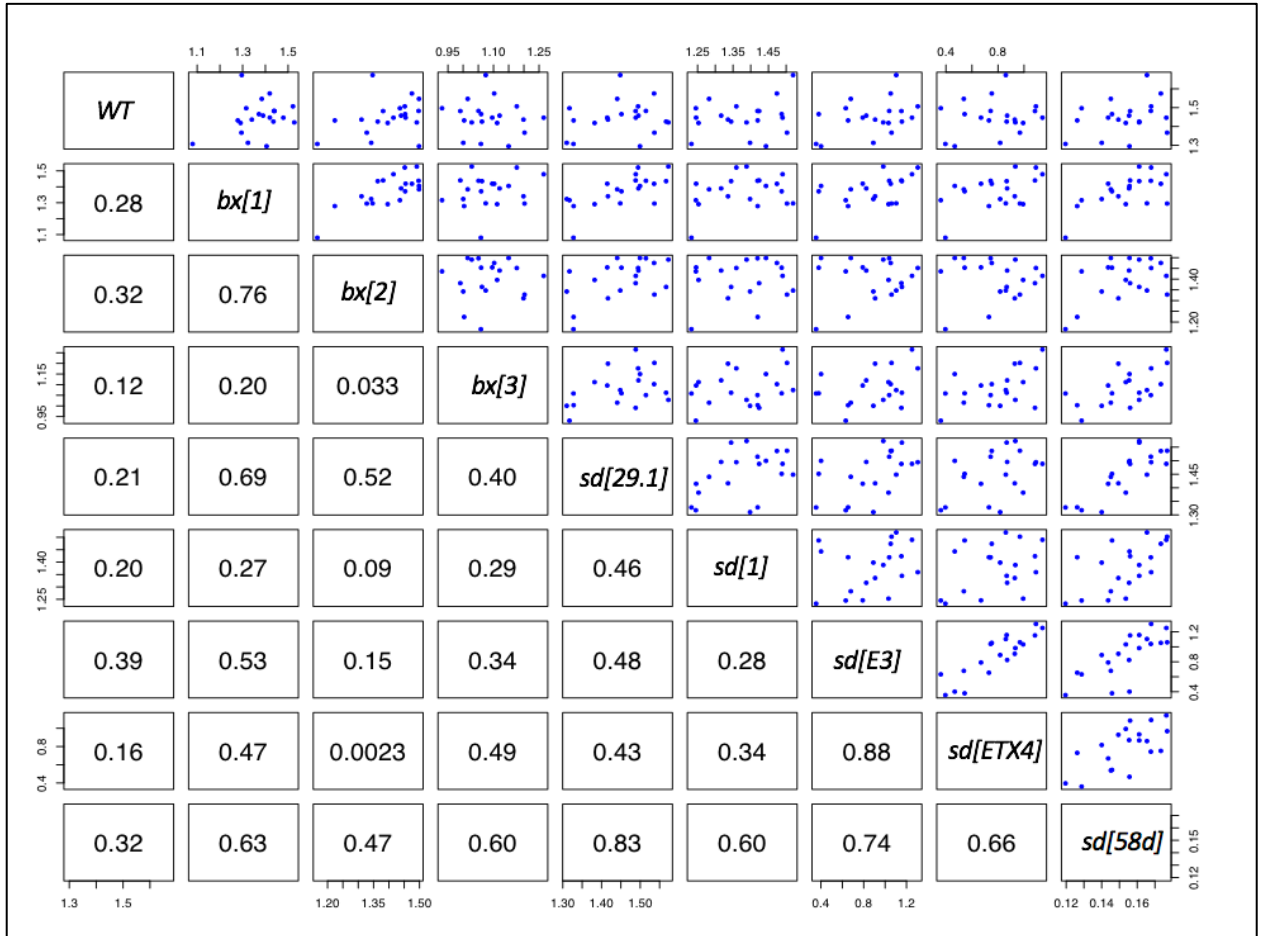


Figure 3.33: Correlation values among *beadex* and *scalloped* mutant alleles for wing size among 20 DGRP strains. Each blue dot represents the model adjusted mean for a unique DGRP strain (Table 3.9). N=3632.

Average estimate of *scalloped* mutant intra-line variability among DGRP strains

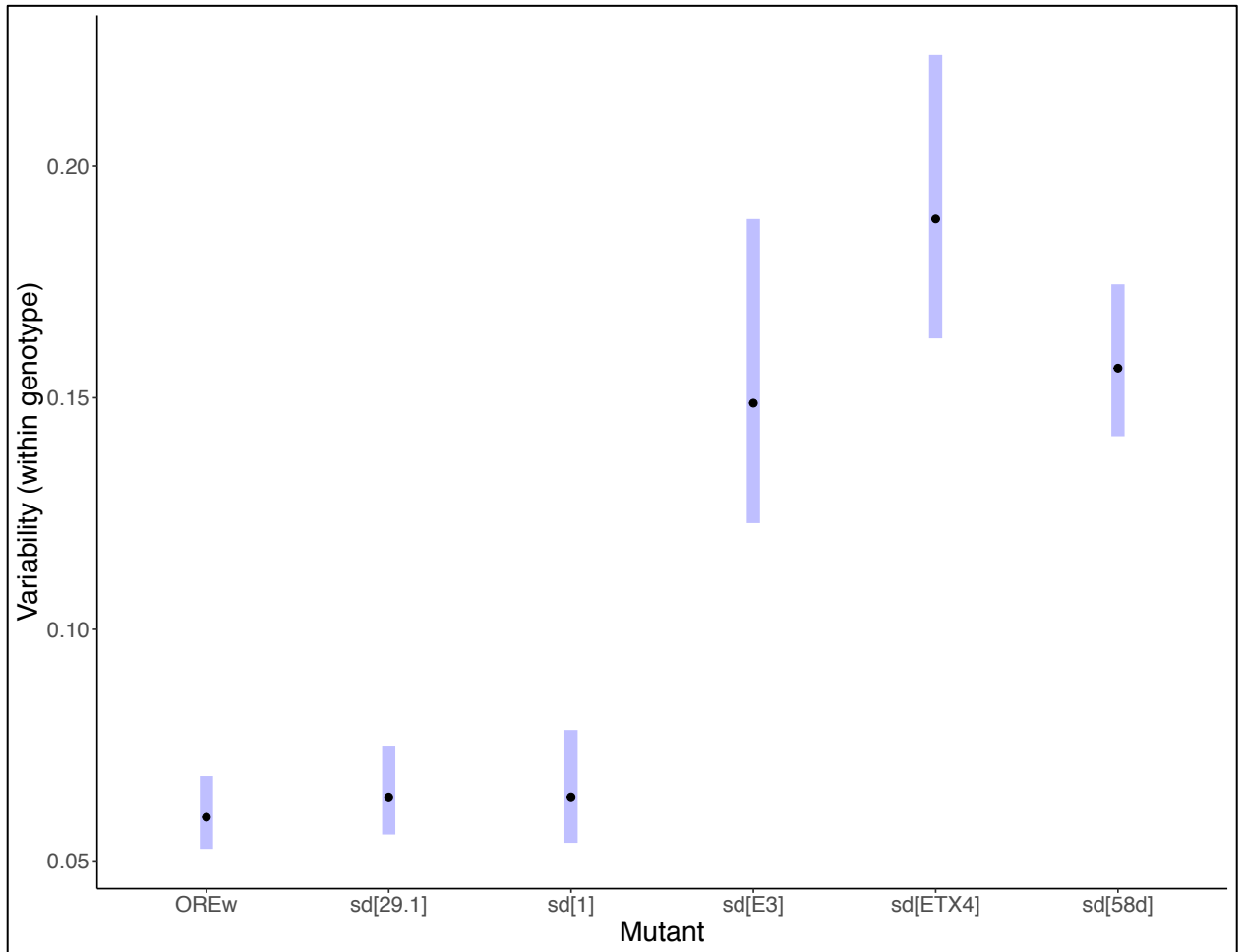


Figure 3.34: The mean variability effect of each *scalloped* mutant allele in 20 DGRP

strains. Levene's means reflect fixed model estimates (Table 3.9). Error bars represent

95% CI. N=3632.

Average estimate of *scalloped* mutant intra-line variability among DGRP strains

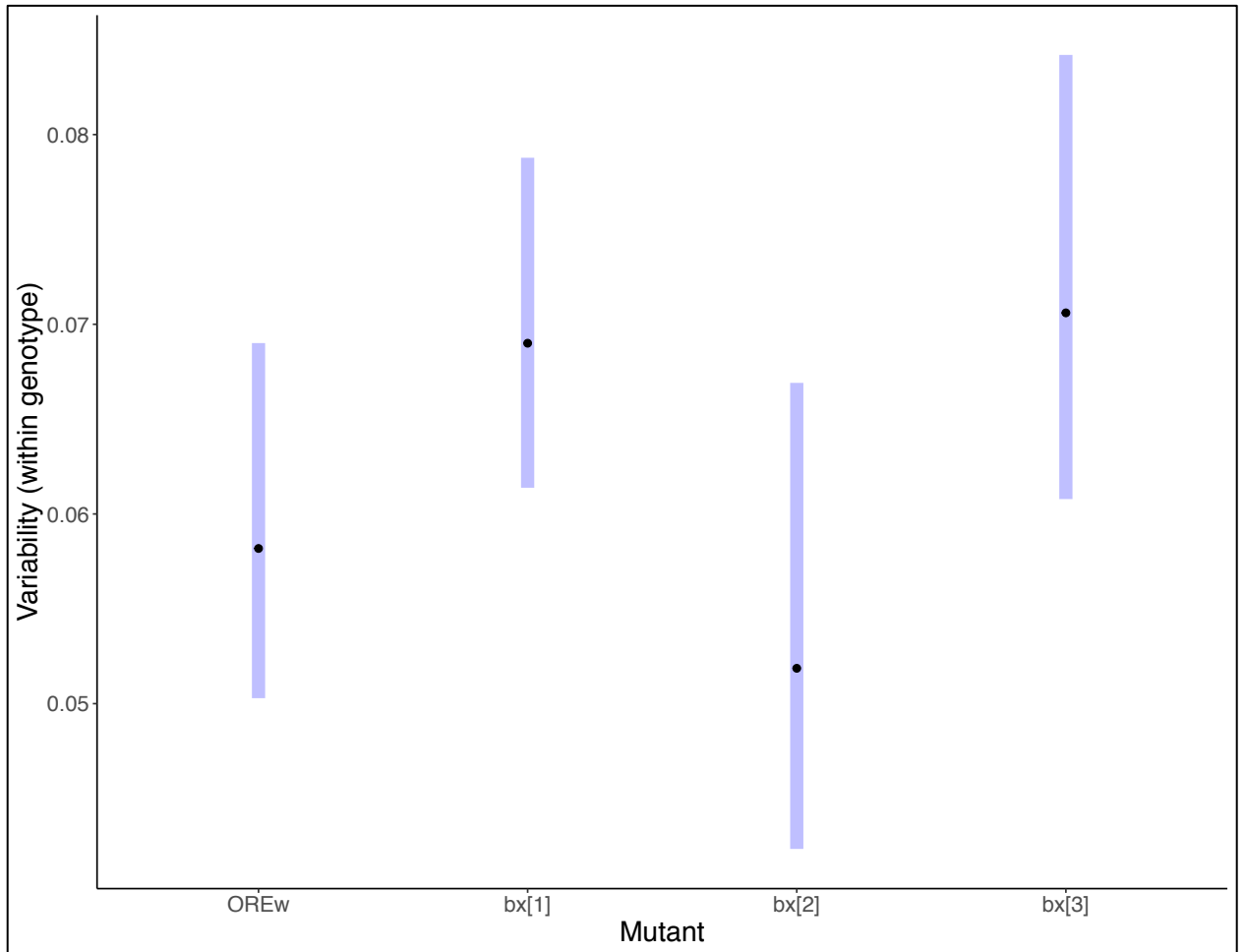


Figure 3.35: The mean variability effect of each *beadex* mutant allele in 20 DGRP strains.

Levene's means reflect fixed model estimates (Table 3.9). Error bars represent 95% CI. N

=2494.

**Among line variability in environmental sensitivity (variation within lines) across
scalloped mutant alleles**

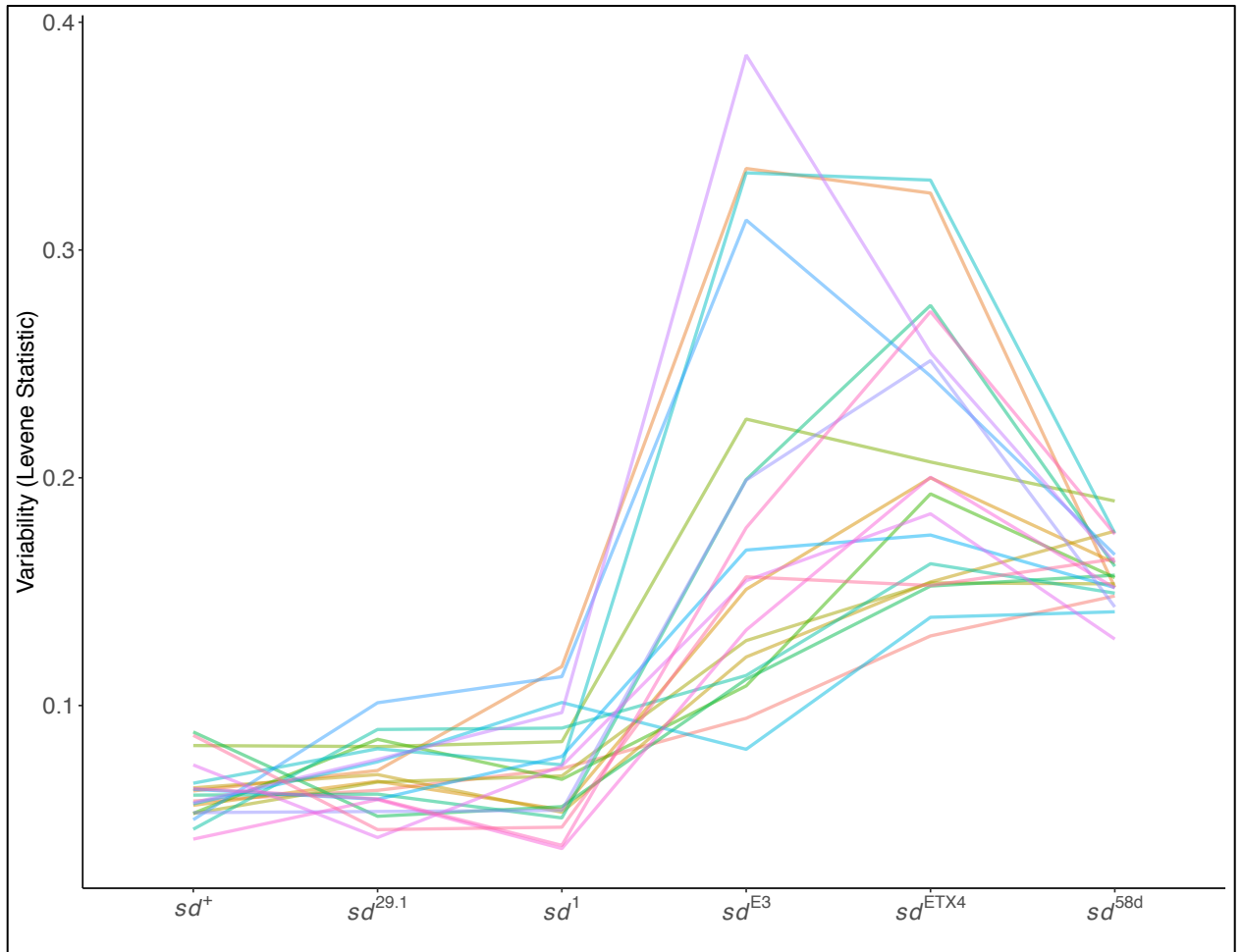


Figure 3.36: A reaction norms plot showing the intra-line variability in *scalloped* mutant wing size among 20 DGRP strains. Lines represent model adjusted Levene's means for each mutant allele (Table 3.9). N=3632.

Intra-line variability in wing size among *beadex* mutant alleles

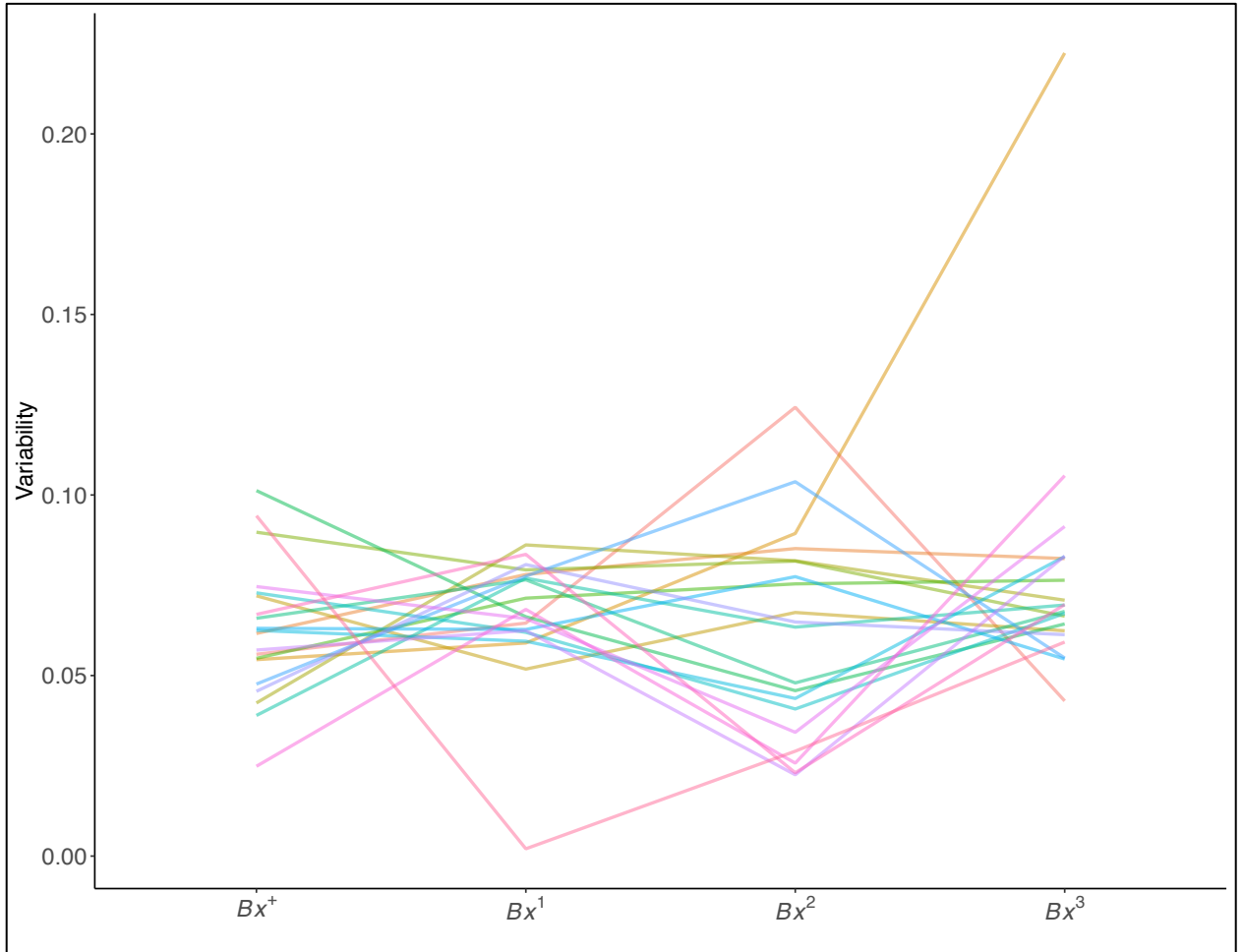


Figure 3.37: A reaction norms plot showing the intra-line variability in *beadex* mutant wing size among 20 DGRP strains. Lines represent raw Levene's means for each mutant allele (Table 3.9).. N=2494.

Correlation of intra-line variability and wing size among *beadex* mutant alleles

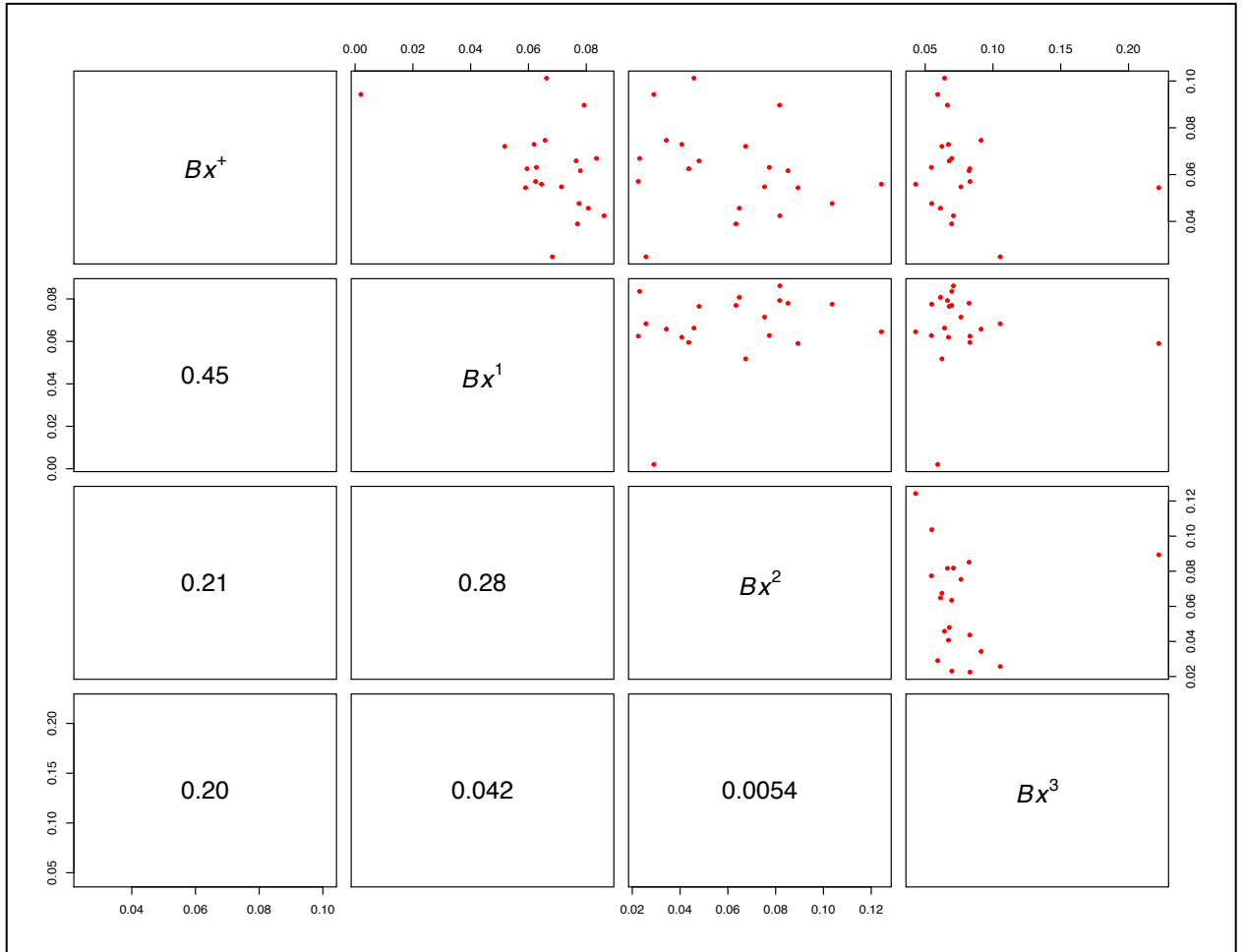


Figure 3.39: Correlation values among *beadex* mutant alleles for Levene's statistic and in 20 DGRP strains. Each blue dot represents the raw means for a unique DGRP strain. N= 2494. Pearson's correlation: $bx[+]:bx[1]$, $P= 0.04$.

Titrated knockdown of *scalloped* and *vestigial* expression

One proposed explanation for background dependence is that the sensitivity of a mutant allele to background dependence may be embedded in genetic architecture of its respective trait. As such, background dependent phenotypic variance may reflect strain specific robustness, or tolerance, to perturbed gene activity of either the focal gene or compensatory genes in the gene network. Given that developmental genes often exhibit functional threshold boundaries, gene regulatory networks are consequently characterized by ubiquitous, nonlinear quantitative relationships between genes and gene products. As such, the apparent strain specific sensitivity to mutation, or genetic background effects, may be due to intrinsic differences in the threshold ranges of genes in each strains network. To examine whether background dependence can be explained by naturally occurring variation in gene expression, we designed an experiment using RNA-interference and temperature manipulation to overexpress and knock down the expression of two functionally related genes, *scalloped* and *vestigial*, in two wildtype laboratory strains (Samarkand and Oregon-R). Given the functions of *scalloped* and *vestigial* are closely linked during development, the parallel function of these genes may make them more likely to exhibit a similar relationship than genes with functions more distantly related. Our experimental design was to use qPCR to monitor transcript expression of both genes in both strains, as well as several other genes within the regulatory networks (to examine potential compensatory responses), in third instar imaginal wing discs. We would then compare the gene expression data to the respective

adult wing phenotypes. Unfortunately, due to unforeseen circumstances, we only collected adult phenotype data of *scalloped* and *vestigial* knockdowns. Observation of our *nubbin*-Gal4 driver with the *vestigial* overexpression lines revealed an unreported expression pattern in segments of the legs. Consequently, ectopic expression of *vestigial* in the legs resulted in mature pupae with severe defects in many of the leg segments (in both strains), preventing them from successfully eclosing. However, manual dissection of mature pupae from the pupal case also revealed viable progeny with severely perturbed wing tissue at 16, 18, 21 and 24 degrees. Wings were not suitable for dissection, as their wings did not undergo wing expansion. Observation of our *nubbin*-Gal4 driver with the *scalloped* overexpression lines at 16, 18 and 21 degrees showed all but absent wing tissue, much of which appeared to be transformation of wing to cuticle tissue. Wings among all temperatures were so severely perturbed they could not be accurately dissected. Interestingly, *scalloped* overexpression with the *nubbin*-Gal4 driver showed differences in lethality among different temperature regimes and between strains. In Oregon, *scalloped* overexpression with the *nubbin*-Gal4 driver was viable at 16, 18 and 21 degrees. However, the same cross in the Samarkand strain was only viable at 16 degrees. Examination of Samarkand vials at 18 and 21 demonstrated most die during second instar, although rare occurrences of dead third instar larvae and prepupae were also observed. Two other *vestigial*-Gal4 drivers were also tested, however crosses with both *vestigial*-Gal4's to a UAS-*GFP* revealed an incomplete expression pattern in the wing pouch (making them unsuitable for our experiment).

Knockdown *scalloped* and *vestigial* with the *nubbin*-Gal4 demonstrated varying results with regard to wing size and background dependence. The phenotypic range among differing temperature regimes for *vestigial* knockdowns was much narrower than the phenotypic range observed for *scalloped*. Effects of the *vestigial* RNAi on wing size were substantially stronger than expected, even for flies reared at 16°C. The goal of the temperature regimes was to titrate the knockdown such that the lower regime would produce flies with phenotypes that overlapped wildtype. However, the effects of the *vestigial* knockdown never overlapped with the wildtype phenotype in either strain, even at 16°C (Figure 3.40). Interestingly, among temperature regimes that demonstrate severe reductions in wing size (18-29°C) mean estimates of wing size were very similar between strains. Yet the magnitude of difference in mean size effects increases as phenotypic estimates become more moderate (16°C). At 16°C, the higher estimate of mean wing size in Samarkand does not overlap mean wing size in Oregon, whereas mean size estimates overlap at all other temperatures. The regression model for *vestigial* knockdown overestimated the slopes and differences between strains, indicating a poor fit (figure not shown). Another notable result is differences in plasticity between the wildtype strains. Among different temperature regimes, the magnitude of difference in mean wing of size between strains varied with temperature.

The phenotypic range among *scalloped* knockdowns was much more complete, and mean size estimates at 16°C were either close to, or overlapped wildtype (Samarkand and Oregon, respectively) (Figure 3.41). Interestingly, the estimates of

scalloped knockdown wing size was greater in Oregon than Samarkand at the lower temperature regimes (16°C, 18°C), yet among the highest temperatures (24°C, 29°C), the reciprocal is true. Estimates of wing size also overlap less at the two temperature extremes. Together, this indicates a discrepancy in the general magnitude of difference in mean wing size among temperatures between Oregon and Samarkand (Figure 3.42).

Mean wing size in Oregon and Samarkand by *nubbin-GAL4 / UAS-vg.RNAi*

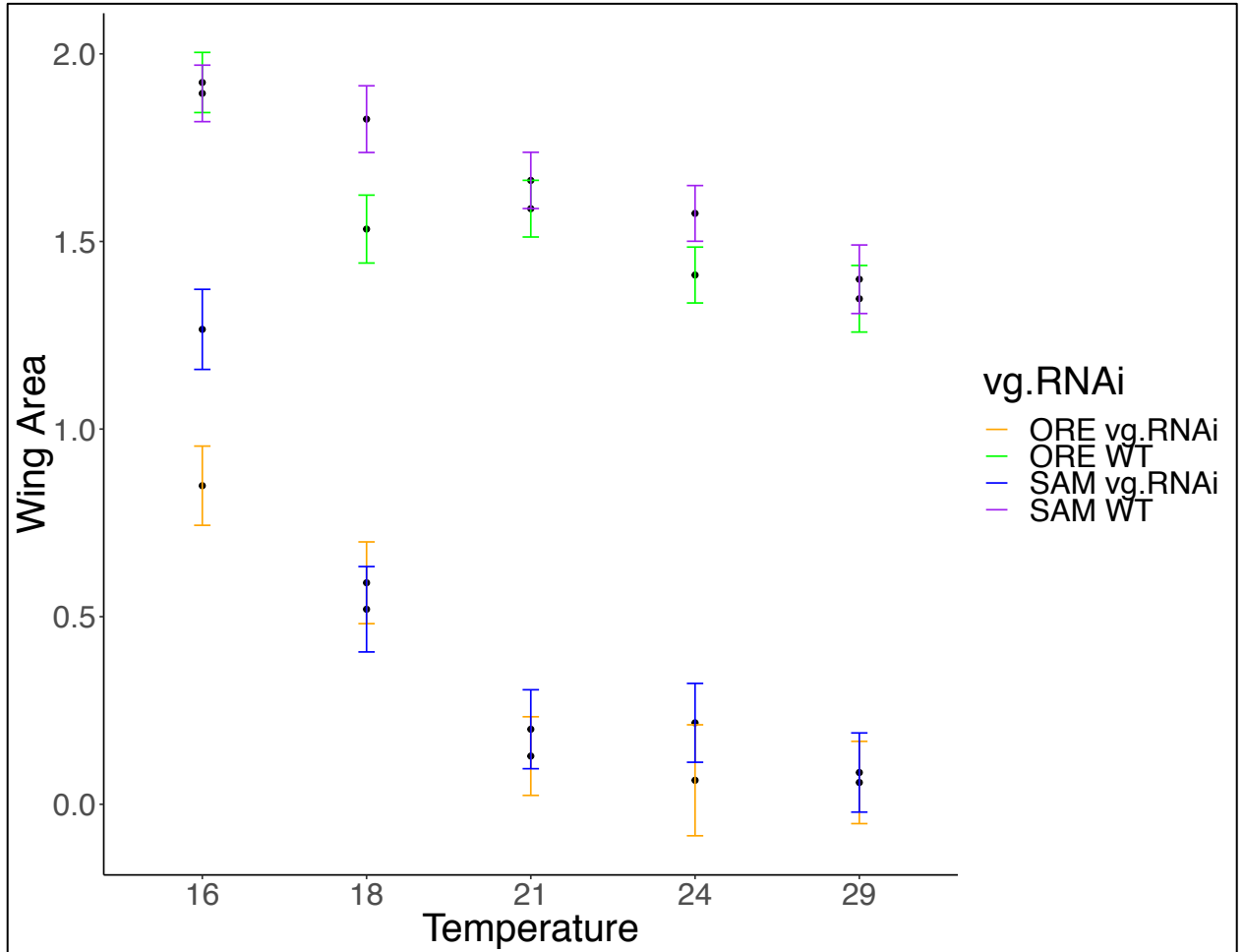


Figure 3.40: Model adjusted estimates of mean wing size by *scalloped* knockdown with *nubbin-Gal4* driver, at differing temperature regimes. Error bars represent 95% CI.

Oregon, N= 132, Samarkand, N= 137.

Mean wing size in Oregon and Samarkand by *nubbin-GAL4 / UAS-sd.RNAi*

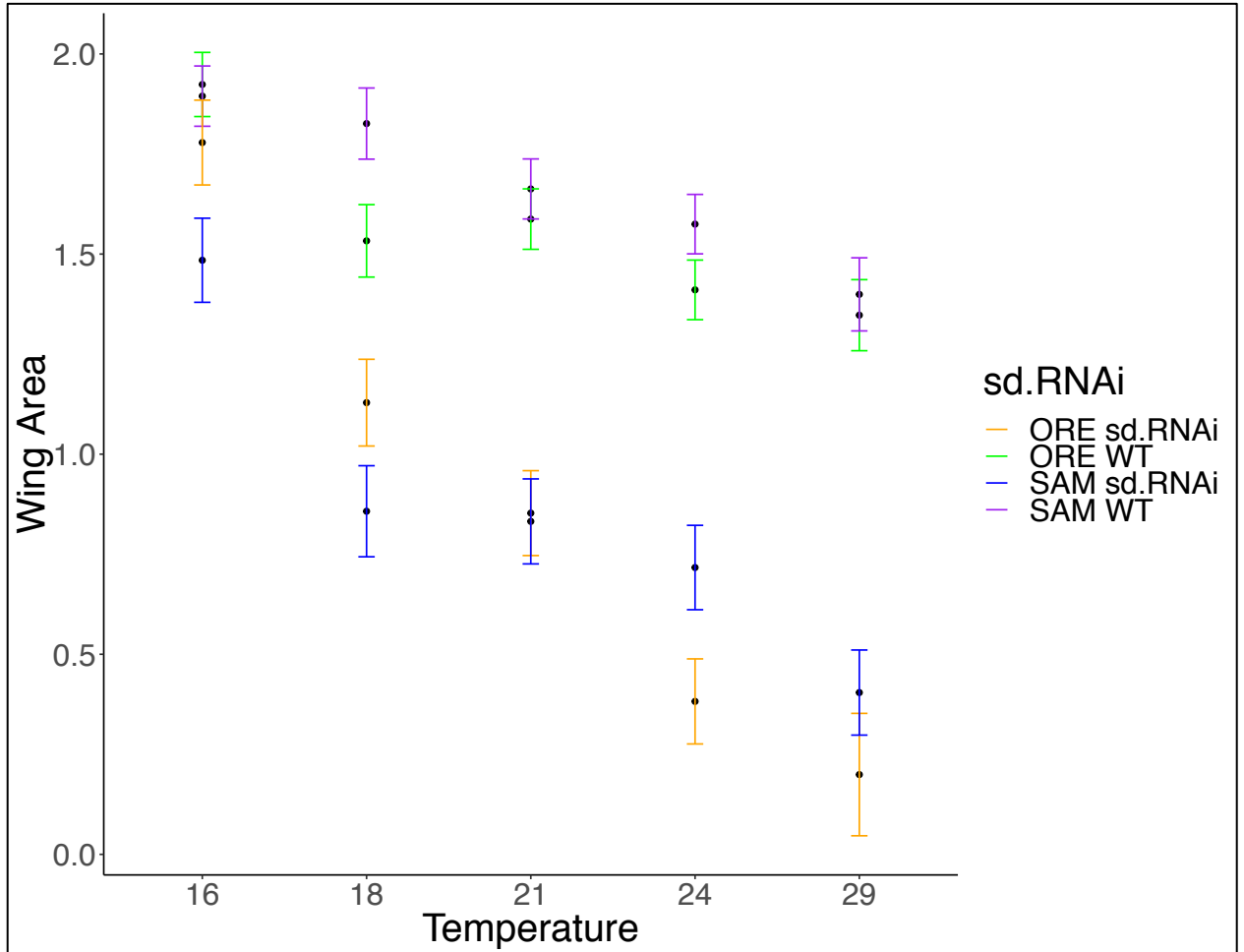


Figure 3.41: Model adjusted estimates of mean wing size by *vestigial* knockdown with the *nubbin-Gal4* driver, at differing temperature regimes. Error bars represent 95% CI.

Oregon, N= 113, Samarkand, N= 135.

Temperature modulation of *scalloped* expression by *nubbin* GAL4/ UAS-*sd.RNAi*

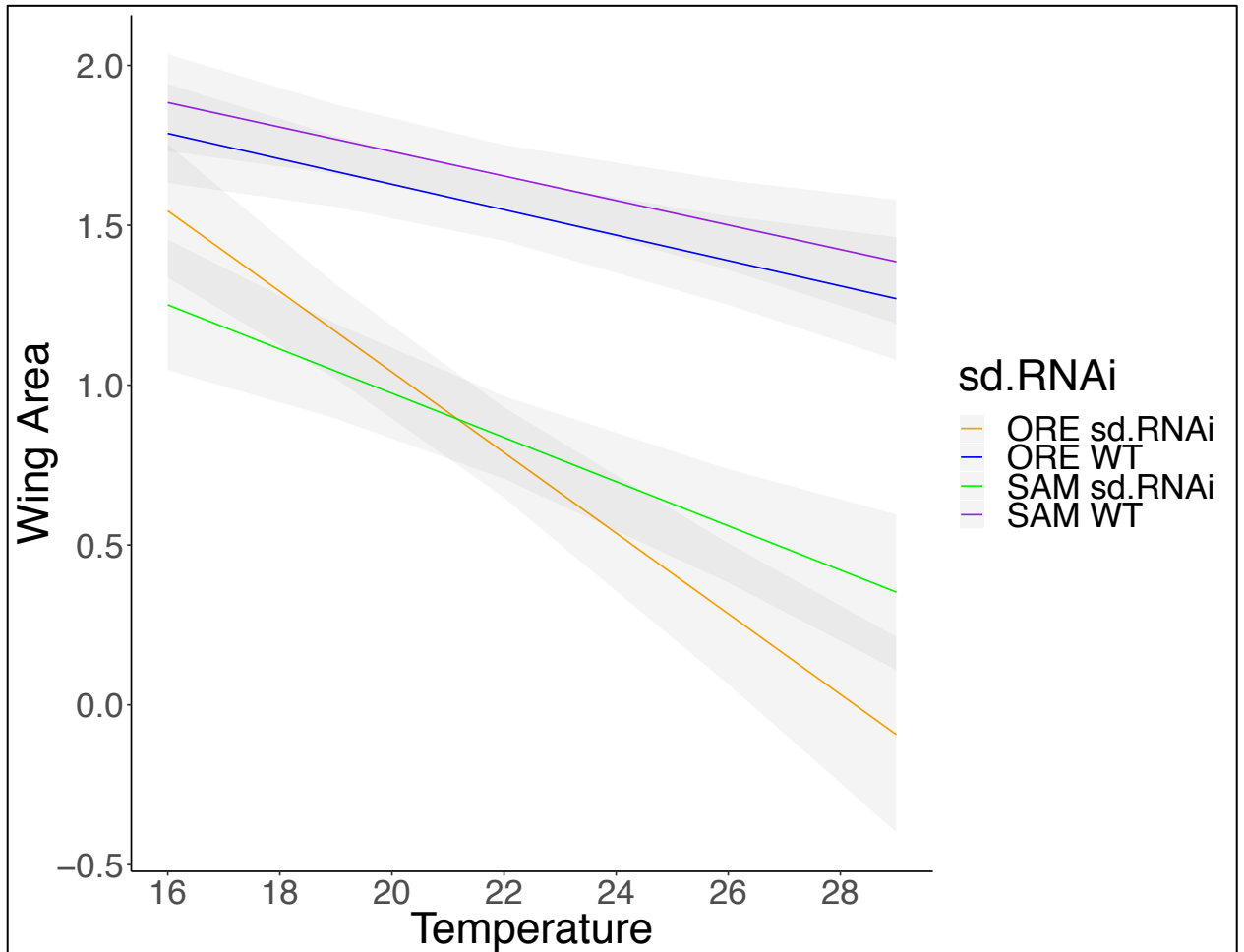


Figure 3.42: Estimated regression of titrated knockdown of *scalloped* expression by via *nubbin* Gal4 at differing temperature regimes, in two genetically distinct wildtype strains. Grey areas represent 95% confidence regions. Oregon, N= 113, Samarkand, N= 135.

4.0 Discussion

Phenotypic analysis of *scalloped*, *beadex*, *cut* and *bifid*

Previous work has demonstrated that background dependence of several alleles in two functionally related *Drosophila* wing genes, *scalloped* and *vestigial*, exhibit a correlated response to background dependence (Chandler et al., 2017). An allelic series in both genes also suggested a predictive relationship between the magnitude of phenotypic effect of a mutant allele and its magnitude of background dependence, irrespective of the identities of the alleles within its genotype (Chandler et al., 2017). However, it was unclear whether this attribute was generalizable to other alleles or genes that function in the regulatory network. Here we have analyzed the phenotypes in hemizygous males for several X-chromosome linked genes in the wing regulatory network, including *cut*, *beadex*, *bifid* (*omb*), as well as additional *scalloped* alleles, among many genetically distinct inbred DGRP wild type strains. All F1 mutant hemizygous males we analyzed were genetically identical except for their respective Oregon-R mutant allele in our focal genes, and unique autosomal DGRP chromosomes. Every individual was heterozygous on the autosomes for a given DGRP strain and the shared Oregon-R strain. Wing size was used as a proxy to assess degree of perturbation. For *scalloped* lethal alleles, progeny were screened for any viable hemizygous males, and count data of the relative number of males and females that successfully eclosed and was documented in blocks three and four (Supplemental Figure 1). We also reanalyzed our results by contrasting the quantitative measures of wing size to a scoring system on a

semi-quantitative scale. A second study repeating the quantitative analysis was also done with the *beadex* and *scalloped* alleles in a subset of 20 DGRP lines included in the original study.

One aim of this study was to confirm if alleles with moderate phenotypic effects exhibit more background dependence than alleles weak or severe effects, as demonstrated by Chandler et al. (2017). In our first study, estimates of mean wing size among all DGRP strains was increased in *sd[E3]* and *sd[ETX4]*, relative to *sd[1]* and the control (Table 3.1). Similarly, mean wing size estimates for *sd[E3]* and *sd[ETX4]* in our second study were intermediate of estimates for weak alleles (control, *sd[29.1]* and *sd[1]*), and the severe allele (*sd[58d]*) (Table 3.9). Variances for *sd[E3]* and *sd[ETX4]* were also notably increased in both studies compared to other alleles. In fact, variances of the moderate alleles were always at least twice as high as for the weak allele (*sd[1]*), and in the first study, the variance of *sd[E3]* was 5 times higher than that of *sd[1]* (Table 3.1). Taken together, estimates of mean wing size and variance confirm *sd[E3]* and *sd[ETX4]* exhibit moderate phenotypic effects relative to other *scalloped* alleles in both studies, and more notably, exhibit increased background dependent phenotypic variance than alleles at either end of the phenotypic spectrum. One interesting contrast of our study with Chandler et al. (2017) is we observed a much greater range in phenotypes among the DGRP strains, considering all *scalloped* Oregon mutant alleles. The increase in phenotypic range among DGRP strains relative to the same mutant alleles in the Samarkand strain (Chandler et al. 2017) suggests the presence of a recessive enhancer

allele not present in the Samarkand strain, as all DGRP crosses were heterozygous on the autosomes. This might also explain why none of the genetic variation in the DGRP strains rescued any of the lethal *scalloped* alleles, despite the fact we see decreased severity of the other *scalloped* mutants among a select few DGRP strains. These same alleles showed some “escapers” in both the pure Samarkand and Oregon-R strains used in Chandler et al. (2017). Additionally, the discrepancy between modulation of the severe wing phenotypes and lethal phenotypes indicates an independence between compensatory mechanisms that underline the modulation of viability and wing development.

For other genes, the relationship between the magnitude of phenotypic effect and variance was less clear. For the *cut* alleles, variance marginally increased with increased estimates of mean wing size (Table 3.2). However, estimates of mean wing size for both *cut* alleles compared to the wildtype indicate the effects on wing size of the mutants are relatively small, and the estimate of variance for the wildtype control is actually higher than for the weakest allele (*cut[K]*). Moreover, wing size in both mutant alleles overlapped wildtype estimates in some of the DGRP strains, indicating the mutational effects of the *cut* alleles included in our study may only be reflective of mutational effects on the weaker end of the phenotypic spectrum. In *beadex*, estimates of mean wing size for each allele was similar between studies, yet estimates of variances differ. While variances estimate in the original study are similar among alleles, the magnitudes of the variances between alleles are somewhat different in the second

study. This indicates the original panel of 20 DGRP strains, used to analyze the *beadex* mutants did not capture the full spectrum of phenotypic effects, especially since the *beadex* alleles exhibited modest correlations with the *scalloped* alleles (and the DGRP strains of the second study were chosen to reflect a complete phenotypic spectrum of *scalloped*). One concern of the original study was the care taken among experimenters to accurately phenotype the *cut* and *beadex* alleles. The ImageJ macro is extremely sensitive to the quality of the image and wing dissection (i.e. dissecting the whole wing, and only wing tissue), especially with regard to any residual cuticle tissue attached to the wing. For alleles with weak effects on wing tissue (as is the case with most of alleles in our studies), any presence of non-wing tissue will compromise true estimates of wing area and obscure any subtle perturbations. While I dealt with this for all the data I collected, this may not have been the case for the experiments performed by the collaborating undergraduates. Thus, prior to submitting this work for peer reviewed publication, images from the undergraduates will be checked and debris digitally removed if necessary.

Another biological consideration when interpreting our results is the mutational effects on wing size of alleles in our study was more limited than expected. Alleles in *cut* and *bifid* only exhibited weak phenotypic effects, and only the allelic series in the *scalloped* gene demonstrated a full range of weak to severe phenotypic effects. This is reflected in comparisons of mean wing size estimates. Given the magnitude of background dependent variance for wing size in the weak *scalloped* alleles, it may not be

surprising that the relationship between wing size and variance was not observed for any of the alleles in other genes. One concern of our analysis with our weaker effect alleles was how well wing area captured subtle phenotypic effects, particularly with respect to the weak phenotypic effects of the *bifid* alleles. Estimates of mean wing size for *bifid* alleles were not statistically different from one another, which is thought to reflect that *bifid* mutants often exhibited venation defects, rather than any perturbations to wing size (which was not clear prior to this study). For *scalloped*, particularly *sd[1]*, weak phenotypes often presented as bristle loss only along the margin of the wing or minor perturbations to distal wing tissue. As such, estimates of wing size among these alleles may be reflecting natural variation in wildtype wing size among DGRP strains, rather than any perturbation effects, and/or underestimate the magnitude of mutational effects among strains. This was partly addressed by conducting semi-quantitative analysis of the *scalloped* and *bifid* alleles with two separate semi-quantitative scales. A wing score was assigned to all *bifid* alleles and *scalloped* samples of the original study, including (*sd[+]*, *sd[1]*, *sd[E3]* and *sd[ETX4]*). The scoring systems were representative of the range of phenotypes of all alleles for each respective gene and higher scores indicate a more severe phenotype (Supplemental Figure 1). In *scalloped*, the quantitative estimates of wing size were highly correlated with wing scores (corr = 0.89). However, there were discrepancies in the degree of correlation among alleles. While estimates of wing size and wing scores in *sd[E3]* and *sd[ETX4]* were highly correlated, correlation was lower in *sd[1]*. Similarly, correlation in the semi-

quantitative and quantitative measures of the *bifid* alleles was low. This was expected, as estimates of mean wing size were not different among *bifid* alleles, yet the semi-quantitative approach demonstrated significant differences in their phenotypic effects (figure).

These differences may be interpreted in two ways. On one hand, differences in correlations for *scalloped* may reflect experimenter error, such that scoring of phenotypes with moderate or severe effects was more accurate than the scoring of phenotypes with weaker effects. On the other hand, the semi-quantitative scale is thought to have been successful in capturing the background dependence of weak phenotypes clouded by quantitative approach. This is the preferred interpretation, as qualitative observation showed there were many more observable perturbations to all *bifid* and *sd[1]* wings than wildtypes, despite the relative similarities in mean wing size estimates. Assigning wing scores to the other weak mutant alleles of this study may also expose more phenotypic variance than estimates of wing size indicate, and the results from the semi-quantitative wing scores did suggest a much greater degree of correlation among alleles. This, in combination with the increase in correlations in the second study, suggests that there are biologically meaningful correlations among mutant alleles within and between genes, but even greater care in experimental design and assessing phenotypic effects must be considered.

An unlikely but alternative explanation for limited phenotypic variance observed among the *beadex* and *cut* alleles is phenotypic variance may be constrained by pleiotropy of each gene. In addition to their roles in wing development, *beadex* and *cut* have functional roles in the development of other *Drosophila* traits. *beadex* activity is necessary for leg and ovum development, as well as the behavioral response to ethanol (Kairamkonda & Nongthomba, 2018; Pueyo & Couso, 2004). *cut* has a functional role in the development of Malpighian tubules, the central nervous system, and many sensor organs including the antenna and auditory organs (Blochlinger, Jan, & Jan, 1974; Dong, Dicks, & Panganiban, 2002; Ebacher, Todi, Eberl, & Boekhoff-Falk, 2007). The pleiotropic effects of these genes suggests their molecular functions are fundamental biological machineries, involved in many developmental processes (He & Zhang, 2006). This is true for *beadex*, which encodes a LIM protein containing a double-zinc finger motif that is vital to many protein-protein interactions (Milan et al., 1998). Limited phenotypic variance of *beadex* and *cut* in the wing may thus reflect an evolutionary compromise, dependent on how deleterious their mutant alleles historically have been to the development of other traits. If this is the case, innate constraints on phenotypic effects in the wing may be higher for *beadex* and *cut* compared to *scalloped*, limiting the magnitude of phenotypic variance possible. Although this explanation is a possibility, other caveats we mention, including limited phenotypic range and poor quality control of phenotypic analysis, we believe better explain the limited range of phenotypic variance among alleles of among these genes.

Despite the limited phenotypic range of most of the genes in our studies, one notable result was correlations for wing size among alleles of the same gene were generally high. In contrast, although correlations among how the DGRP responded to mutations were positive, generally speaking correlations between alleles in different genes were often of very small or modest effect. Correlations to background dependence among alleles between genes also demonstrates an inconsistent relationship between the magnitude of phenotypic effect and a correlated response to background dependence. While alleles of the same gene in similar phenotypic classes tend to be highly correlated, correlations in background dependence between genes are variable. For example, all alleles in each *scalloped* phenotypic class (weak, moderate, severe) were highly correlated, as were both weak *cut* alleles, both weak *beadex* alleles and both moderate *bifid* alleles. However, comparisons of the *scalloped* and *bifid* wing scores indicate correlations are weak to moderate at best, regardless of phenotypic class. In *scalloped*, the correlation of background effects was highest among the moderate alleles, which were significantly correlated in both studies (Corr = 0.82 & 0.85). Wing size estimates of both weak alleles were also significantly correlated, as was the correlation between the stronger moderate allele (*sd[ETX4]*) and the severe allele. Most of the other correlations among *scalloped* alleles were moderate to high between studies. In *cut*, correlation between the two mutant alleles was significant (corr = 0.82). The *Beadex* mutant alleles also significantly correlated in the first study ($bx[1]:bx[2]= 0.89$, $bx[1]:bx[3]= 0.92$, $bx[2]:bx[3]= 0.73$), with similar (but slightly reduced)

correlations in the second study (Figure 3.33). Reduced correlations in the second study are thought to reflect decreased control of environmental conditions.

In block two, all *scalloped* and *beadex* vials were exposed to an unintentional temperature increase (<28 degrees) for an unknown amount of time. Given the sensitivity of these mutants to environmental effects (as discussed further down), this probably compromised some of the correlations. Interestingly, mean size effects of *bx[3]* was significantly correlated with *sd[ETX4]* (corr = 0.44), and moderately correlated with *sd[E3]* (0.36). As all three alleles fall into the moderate phenotypic class (which we later discuss are more sensitive to environmental effects), high correlations may indicate a similar response to perturbed environmental conditions. Unfortunately, convergence errors emerged when modeling estimates of random effects for the model, so this is inconclusive. One caveat is *bx[1]* remained significantly correlated for all *scalloped* alleles except *sd[1]*, so correlations are probably not completely explained solely by similarities in magnitude of phenotypic effect. Given the lack of variation in mean wing size estimates among *bifid* alleles, quantitative correlations for *bifid* alleles were ignored. However, correlations in mean wing score for *scalloped* and *bifid* were computed. For *scalloped*, the correlation between the two moderate alleles was essentially the same for estimates of wing size and wing scores (4% increased correlation in wing scores). Strikingly, correlations of both moderate alleles with *sd[1]* increased significantly, by about 40%. The dramatic increase in correlation likely reflects the increase in observable phenotypes for *sd[1]* with semi-quantitative analysis. In *bifid*,

most of the alleles are significantly correlated, except *bifid[1]* is only correlated with *bi[QD]*. The discordance in background dependence between *scalloped* and the other genes, but similar response between *scalloped* and *vestigial* in other work, may be because of the close relationship between *scalloped* and *vestigial* function. *Scalloped* and *vestigial* function in parallel during wing development, as proteins from both genes together form a transcription factor complex that directly regulates the activity of wing genes downstream (Pimmett et al., 2017; Simmonds et al., 1998). Thus, it might be expected that they or other sets of genes with similar associations, will exhibit comparable attributes of background dependence. Correspondingly, the lack of correlation between *bifid* and *scalloped* may be because the genotypic and phenotypic effects of *bifid* mutants are quite distinct from *scalloped* and the other genes. While *scalloped*, *cut* and *beadex* mutants all perturb wing tissue in the distal regions of the wing, mutant effects of *bifid* mostly manifest in the vein tissue.

Higher correlations in background dependence of among *beadex*, *cut* and *scalloped* alleles may reflect overlap in their developmental programs, and consequently, similar robustness mechanisms to perturbed distal wing tissue. For example, all three of these genes are involved in regulating activity at the D/V boundary of the wing disc. It is known that loss of *scalloped* expression reduces expression of *wingless* at the D/V boundary and restoring *wingless* at the D/V boundary partially rescues the *scalloped* phenotype (Srivastava & Bell, 2003). Correct localization of *apterous* (regulated by *beadex*) is also critical to differentiating the ventral and dorsal

regions of the wing, and consequently distinguish the cell populations that make up these regions. Moreover, *apterous* selects genes involved in distal cell fates (Milán & Cohen, 2003). *Cut* also works in a feedback loop with Notch and other wing genes (*serrate*, *delta*) to restrict Notch activity to the D/V boundary (De & Bray, 1997). Interestingly, Notch signalling has been demonstrated to be involved in inducing apoptosis of mistaken cell fates at the D/V boundary (Milán, Pérez, & Cohen, 2002). As such, correlations likely reflect an interaction between similarities to sensitivity to the environment, magnitude of phenotypic effect (as *scalloped* and *beadex* alleles still demonstrate modest correlations in the first study despite temporal separation in experiments), and how closely related the genes are within the regulatory network. Correlations between the *cut* alleles and *sd[1]* were higher than correlations among *bx[1]* and *sd[1]*, despite the temporal separation of experiments with *scalloped* and *cut*, but not *scalloped* and *beadex*.

The central goal of our study was to understand if any predictive or generalizable patterns of background dependence exists with regard to either the phenotypic effects of a mutant allele, or the intragenic relations between genes that function in the same regulatory network. A critical caveat to our study is all genes in the *Drosophila* wing network we included in our study are transcription factors, and on the X-chromosome. These attributes may challenge whether our results are truly generalizable to either more dosage sensitive genes that encode kinases, receptors or second messengers, or autosomal genes which do not already have innate properties of dosage compensation.

Genes on the X-chromosome in *Drosophila* are likely biased towards canalized dosage compensation, as dosage compensation is an innate property of the *Drosophila* X-chromosome due to its role in sex determination. The expression of genes on the *Drosophila* X-chromosome is upregulated in male flies to equalize the increased dosage by the activity of two X-chromosomes in female flies (Salz & Erickson, 2010). Despite the fact the alleles in our study were transcription factors on the X-chromosome, the generalizability of our results to autosomal or functionally distinct genes is supported by pre-existing literature. For example, Chandler et al., (2017) demonstrate moderate effect alleles in the second chromosome *vestigial* gene (another transcription factor in the *Drosophila* wing regulatory network), are more sensitive to background dependence, which is congruent with the increased background dependence of moderate alleles in the X-chromosome *scalloped* and *beadex* alleles included in our studies. The phenotypic response of alleles in *scalloped* and *vestigial* also exhibit a high degree of correlation to background dependence, echoing the intergenic correlations we observed among the *beadex*, *bifid*, *cut* and *scalloped* alleles. Polaczyk, Gasperini and Gibson (1998) also demonstrate the phenotypic effect of two mutant alleles in two genes, *eclipse* and *seven*, are highly correlated among the seventeen genetically distinct inbred *Drosophila* strains they assessed. Notably, *eclipse* and *seven* are dosage sensitive kinases that function in the signal transduction pathway controlling determination of the identity of the R7 photoreceptor in the *Drosophila* eye genes. Their results, in conjunction with our study, supports the notion that intragenic correlations among mutant alleles, and

intergenic correlation to background dependence among genes, is not likely just an attribute of the transcription factors.

The statistical approach we employed to distinguish fixed and random estimates was deliberately used to separate the relative contributions of genetic and environmental effects to the phenotypic variance for each mutant allele. Broad sense heritability estimates indicate contribution of genetic effects to *scalloped* phenotypes was similar between studies. Estimates for both moderate alleles illustrates the contribution of genetic effects was always more deterministic than any environmental effects ($H^2 > 0.5$), regardless of the study or analysis of wing size or wing scores. This was a marked contrast to contributions of genetic effects to phenotypic variance of other *scalloped* alleles, which never accounted for more than 33% of the phenotypic variance. The discrepancy in sensitivities to genetic effects is thoroughly explained by differences thought to underlying robustness and genetic canalization. It is expected that most strains will be able to mitigate the effects of a weak alleles because their perturbation is minimal in the regulatory network. On the other hand, even the most robust systems are unlikely to overcome drastic reductions in gene activity by severe alleles. Consequently, differences in the degree of genetic canalization or robustness between strains will become most apparent by introduction of a moderate allele that falls somewhere between these two extremes. This phenomenon would also explain the significantly high correlation between *sd[29.1]* and *sd[58d]* wing size and *bi[1]* and *bi[QD]* wing scores, despite these alleles being at opposite ends of the their phenotypic

spectrums. If phenotypic variance is expected to be minimal for alleles with weak or severe effects, a high degree of correlation probably reflects a similar response to size and environmental effects, rather than any modulating activities of the genetic background. Moreover, the rank order of the heritability estimates (estimation of the relative contribution of genetic effects) among the *scalloped* alleles corresponds to an increasing magnitude of perturbation, up to the severe allele, as you would expect; heritability estimates are $sd[29.1] < sd[1] < sd[E3] < sd[ETX4]$, and $sd[58d]$ is most like $sd[29.1]$. For alleles of the other genes, the relationship between heritability estimates and mutant effects is less clear. In *cut*, there is no obvious relationship between mean wing size estimates and the contribution of genetic effects. In *beadex*, heritability estimates were the same for all alleles in the first study, and were mostly similar in the second study. In the second study, the contribution of genetic effects was greatest for the weak allele and least for the moderate allele. Heritability estimates could not be computed for *bifid*, as block was not modeled as a random effect in the study. The inconsistency of this relationship result may be due to the same factors thought to distinguish the unique *scalloped* relationship between mean wing size and phenotypic variance, including reduced representation of phenotypic effects among alleles.

Given that environmental effects were demonstrated to account for most of the phenotypic variation among all genes in our study (as indicated by the heritability estimates), it is evident that these effects are important modulators of the correlation among alleles within and between genes. In the original *scalloped* study, the

contribution of block effects was estimated to be 0.003. This estimate was similar to block effects for the studies with other genes. To put this estimate into context, it is thought that environmental variation introduced approximately as half as much variation into wing size among DGRP strains as the effect of the weak *scalloped* mutation. Taking into account the magnitude of phenotypic variance we observe (especially for the moderate alleles), the contributions of genetic effects indicated by the heritability estimates, and the time needed to complete all blocks, block effects were thought to be relatively modest among our studies. In the second study with *beadex* and *scalloped*, block effects were increased (0.02), despite the shorter time frame between measuring replicate vials. This increase was expected because of the unintentional temperature increase. Additional fluctuations in rearing conditions, such as humidity, food quality, larval density and light cycles, was expected to explain most of the interline variation among otherwise genetically identical individuals.

Although intra-line variation was not the focus of this study, analysis revealed important distinctions between how mutant alleles respond to genetic and environmental effects. This statistical analysis was only possible for *scalloped* and *beadex*, due to the need for large sample sizes for sufficient accuracy of estimates. For *scalloped*, we observe a discrepancy in the magnitude of correlation between $sd[1]$ and the moderate alleles between the two studies, where correlations in intra-line variance was somewhat reduced in the first study (Figures 3.24 and 3.28). This result is not unexpected, as the timeframe of this experiment was much longer (eight blocks over

size months vs. two blocks over two weeks). However, *sd[1]* still demonstrate correlations with the moderate alleles in the first study, and moderate alleles are highly correlated in both studies. Our second study showed that correlations in intra-line variation among the *scalloped* alleles was highest between alleles of adjacent phenotypic classes (i.e. weak alleles best correlated with moderate alleles, and severe alleles best correlated with moderate alleles). Estimates of intra-line variability were highest for the moderate alleles, and the magnitude of difference in intra-line variability among strains was dramatically higher than the weaker *scalloped* alleles. This may reflect the intrinsic robustness of the network to mutations with relatively weak effects, and a limited capacity to modulate severe phenotypic effects. The low correlation among the mutant alleles with the wildtype control illustrates an increased environmental sensitivity of the *scalloped* mutants, rather than any kind of intrinsic sensitivity of their respective wildtype strains. This trend largely echoes the kinds of correlations observed for among line variability (i.e. among line variability and magnitude is highest for alleles with moderate effects, limited correlation of mutants with wildtype). Interestingly, estimates of mean intra-line variation in *beadex* also indicates more intra-line variation in the *bx[3]* (moderate) allele than either of the weak *beadex* alleles, which corresponds with its increase in background dependence. This was not something demonstrated in the original study.

An important consideration of this discrepancy is correlations and comparisons among the *scalloped* and *beadex* alleles is improved because both were analyzed at the

same time, and greater care was taken to measure phenotypic effects. As such, our second study may more reliably report the intergenic correlations and mean estimates of the *beadex* and *scalloped* alleles. Moreover, both the *scalloped* and *beadex* data from the second study support the notion that the sensitivity to variation within and among strains is generally greater for moderate alleles than weak alleles, which counters our speculation from that original data that this relationship may only be characteristic of *scalloped* and *vestigial*, or genes with similar affinities to one another. We also observed a strong positive correlation between the severity of a *scalloped* mutant phenotype (measured by absolute deviation from wildtype), and the degree of intra-line variation, irrespective of allelic effects (Figure 3.27, $r = 0.88$). However, the identity of the mutant does have a significant effect on this relationship ($P=0.01$), and intra-line variation is increased in the moderate alleles. The weak correlations between the intra-line variance of the wildtype strains and their respective mutant alleles also indicates environmental sensitivity is an attribute of mutational effects, rather than any intrinsic sensitivity of a particular strain. This is further supported by the lack of relationship between the magnitude of intra-line variation within the wildtype strain, and the magnitude of deviation of mutant alleles from their respective wildtypes.

To conclude, here we have demonstrated that background dependence of *scalloped*, *beadex*, *cut* and *bifid* is generally well correlated among alleles of the same gene, especially among alleles of similar phenotypic classes (weak, moderate, severe). Similarly, positive correlations among mutant alleles of different genes that function in

the same regulatory network exhibit varying, but often modest correlations. Collectively, data among all genes analyzed suggests that the degree of background dependence and environmental sensitivity of genes that function in the same regulatory network may be predictable, especially if they are in close proximity (as was the case with *scalloped* and *vestigial*, as well as *scalloped* and *cut*). We also confirm in *scalloped* and *beadex* that moderate alleles exhibit a greater degree of sensitivity to background dependence, and in *scalloped*, much of the phenotypic variation of these alleles can be attributed to heritable genetic variation. We also report no rescue of the *scalloped* lethal alleles among any examined DGRP strains, indicating an independence between suppression mechanisms influencing wing development and viability (whatever traits are contributing to lethality). Furthermore, analysis with Levene's statistics and deviations also revealed a strong positive relationship between wildtype wing size and deviation (or severity) among mutant alleles. However, the wildtype condition and sensitivity to either genetic (background dependence) or environmental effects (intra-line variability) is not well correlated with mutant effects. Additionally, high correlations of wing size and wing scores among the *scalloped* alleles indicates an importance and reliability of doing semi-quantitative phenotypic analysis to capture the full spectrum of phenotypic effects. Our data illustrates that estimates of wing size and correlations of background dependence among and between genes was largely consistent across studies. It is expected that going back and improving the quality of phenotypic analysis with the *beadex* alleles will further reflect the repeatability of our results.

Phenotypic analysis of *scalloped* and *vestigial* knockdown

Previous work has demonstrated background dependent differences among *scalloped* and *vestigial* mutants between the Oregon-R and Samarkand strains . On average, the mutation effects of these genes are much greater than Oregon-R than Samarkand. One hypothesis is that the regulatory network of *scalloped* and *vestigial* is less robust to perturbation in Oregon-R than Samarkand, which may be due to intrinsic differences in gene expression of either these focal genes. To test this idea, we knocked down *scalloped* and *vestigial* expression with a nubbin-Gal4 (that expresses ubiquitously in the wing pouch) at different temperature regimes to titrate expression. In *scalloped*, our data demonstrate that the knockdown response at our different temperature regimes differs between backgrounds. In Samarkand, mean estimates of wing size are larger than Oregon-R at both lower temperatures (Figure 3.41). However, at the two highest temperatures, estimates of mean wing size are smaller than Samarkand. This demonstrates that mean wing size in both backgrounds decreases as temperature increases (as expected with increased *scalloped* knockdown), however the slope of this effect is much greater in Oregon-R. (Figure 3.42). This data indicates that although on average, although Oregon-R wings are larger than Samarkand with weak knockdown, the rate at which the wings become perturbed with increasing expression is greater. This suggests an increased sensitivity of Oregon-R to *scalloped* knockdown in accordance with data that demonstrates hypomorphic mutants in *scalloped* in the Oregon-R strain are more severely perturbed. Moreover, the smaller estimates of Samarkand at the

lower temperatures may hint at an increased sensitivity to *scalloped* overexpression, although this hypothesis remains to be tested. Interestingly, the plasticity response to the different temperature regimes among the wildtype controls also differs.

Despite the differences we see between strains for *scalloped* expression, the response to *vestigial* knockdown is similar between strains. The only temperature regime where estimates of mean wing size do not overlap is at 16°C. However, one thing to note is that among temperature regimes, for both strains, *vestigial* knockdown does not even come close to overlapping with the wildtype phenotype. Thus, it is evident our RNAi line driven by the nubbin-Gal4 is very strong, and was unsuccessful at titrating expression to reflect a full range of phenotypic effects (i.e. weak to severe effects). All temperature regimes with the exception of 16°C reflect severe perturbation to wing tissue. This suggests that background dependence when *vestigial* expression is severely perturbed, which is expected given our the general relationship outlined in our hypothetical models (Supplemental figures 3-5). Interestingly, at 16°C, wings are moderately perturbed and we see a clear difference in the size estimates of Samarkand and Oregon-R, whereby the mean wing size of Samarkand is notably larger, and does not overlap with Oregon-R. This result may hint at a potential difference between strains at lower temperatures, such that Samarkand is less sensitive to weak-moderate knockdown. However, this speculation remains to be tested.

References

- Apidianakis, Y., Nagel, A. C., Chalkiadaki, A., Preiss, A., & Delidakis, C. (1999). Overexpression of the *m4* and *mα* genes of the E(spl)-Complex antagonizes Notch mediated lateral inhibition. *Mechanisms of Development*, *86*(1), 39–50. [https://doi.org/10.1016/S0925-4773\(99\)00099-4](https://doi.org/10.1016/S0925-4773(99)00099-4)
- Barkoulas, M., van Zon, J. S., Milloz, J., van Oudenaarden, A., & Félix, M.-A. (2013). Robustness and Epistasis in the *C. elegans* Vulval Signaling Network Revealed by Pathway Dosage Modulation. *Developmental Cell*, *24*(1), 64–75. <https://doi.org/10.1016/j.devcel.2012.12.001>
- Bataillon, T. (2003). Shaking the ‘deleterious mutations’ dogma? *Trends in Ecology & Evolution*, *18*(7), 315–317. [https://doi.org/10.1016/S0169-5347\(03\)00128-9](https://doi.org/10.1016/S0169-5347(03)00128-9)
- Bejarano, F., Luque, C. M., Herranz, H., Sorrosal, G., Rafel, N., Pham, T. T., & Milán, M. (2008). A Gain-of-Function Suppressor Screen for Genes Involved in Dorsal–Ventral Boundary Formation in the *Drosophila* Wing. *Genetics*, *178*(1), 307–323. <https://doi.org/10.1534/genetics.107.081869>
- Bejarano, F., Smibert, P., & Lai, E. C. (2010). MiR-9a prevents apoptosis during wing development by repressing *Drosophila* LIM-only. *Developmental Biology*, *338*(1), 63–73. <https://doi.org/10.1016/j.ydbio.2009.11.025>
- Blochlinger, K., Jan, L. Y., & Jan, Y. N. (n.d.). *Postembryonic patterns of expression of cut, a locus regulating sensory organ identity in Drosophila*. 10.

Boer, T. E. de, Roelofs, D., Vooijs, R., Holmstrup, M., & Amorim, M. J. B. (2018).

Population-specific transcriptional differences associated with freeze tolerance in a terrestrial worm. *Ecology and Evolution*, 8(7), 3774–3786.

<https://doi.org/10.1002/ece3.3602>

Bonyadi, M., Rusholme, S. A. B., Cousins, F. M., Su, H. C., Biron, C. A., Farrall, M., &

Akhurst, R. J. (1997). Mapping of a major genetic modifier of embryonic lethality in TGF β 1 knockout mice. *Nature Genetics*, 15(2), 207–211.

<https://doi.org/10.1038/ng0297-207>

Burnett, C., Valentini, S., Cabreiro, F., Goss, M., Somogyvári, M., Piper, M. D., ... Gems, D.

(2011). Absence of effects of Sir2 overexpression on lifespan in *C. elegans* and *Drosophila*. *Nature*, 477(7365), 482–485. <https://doi.org/10.1038/nature10296>

Bush, W. S., & Moore, J. H. (2012). Chapter 11: Genome-Wide Association Studies. *PLoS*

Computational Biology, 8(12). <https://doi.org/10.1371/journal.pcbi.1002822>

Castellani, C., Cuppens, H., Macek, M., Cassiman, J. J., Kerem, E., Durie, P., ... Elborn, J. S.

(2008). Consensus on the use and interpretation of cystic fibrosis mutation analysis in clinical practice. *Journal of Cystic Fibrosis : Official Journal of the European Cystic Fibrosis Society*, 7(3), 179–196.

<https://doi.org/10.1016/j.jcf.2008.03.009>

Chandler, C. H., Chari, S., Kowalski, A., Choi, L., Tack, D., DeNieu, M., ... Dworkin, I.

(2017). How well do you know your mutation? Complex effects of genetic

background on expressivity, complementation, and ordering of allelic effects.

PLoS Genetics, 13(11), e1007075. <https://doi.org/10.1371/journal.pgen.1007075>

Chandler, C. H., Chari, S., Tack, D., & Dworkin, I. (2014). Causes and Consequences of Genetic Background Effects Illuminated by Integrative Genomic Analysis.

Genetics, 196(4), 1321–1336. <https://doi.org/10.1534/genetics.113.159426>

Chari, S., & Dworkin, I. (2013). The Conditional Nature of Genetic Interactions: The Consequences of Wild-Type Backgrounds on Mutational Interactions in a

Genome-Wide Modifier Screen. *PLoS Genetics*, 9(8), e1003661.

<https://doi.org/10.1371/journal.pgen.1003661>

Connahs, H., Rhen, T., & Simmons, R. B. (2016). Transcriptome analysis of the painted lady butterfly, *Vanessa cardui* during wing color pattern development. *BMC*

Genomics, 17(1). <https://doi.org/10.1186/s12864-016-2586-5>

d'Adda di Fagagna, F. (2014). A direct role for small non-coding RNAs in DNA damage response. *Trends in Cell Biology*, 24(3), 171–178.

<https://doi.org/10.1016/j.tcb.2013.09.008>

De, J. F. C., & Bray, S. (1997). Feed-back mechanisms affecting Notch activation at the dorsoventral boundary in the *Drosophila* wing. *Development*, 124(17), 3241–3251.

Debat, V., Debelle, A., & Dworkin, I. (2009). Plasticity, Canalization, and Developmental Stability of the *Drosophila* Wing: Joint Effects of Mutations and Developmental

Temperature. *Evolution*, 63(11), 2864–2876. <https://doi.org/10.1111/j.1558-5646.2009.00774.x>

Domingo, J., Baeza-Centurion, P., & Lehner, B. (2019). The Causes and Consequences of Genetic Interactions (Epistasis). *Annual Review of Genomics and Human Genetics*, 20(1), null. <https://doi.org/10.1146/annurev-genom-083118-014857>

Dong, P. D. S., Dicks, J. S., & Panganiban, G. (2002). Distal-less and homothorax regulate multiple targets to pattern the *Drosophila* antenna. *Development*, 129(8), 1967–1974.

Dowell, R. D., Ryan, O., Jansen, A., Cheung, D., Agarwala, S., Danford, T., ... Boone, C. (2010). Genotype to Phenotype: A Complex Problem. *Science*, 328(5977), 469–469. <https://doi.org/10.1126/science.1189015>

Dworkin, I., & Gibson, G. (2006). Epidermal Growth Factor Receptor and Transforming Growth Factor- β Signaling Contributes to Variation for Wing Shape in *Drosophila melanogaster*. *Genetics*, 173(3), 1417–1431. <https://doi.org/10.1534/genetics.105.053868>

Ebacher, D. J. S., Todi, S. V., Eberl, D. F., & Boekhoff-Falk, G. E. (2007). Cut mutant *Drosophila* auditory organs differentiate abnormally and degenerate. *Fly*, 1(2), 86–94. <https://doi.org/10.4161/fly.4242>

El-Brolosy, M. A., Rossi, A., Kontarakis, Z., Kuenne, C., Günther, S., Fukuda, N., ... Stainier, D. Y. R. (2018). *Genetic compensation is triggered by mutant mRNA degradation* [Preprint]. <https://doi.org/10.1101/328153>

- El-Brolosy, M. A., & Stainier, D. Y. R. (2017). Genetic compensation: A phenomenon in search of mechanisms. *PLoS Genetics*, *13*(7), e1006780.
<https://doi.org/10.1371/journal.pgen.1006780>
- Estibeiro, J. P., Brook, F. A., & Copp, A. J. (1993). Interaction between splotch (Sp) and curly tail (ct) mouse mutants in the embryonic development of neural tube defects. *Development (Cambridge, England)*, *119*(1), 113–121.
- Félix, M.-A., & Barkoulas, M. (2015). Pervasive robustness in biological systems. *Nature Reviews Genetics*, *16*(8), 483–496. <https://doi.org/10.1038/nrg3949>
- Flatt, T. (2005). The Evolutionary Genetics of Canalization. *The Quarterly Review of Biology*, *80*(3), 287–316. <https://doi.org/10.1086/432265>
- Fowler, J. E., & Freeling, M. (1996). Genetic analysis of mutations that alter cell fates in maize leaves: Dominant Liguleless mutations. *Developmental Genetics*, *18*(3), 198–222. [https://doi.org/10.1002/\(SICI\)1520-6408\(1996\)18:3<198::AID-DVG2>3.0.CO;2-4](https://doi.org/10.1002/(SICI)1520-6408(1996)18:3<198::AID-DVG2>3.0.CO;2-4)
- Gonçalves, E., Carrasquinho, I., St. Aubyn, A., & Martins, A. (2013). Broad-sense heritability in mixed models for grapevine initial selection trials. *Euphytica*, *189*(3), 379–391. <https://doi.org/10.1007/s10681-012-0787-9>
- Green, R. M., Fish, J. L., Young, N. M., Smith, F. J., Roberts, B., Dolan, K., ... Hallgrímsson, B. (2017). Developmental nonlinearity drives phenotypic robustness. *Nature Communications*, *8*(1). <https://doi.org/10.1038/s41467-017-02037-7>

- Guo, T., Lu, Y., Li, P., Yin, M.-X., Lv, D., Zhang, W., ... Zhang, L. (2013). A novel partner of Scalloped regulates Hippo signaling via antagonizing Scalloped-Yorkie activity. *Cell Research*, 23(10), 1201–1214. <https://doi.org/10.1038/cr.2013.120>
- Guss, K. A. (2001). Control of a Genetic Regulatory Network by a Selector Gene. *Science*, 292(5519), 1164–1167. <https://doi.org/10.1126/science.1058312>
- Guss, Kirsten A., Benson, M., Gubitosi, N., Brondell, K., Broadie, K., & Skeath, J. B. (2013). Expression and Function of Scalloped During *Drosophila* Development. *Developmental Dynamics : An Official Publication of the American Association of Anatomists*, 242(7). <https://doi.org/10.1002/dvdy.23942>
- Hallgrimsson, B., Green, R. M., Katz, D. C., Fish, J. L., Bernier, F. P., Roseman, C. C., ... Marcucio, R. S. (2019). The developmental-genetics of canalization. *Seminars in Cell & Developmental Biology*, 88, 67–79. <https://doi.org/10.1016/j.semcdb.2018.05.019>
- Harrison, R., Papp, B., Pál, C., Oliver, S. G., & Delneri, D. (2007). Plasticity of genetic interactions in metabolic networks of yeast. *Proceedings of the National Academy of Sciences*, 104(7), 2307–2312. <https://doi.org/10.1073/pnas.0607153104>
- He, X., & Zhang, J. (2006). Toward a Molecular Understanding of Pleiotropy. *Genetics*, 173(4), 1885–1891. <https://doi.org/10.1534/genetics.106.060269>
- Helwig, U., Imai, K., Schmahl, W., Thomas, B. E., Varnum, D. S., Nadeau, J. H., & Balling, R. (1995). Interaction between undulated and Patch leads to an extreme form of

spina bifida in double-mutant mice. *Nature Genetics*, 11(1), 60–63.

<https://doi.org/10.1038/ng0995-60>

Hoffmann, A. A., Hallas, R., Sinclair, C., & Partridge, L. (2001). Rapid Loss of Stress

Resistance in *Drosophila Melanogaster* Under Adaptation to Laboratory Culture.

Evolution, 55(2), 436–438. <https://doi.org/10.1111/j.0014-3820.2001.tb01305.x>

Højland, D. H., Jensen, K.-M. V., & Kristensen, M. (2014). Adaptation of *Musca domestica*

L. Field Population to Laboratory Breeding Causes Transcriptional Alterations.

PLOS ONE, 9(1), e85965. <https://doi.org/10.1371/journal.pone.0085965>

Houle, D. (1998). How should we explain variation in the genetic variance of traits?

Genetica, 102–103(1–6), 241–253.

Hubbard, J. K., Uy, J. A. C., Hauber, M. E., Hoekstra, H. E., & Safran, R. J. (2010).

Vertebrate pigmentation: From underlying genes to adaptive function. *Trends in*

Genetics, 26(5), 231–239. <https://doi.org/10.1016/j.tig.2010.02.002>

Johnson, K. R., Zheng, Q. Y., & Noben-Trauth, K. (2006). Strain background effects and

genetic modifiers of hearing in mice. *Brain Research*, 1091(1), 79–88.

<https://doi.org/10.1016/j.brainres.2006.02.021>

Kacser, H., & Burns, J. (n.d.). *The Molecular Basis of Dominance*. 28.

Kairamkonda, S., & Nongthomba, U. (2018). Beadex, a *Drosophila* LIM domain only

protein, function in follicle cells is essential for egg development and fertility.

Experimental Cell Research, 367(1), 97–103.

<https://doi.org/10.1016/j.yexcr.2018.03.029>

- Kebaara, B., Nazarenus, T., Taylor, R., & Atkin, A. L. (2003). Genetic background affects relative nonsense mRNA accumulation in wild-type and upf mutant yeast strains. *Current Genetics*, *43*(3), 171–177. <https://doi.org/10.1007/s00294-003-0386-3>
- Keene, J. D. (2007). RNA regulons: Coordination of post-transcriptional events. *Nature Reviews Genetics*, *8*(7), 533–543. <https://doi.org/10.1038/nrg2111>
- Kopp, A., & Duncan, I. (1997). Control of cell fate and polarity in the adult abdominal segments of *Drosophila* by optomotor-blind. *Development (Cambridge, England)*, *124*(19), 3715–3726.
- Korona, R. (1996). Genetic Divergence and Fitness Convergence Under Uniform Selection in Experimental Populations of Bacteria. *Genetics*, *143*(2), 637–644.
- Lessel, C. E., Parkes, T. L., Dickinson, J., & Merritt, T. J. S. (2017). Sex and Genetic Background Influence Superoxide Dismutase (cSOD)-Related Phenotypic Variation in *Drosophila melanogaster*. *G3: Genes/Genomes/Genetics*, *7*(8), 2651–2664. <https://doi.org/10.1534/g3.117.043836>
- Li, L., Lyu, X., Hou, C., Takenaka, N., Nguyen, H. Q., Ong, C.-T., ... Corces, V. G. (2015). Widespread Rearrangement of 3D Chromatin Organization Underlies Polycomb-Mediated Stress-Induced Silencing. *Molecular Cell*, *58*(2), 216–231. <https://doi.org/10.1016/j.molcel.2015.02.023>
- Liu, X., Grammont, M., & Irvine, K. D. (2000). Roles for scalloped and vestigial in Regulating Cell Affinity and Interactions between the Wing Blade and the Wing

Hinge. *Developmental Biology*, 228(2), 287–303.

<https://doi.org/10.1006/dbio.2000.9939>

Mackay, T. F. C., Richards, S., Stone, E. A., Barbadilla, A., Ayroles, J. F., Zhu, D., ... Gibbs,

R. A. (2012). The *Drosophila melanogaster* Genetic Reference Panel. *Nature*,

482(7384), 173–178. <https://doi.org/10.1038/nature10811>

McCarroll, S. A., & Hyman, S. E. (2013). Progress in the Genetics of Polygenic Brain

Disorders: Significant New Challenges for Neurobiology. *Neuron*, 80(3), 578–587.

<https://doi.org/10.1016/j.neuron.2013.10.046>

Micchelli, C. A., Rulifson, E. J., & Blair, S. S. (n.d.). *The function and regulation of cut*

expression on the wing margin of Drosophila: Notch, Wingless and a dominant

negative role for Delta and Serrate. 11.

Milan, M., Diaz-Benjumea, F. J., & Cohen, S. M. (1998). Beadex encodes an LMO protein

that regulates Apterous LIM-homeodomain activity in *Drosophila* wing

development: A model for LMO oncogene function. *Genes & Development*,

12(18), 2912–2920. <https://doi.org/10.1101/gad.12.18.2912>

Milán, M., Pérez, L., & Cohen, S. M. (2002). Short-Range Cell Interactions and Cell

Survival in the *Drosophila* Wing. *Developmental Cell*, 2(6), 797–805.

[https://doi.org/10.1016/S1534-5807\(02\)00169-7](https://doi.org/10.1016/S1534-5807(02)00169-7)

Montagne, J., Groppe, J., Guillemin, K., Krasnow, M. A., Gehring, W. J., & Affolter, M.

(n.d.). *The Drosophila Serum Response Factor gene is required for the formation*

of intervein tissue of the wing and is allelic to blistered. 9.

- Muller, R. (2006). Dynamic and Compensatory Responses of Arabidopsis Shoot and Floral Meristems to CLV3 Signaling. *THE PLANT CELL ONLINE*, 18(5), 1188–1198.
<https://doi.org/10.1105/tpc.105.040444>
- Nadeau, J. H. (2001). Modifier genes in mice and humans. *Nature Reviews Genetics*, 2(3), 165–174.
- Neretti, N., Wang, P.-Y., Brodsky, A. S., Nyguen, H. H., White, K. P., Rogina, B., & Helfand, S. L. (2009). Long-lived Indy induces reduced mitochondrial reactive oxygen species production and oxidative damage. *Proceedings of the National Academy of Sciences*, 106(7), 2277–2282.
<https://doi.org/10.1073/pnas.0812484106>
- Paumard-Rigal, S., Zider, A., Vaudin, P., & Silber, J. (1998). Specific interactions between vestigial and scalloped are required to promote wing tissue proliferation in *Drosophila melanogaster*. *Development Genes and Evolution*, 208(8), 440–446.
<https://doi.org/10.1007/s004270050201>
- Pejaver, V., Hsu, W.-L., Xin, F., Dunker, A. K., Uversky, V. N., & Radivojac, P. (2014). The structural and functional signatures of proteins that undergo multiple events of post-translational modification. *Protein Science*, 23(8), 1077–1093.
<https://doi.org/10.1002/pro.2494>
- Pimmett, V. L., Deng, H., Haskins, J. A., Mercier, R. J., LaPointe, P., & Simmonds, A. J. (2017). The activity of the *Drosophila* Vestigial protein is modified by Scalloped-

dependent phosphorylation. *Developmental Biology*, 425(1), 58–69.

<https://doi.org/10.1016/j.ydbio.2017.03.013>

Poelwijk, F. J., Krishna, V., & Ranganathan, R. (2016). The Context-Dependence of Mutations: A Linkage of Formalisms. *PLOS Computational Biology*, 12(6),

e1004771. <https://doi.org/10.1371/journal.pcbi.1004771>

Polaczyk, P. J., Gasperini, R., & Gibson, G. (1998). Naturally occurring genetic variation affects *Drosophila* photoreceptor determination. *Development genes and evolution*, 207(7), 462-470.

Pueyo, J. I., & Couso, J. P. (2004). Chip-mediated partnerships of the homeodomain proteins Bar and Aristaless with the LIM-HOM proteins Apterous and Lim1 regulate distal leg development. *Development*, 131(13), 3107–3120.

<https://doi.org/10.1242/dev.01161>

Rossi, A., Kontarakis, Z., Gerri, C., Nolte, H., Hölper, S., Krüger, M., & Stainier, D. Y. R. (2015). Genetic compensation induced by deleterious mutations but not gene

knockdowns. *Nature*, 524(7564), 230–233. <https://doi.org/10.1038/nature14580>

Salz, H., & Erickson, J. W. (2010). Sex determination in *Drosophila*: The view from the top. *Fly*, 4(1), 60–70. <https://doi.org/10.4161/fly.4.1.11277>

Schuermann, A., Helker, C. S. M., & Herzog, W. (2015). Metallothionein 2 regulates endothelial cell migration through transcriptional regulation of vegfc expression.

Angiogenesis, 18(4), 463–475. <https://doi.org/10.1007/s10456-015-9473-6>

- Schultz, B. B. (1985). Levene's Test for Relative Variation. *Systematic Biology*, 34(4), 449–456. <https://doi.org/10.1093/sysbio/34.4.449>
- Shen, J., Dorner, C., Bahlo, A., & Pflugfelder, G. O. (2008). Optomotor-blind suppresses instability at the A/P compartment boundary of the *Drosophila* wing. *Mechanisms of Development*, 125(3), 233–246. <https://doi.org/10.1016/j.mod.2007.11.006>
- Simmonds, A. J., Liu, X., Soanes, K. H., Krause, H. M., Irvine, K. D., & Bell, J. B. (1998). Molecular interactions between Vestigial and Scalloped promote wing formation in *Drosophila*. *Genes & Development*, 12(24), 3815–3820. <https://doi.org/10.1101/gad.12.24.3815>
- Sittig, L. J., Carbonetto, P., Engel, K. A., Krauss, K. S., Barrios-Camacho, C. M., & Palmer, A. A. (2016). Genetic Background Limits Generalizability of Genotype-Phenotype Relationships. *Neuron*, 91(6), 1253–1259. <https://doi.org/10.1016/j.neuron.2016.08.013>
- Srivastava, A. (2004). Molecular and Functional Analysis of scalloped Recessive Lethal Alleles in *Drosophila melanogaster*. *Genetics*, 166(4), 1833–1843. <https://doi.org/10.1534/genetics.166.4.1833>
- Srivastava, Ajay, & Bell, J. B. (2003). Further developmental roles of the Vestigial/Scalloped transcription complex during wing development in *Drosophila melanogaster*. *Mechanisms of Development*, 120(5), 587–596. [https://doi.org/10.1016/S0925-4773\(03\)00037-6](https://doi.org/10.1016/S0925-4773(03)00037-6)

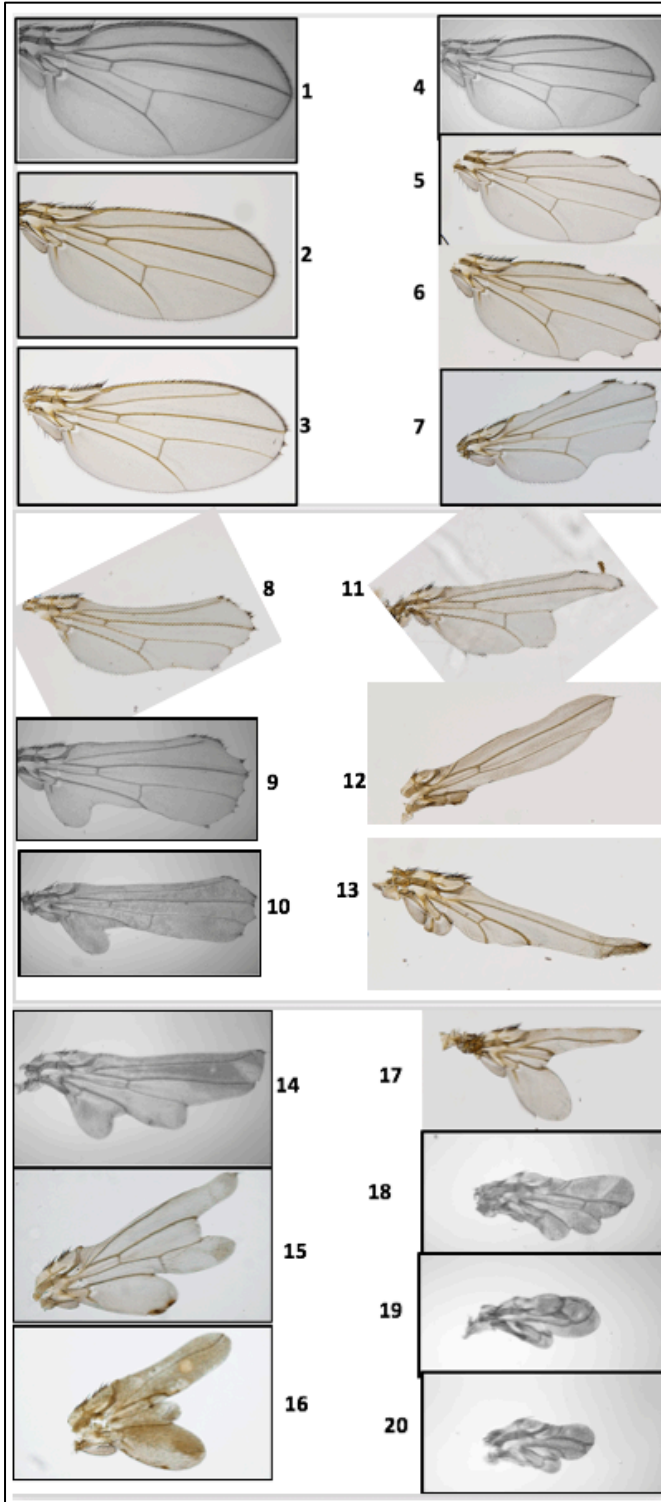
- Strassburg, K., Walther, D., Takahashi, H., Kanaya, S., & Kopka, J. (2010). Dynamic Transcriptional and Metabolic Responses in Yeast Adapting to Temperature Stress. *OMICS: A Journal of Integrative Biology*, *14*(3), 249–259.
<https://doi.org/10.1089/omi.2009.0107>
- Swarup, S., & Verheyen, E. M. (2012). Wnt/Wingless Signaling in *Drosophila*. *Cold Spring Harbor Perspectives in Biology*, *4*(6).
<https://doi.org/10.1101/cshperspect.a007930>
- Tam, V., Patel, N., Turcotte, M., Bossé, Y., Paré, G., & Meyre, D. (2019). Benefits and limitations of genome-wide association studies. *Nature Reviews Genetics*, *1*.
<https://doi.org/10.1038/s41576-019-0127-1>
- Taneja, N. K., Dhingra, S., Mittal, A., Naresh, M., & Tyagi, J. S. (2010). Mycobacterium tuberculosis Transcriptional Adaptation, Growth Arrest and Dormancy Phenotype Development Is Triggered by Vitamin C. *PLOS ONE*, *5*(5), e10860.
<https://doi.org/10.1371/journal.pone.0010860>
- Threadgill, D. W., Dlugosz, A. A., Hansen, L. A., Tennenbaum, T., Lichti, U., Yee, D., ... Magnuson, T. (1995). Targeted Disruption of Mouse EGF Receptor: Effect of Genetic Background on Mutant Phenotype. *Science*, *269*(5221), 230–234.
- Tissenbaum, H. A., & Guarente, L. (2001). Increased dosage of a sir-2 gene extends lifespan in *Caenorhabditis elegans*. *Nature*, *410*(6825), 227–230.
<https://doi.org/10.1038/35065638>

- Ungerer, M. C., Linder, C. R., & Rieseberg, L. H. (n.d.). *Effects of Genetic Background on Response to Selection in Experimental Populations of Arabidopsis thaliana*. 10.
- Wang, P.-Y., Neretti, N., Whitaker, R., Hosier, S., Chang, C., Lu, D., ... Helfand, S. L. (2009). Long-lived Indy and calorie restriction interact to extend life span. *Proceedings of the National Academy of Sciences of the United States of America*, 106(23), 9262–9267. <https://doi.org/10.1073/pnas.0904115106>
- Weihe, U., Milán, M., & Cohen, S. M. (2001). Regulation of Apterous activity in *Drosophila* wing development. *Development (Cambridge, England)*, 128(22), 4615–4622.
- Williams, J. A., Paddock, S. W., & Carroll, S. B. (n.d.). *Pattern formation in a secondary field: A hierarchy of regulatory genes subdivides the developing Drosophila wing disc into discrete subregions*. 14.
- Wright, J., Morales, M. M., Sousa-Menzes, J., Ornellas, D., Sipes, J., Cui, Y., ... Guggino, S. E. (2008). Transcriptional adaptation to Clcn5 knockout in proximal tubules of mouse kidney. *Physiological Genomics*, 33(3), 341–354. <https://doi.org/10.1152/physiolgenomics.00024.2008>
- Yoshiki, A., & Moriwaki, K. (2006). Mouse Phenome Research: Implications of Genetic Background. *ILAR Journal*, 47(2), 94–102. <https://doi.org/10.1093/ilar.47.2.94>
- Ziv, Y., Bielopolski, D., Galanty, Y., Lukas, C., Taya, Y., Schultz, D. C., ... Shiloh, Y. (2006). Chromatin relaxation in response to DNA double-strand breaks is modulated by a

novel ATM- and KAP-1 dependent pathway. *Nature Cell Biology*, 8(8), 870–876.

<https://doi.org/10.1038/ncb1446>

Supplemental Figure 1: *scalloped* semi-quantitative scale



Supplemental Table 1: Count data from crosses with *scalloped* lethal alleles and the control

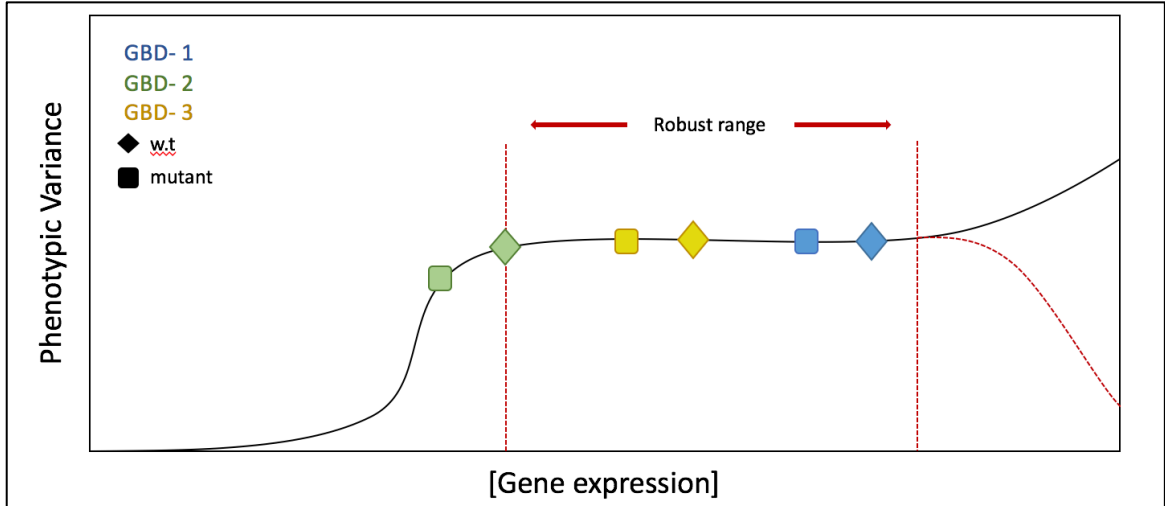
DGRP Line	Mutant	Male	Female	Block
073	sd[G0239]	18	47	B3
069	sd[G0239]	0	0	B3
385	sd[G0239]	17	40	B3
217	sd[G0239]	21	49	B3
235	sd[G0239]	14	26	B3
491	sd[G0239]	18	40	B3
508	sd[G0239]	28	86	B3
517	sd[G0239]	30	64	B3
596	sd[G0239]	6	11	B3
703	sd[G0239]	4	40	B3
765	sd[G0239]	27	66	B3
744	sd[G0239]	7	21	B3
799	sd[G0239]	13	27	B3
808	sd[G0239]	17	47	B3
229	sd[G0239]	21	51	B3
391	sd[G0239]	10	34	B3
208	sd[G0239]	11	17	B3
228	sd[G0239]	13	47	B3
129	sd[G0239]	3	21	B3
913	sd[G0239]	12	38	B3
073	sd[G0483]	17	48	B3
069	sd[G0483]	17	37	B3
385	sd[G0483]	19	43	B3
217	sd[G0483]	28	58	B3
228	sd[G0483]	12	31	B3
235	sd[G0483]	19	29	B3
491	sd[G0483]	17	27	B3
508	sd[G0483]	19	55	B3
517	sd[G0483]	20	60	B3
596	sd[G0483]	3	9	B3
703	sd[G0483]	16	59	B3
765	sd[G0483]	21	58	B3
744	sd[G0483]	29	44	B3
799	sd[G0483]	11	37	B3
808	sd[G0483]	28	59	B3
229	sd[G0483]	16	37	B3
391	sd[G0483]	20	60	B3
129	sd[G0483]	0	0	B3
913	sd[G0483]	10	41	B3
073	sd[G0309]	17	30	B3
069	sd[G0309]	18	29	B3
385	sd[G0309]	13	33	B3
217	sd[G0309]	26	46	B3
228	sd[G0309]	16	23	B3

235	sd[G0309]	27	64	B3
491	sd[G0309]	14	42	B3
508	sd[G0309]	21	39	B3
517	sd[G0309]	12	45	B3
596	sd[G0309]	22	52	B3
703	sd[G0309]	13	49	B3
765	sd[G0309]	24	50	B3
744	sd[G0309]	19	34	B3
799	sd[G0309]	11	26	B3
808	sd[G0309]	7	28	B3
229	sd[G0309]	18	29	B3
391	sd[G0309]	0	0	B3
129	sd[G0309]	12	32	B3
913	sd[G0309]	28	53	B3
073	OREw	0	0	B3
069	OREw	21	26	B3
385	OREw	22	41	B3
217	OREw	16	17	B3
228	OREw	20	15	B3
235	OREw	15	17	B3
491	OREw	27	34	B3
508	OREw	26	31	B3
517	OREw	25	21	B3
596	OREw	17	36	B3
703	OREw	8	13	B3
765	OREw	41	52	B3
774	OREw	30	31	B3
799	OREw	33	36	B3
808	OREw	29	42	B3
229	OREw	20	27	B3
391	OREw	24	27	B3
129	OREw	16	25	B3
913	OREw	26	28	B3
379	sd[G0239]	18	58	B4
392	sd[G0239]	19	50	B4
439	sd[G0239]	12	21	B4
502	sd[G0239]	10	66	B4
757	sd[G0239]	9	19	B4
894	sd[G0239]	2	4	B4
900	sd[G0239]	26	56	B4
911	sd[G0239]	42	55	B4
373	sd[G0239]	21	50	B4
042	sd[G0239]	20	42	B4
083	sd[G0239]	22	55	B4
158	sd[G0239]	27	42	B4

177	sd[G0239]	29	68	B4
195	sd[G0239]	35	71	B4
239	sd[G0239]	31	78	B4
319	sd[G0239]	19	40	B4
348	sd[G0239]	1	6	B4
371	sd[G0239]	29	62	B4
091	sd[G0239]	29	56	B4
057	sd[G0239]	19	39	B4
379	sd[G0309]	36	62	B4
392	sd[G0309]	17	52	B4
439	sd[G0309]	29	63	B4
502	sd[G0309]	14	47	B4
757	sd[G0309]	12	29	B4
894	sd[G0309]	3	4	B4
900	sd[G0309]	16	30	B4
911	sd[G0309]	22	29	B4
373	sd[G0309]	30	59	B4
042	sd[G0309]	33	67	B4
083	sd[G0309]	17	27	B4
158	sd[G0309]	25	51	B4
177	sd[G0309]	21	45	B4
195	sd[G0309]	30	56	B4
239	sd[G0309]	20	66	B4
319	sd[G0309]	14	46	B4
348	sd[G0309]	36	42	B4
371	sd[G0309]	27	46	B4
091	sd[G0309]	21	60	B4
057	sd[G0309]	27	54	B4
379	sd[G0483]	27	65	B4
392	sd[G0483]	8	30	B4
439	sd[G0483]	19	35	B4
502	sd[G0483]	30	56	B4
757	sd[G0483]	6	22	B4
894	sd[G0483]	1	4	B4
900	sd[G0483]	14	24	B4
911	sd[G0483]	22	42	B4
373	sd[G0483]	27	43	B4
042	sd[G0483]	16	49	B4
083	sd[G0483]	13	27	B4
158	sd[G0483]	25	68	B4
177	sd[G0483]	31	56	B4
195	sd[G0483]	27	55	B4
239	sd[G0483]	32	72	B4
319	sd[G0483]	28	44	B4
348	sd[G0483]	16	39	B4

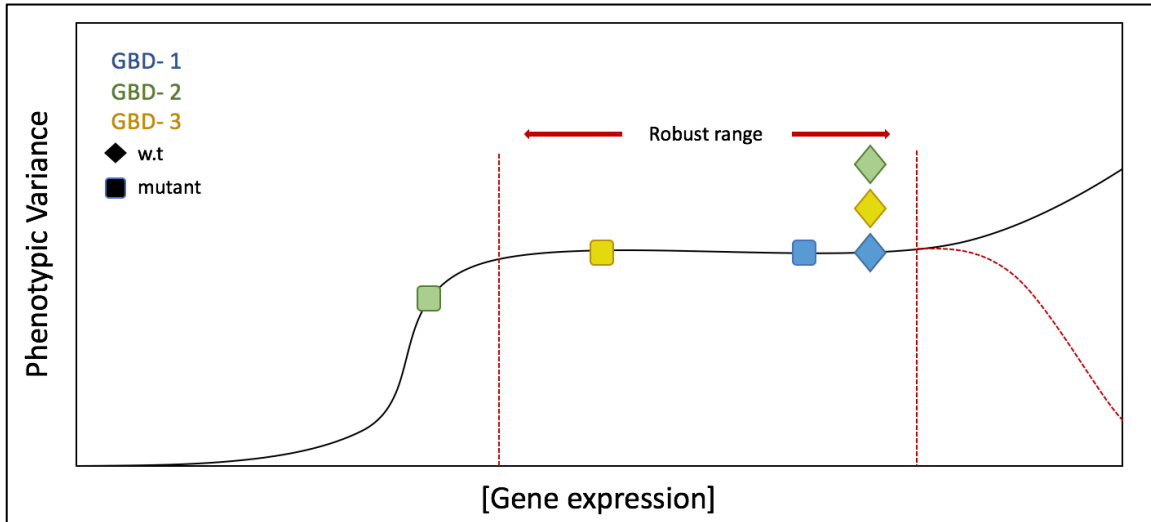
371	sd[G0483]	17	58	B4
091	sd[G0483]	13	22	B4
057	sd[G0483]	18	62	B4
379	OREw	46	58	B4
392	OREw	45	15	B4
439	OREw	39	51	B4
502	OREw	52	47	B4
757	OREw	29	37	B4
894	OREw	0	0	B4
900	OREw	52	49	B4
911	OREw	55	49	B4
373	OREw	35	49	B4
042	OREw	55	52	B4
083	OREw	36	33	B4
158	OREw	40	51	B4
177	OREw	47	50	B4
195	OREw	42	32	B4
239	OREw	51	14	B4
319	OREw	46	53	B4
348	OREw	37	41	B4
371	OREw	33	39	B4
091	OREw	27	32	B4
057	OREw	45	57	B4

Model 1- Genetic background effects are directly related to initial wild-type gene activity in each genetic strain.



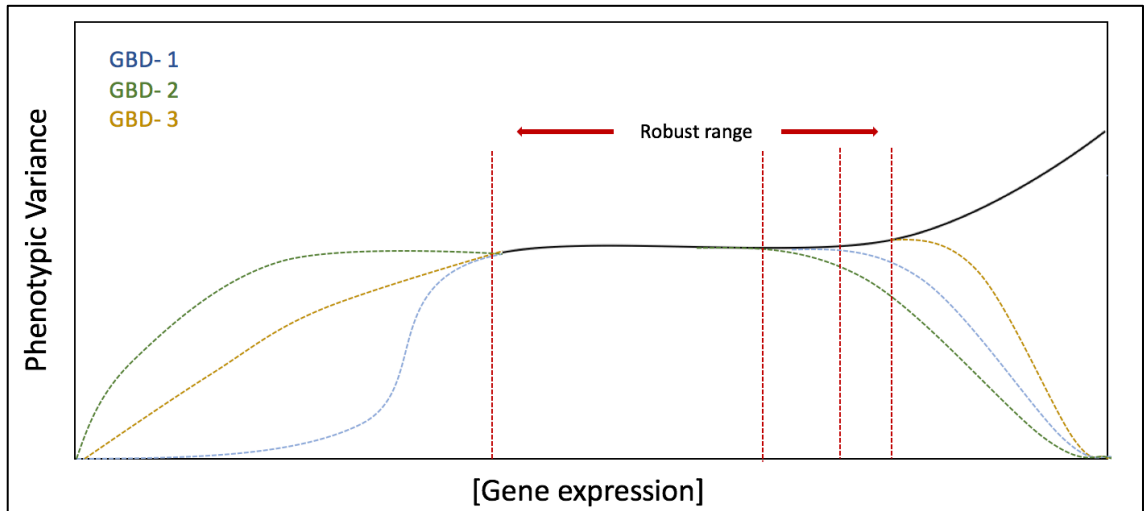
Supplemental Figure 3: Each genetic background (GBD) starts with a different amount of gene activity (we will use gene expression as a proxy) that is sufficient to produce the “wild type” phenotype (the robust range). The hypomorphic mutant allele behaves the same in each genotype (i.e. the same Δ [Gene Activity]), reducing gene expression equally in all strains. This results in backgrounds that start with less wild-type expression being more susceptible to the effects of hypomorphic mutants (green). Conversely, genotypes that are most robust to hypomorphic mutations may be most susceptible to hypermorphic mutations. Genetic background sensitivity thus may be predictable from wild-type analysis of the mutant allele.

Model 2 – Wild type backgrounds differ with respect to mutational robustness



Supplemental Figure 4: Each genetic background (GBD) starts with the same amount of gene expression that is sufficient to produce the “wild type” phenotype (the robust range). However, the hypomorphic mutant allele behaves differently in each genetic background, reducing gene expression unequally between strains. This may suggest the mutant allele itself is sensitive to genetic context (i.e. exhibits differing degrees of robustness/canalization between strains).

Model 3—Each wild type strain differs in the shape of Genotype-Phenotype relationships.



Supplemental Figure 5: Each genetic background (GBD) has its own unique genotype-phenotype curve that exhibits a robust and sensitive range.

Supplemental Figure 6: Dworkin lab standard fly food recipe

Protocol for Making Fly Food

Batch Size ->	Single	Double	Triple	Quadruple
Ingredients				
ddH ₂ O (l)	4.25	8.5	12.75	17
Molasses (g)	390	780	1170	1560
Carageenan (g)	27	54	81	108
Cornmeal (g)	245	490	735	980
Yeast (g)	50	100	150	200
Propionic acid (ml)	12	24	36	48
10% Methyl paraben (ml)	25	50	75	100

- 1.) In a large cooking vessel, measure out the water using a graduated cylinder and once three liters are in there, turn up the heat to low-medium. (Add 5% more water in the winter)
- 2.) Measure and pour molasses using a large beaker. Make sure there is none sticking to the beaker and mix till uniform.
- 3.) Measure carageenan using boat. Add it to the cooker slowly and stir constantly to avoid clumping.
- 4.) Measure cornmeal, add it to the cooker slowly and continue stirring. If you have an electronic mixer keep it on at low speeds to help avoid clumping otherwise continue stirring till you are sure there are no clumps.
- 5.) Measure and add yeast into a SEPARATE vessel/ beaker/ container. Pour 1-2 liters of water depending on the batch size and mix the yeast till it dissolves COMPLETELY. Then add the yeast slurry into the main cooking pot.

PLEASE ADD the CARAGEENAN, CORNMEAL & YEAST as SLOWLY as possible WITH CONSTANT STIRRING to AVOID CLUMPING. It is VERY inconvenient to break the clumps later.

- 6.) Remember to get all the sides clean, stir vigorously till the contents in the cooker look reasonably homogenous. **Stop mixing/ stirring** and turn up heat all the way. Check for bubbling (kind of simmering) at the sides and once you can see the bubbles, cover the cooker (with foil) and let it boil vigorously for 10-15 mins. Watch out for overflow due to boiling especially for large batches. **DO NOT MIX DURING THE BOILING PHASE.**
- 7.) Once it has boiled vigorously, cool the food by either turning the heat to the lowest (which we prefer) or turn it off. Leave the cover on for a while to avoid water loss **BUT STIR/ MIX** the food **INTERMITTENTLY** to avoid clumping and settling.

- 8.) While the food is cooling, please put the vial-pouring machine in the autoclave and turn the autoclave on. The idea is to heat the machine for a while to make pouring food into vials easy.
- 9.) Let the food cool to about 60 deg C. When it is ~60 deg C, prepare 10% Tegosept (Methyl paraben) solution in 95% (or 99%) Ethanol as per the table above. During the cooling period please arrange vials and/or bottles in the appropriate trays, so that they can be used as soon as the food cools down.
- 10.) When food reaches about 60 degrees, add the propionic acid and 10% tegosept to the food. Mix well and begin pouring.

Few tips for better food:

1) To avoid clumps:

- When adding the ingredients add slowly and after EVERY addition stir rigorously till it is uniform.
 - Keep stirring on a regular basis although not continuously after all the ingredients have been added.
- These two steps are enough to ensure non-clumpy food

2) We have observed in the past that the fly food is a bit hard and after a few days it gets crusty and dry.

- This usually happens when too much water escapes while cooking. So try not to let a lot of water evaporate while cooking. Cover the whole vessel with the foil and if you think its going to boil over then leave a teeny-tiny gap in the foil or periodically just open up a small hole on the edge to reduce the pressure.

3) Also the food at times seems to be elastic- meaning if we try to poke holes in the food there is resistance.

- This can be a difficult for the larvae and combined with (2) can render the food almost unpalatable for them (they cannot burrow into the food). This is again in part due to too much water escaping and that corn flour may have gluten in it. If gluten is over-mixed/ stirred it may lead to kind of "elasticky" food. Try to mix the food in pulses and not constantly to correct for this. After adding all the ingredients mix the food for uniform consistency and then turn off the mixer. Then after a while if you find the food getting chunky mix it well for a bit. Turn the mixer off while boiling and then while cooling to about 60 deg C mix in pulses to maintain the consistency.